Journal of Environmental Chemical Engineering 11 (2023) 111303

Contents lists available at ScienceDirect

Journal of Environmental Chemical Engineering

journal homepage: www.elsevier.com/locate/jece

Progress of antibiotics removal from synthetic and real waters and wastewaters by persulfate-based advanced oxidation processes

Enric Brillas

Laboratori d'Electroquímica dels Materials i del Medi Ambient, Secció de Química Física, Facultat de Química, Universitat de Barcelona, Martí i Franquès 1-11, 08028 Barcelona, Spain

ARTICLE INFO

Editor: Stefanos Giannakis

Keywords:
Antibiotics
Catalytic activation
Persulfate
Photocatalytic activation
Thermal activation
UVC activation

ABSTRACT

Bacteriological diseases of humans and animals can be held by the supply of specific antibiotics that allow a larger average-life expectancy. Low concentrations of these recalcitrant compounds have been found in natural waters, which can cause serious health risks to living beings by raising the resistance to bacterial infection, the control of infectious diseases, and the damage of the beneficial bacteria. Antibiotics are very stable at mild conditions and cannot be completely removed in municipal wastewater treatment plants. Over the last decade, potent persulfate (PS)-based advanced oxidation processes (AOPs) are being developed to guaranty the efficient abatement of antibiotics in synthetic and real waters and wastewaters. This review presents a critical and comprehensive analysis of different procedures used to activate PS for form strong oxidants like sulfate radical ($SO_4^{\bullet-}$) and hydroxyl radical ($^{\bullet}OH$), covering up to June 2023. The radical superoxide ion ($O_2^{\bullet-}$) and non-radical singlet oxygen ($^1O_2$) can also be produced and acted as oxidants depending on the experimental conditions. Homogeneous and heterogeneous catalytic, UVC, photocatalytic, thermal, dielectric barrier, and electrochemical processes for PS activation are summarized. Other hybrid methods with 1 activator and combined activation processes are also examined. The fundamentals and characteristics of these treatments are described remarking their oxidation power to abate antibiotics, the effect of operating variables, the generation and identification of radical and non-radical oxidizing agents, the influence of added inorganic anions and natural organic matter, and the detection of by-products produced. Finally, the toxicity of treated antibiotic solutions by PS-based AOPs is discussed.

1. Introduction

Bacteriological diseases of humans and animals can be held by the supply of specific antibiotics, thus increasing their average-life expectancy [1]. The release and accumulation of low concentrations (usually < 10 μg L^{-1}) of antibiotics in many aquatic resources including rivers, lakes, seawater, and even drinking water have been reported due to their widespread use [2]. Wastewaters originated in hospitals, pharmaceutical industries, and houses (also containing the metabolites excreted by humans and animals) are the main sources of these contaminants in the aquatic environment [3]. Urban runoff and leaching from agricultural land also contribute to their flow into the groundwater streams [4]. The low content of these compounds in water bodies can provoke serious health risks to humans and animals by raising the resistance to bacterial infection, the control of infectious diseases, and the damage of the beneficial bacteria [5]. The possible harmful effects of antibiotics have been recognized by the European Directives 2015/495/EU and 2018/840/EU that recommended monitoring the frequency, distribution, occurrence, and inclusion in risk assessment of active compounds such as ciprofloxacin and amoxicillin.

Antibiotics are usually classified in families that possess a similar chemical structure and hence, show the same action mechanism to kill bacteria. Fig. 1 lists the chemical structure and name of the most relevant antibiotics considered in this review. They belong to the families of amphenicols (chloramphenicol), β-lactams (amoxicillin), fluoroquinolones (ciprofloxacin, ofloxacin), macrolides (erythromycin), nitroimidazole (metronidazole), penicillin (amoxicillin), sulfonamides (sulfadiazine, sulfamethazine, sulfamethoxazole), and tetracyclines (tetracycline, oxytetracycline). Trimethoprim, other ubiquitous antibiotic, is not included in any family.

The most usual methods for removing antibiotics from wastewaters are adsorption and biotransformation/biodegradation that are applied in municipal wastewater treatment plants (WWTPs). Nevertheless, these techniques cannot efficiently remove these recalcitrant contaminants

E-mail address: brillas@ub.edu.

https://doi.org/10.1016/j.jece.2023.111303
Received 9 September 2023; Received in revised form 10 October 2023; Accepted 20 October 2023
Available online 24 October 2023

because of their limited and low ability for their abatement being persistent to.

biodegradation due to its chemical nature. As an example, it has been found that only a 40–70% of the concentration of trimethoprim is removed during its treatment in WWTPs, and due to its permanence in the released effluents, it can re-enter again into the environment [6]. To ensure the overall disappearance of antibiotics from wastewaters, more powerful oxidation techniques have been checked. UV irradiation and chlorination have been applied after a biological treatment, but both techniques are not potent enough to degrade most of antibiotics and their metabolites. Other physicochemical and physical methods including coagulation-flocculation and membrane filtration have also

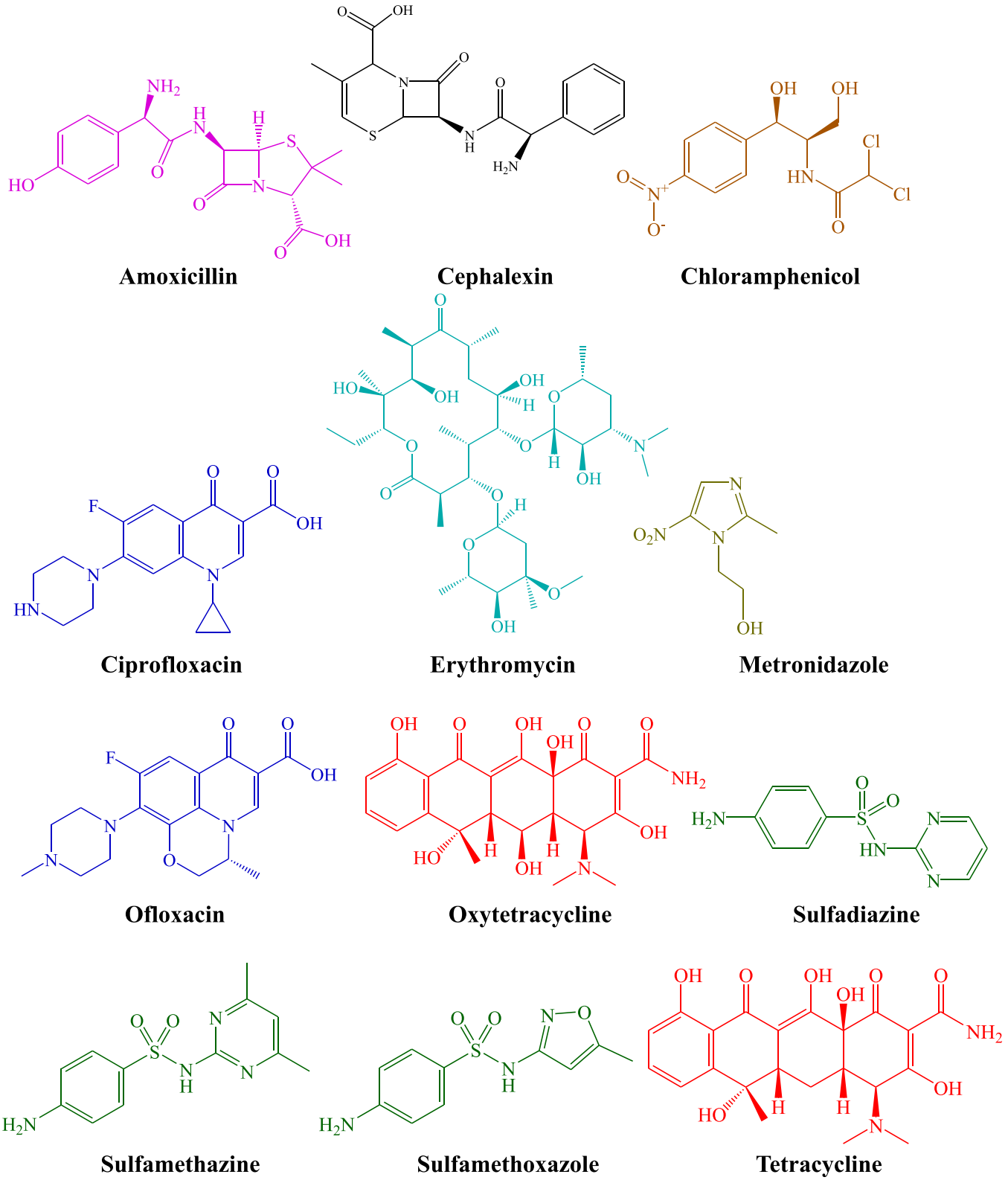

Fig. 1. Chemical structure and name of the most treated antibiotics by persulfate-based AOPs.

been applied to remove these contaminants, but they do not solve their degradation because either they transfer the contaminants from one phase to another or produce concentrates that need to be treated by other methods, respectively [6].

The advanced oxidation processes (AOPs) are much more powerful treatments because they have been specifically designed to efficiently degrade persistent organic pollutants like antibiotics [7,8]. AOPs are environmental-friendly methods that include chemical, photochemical, electrochemical, and photoelectrochemical treatments with the in-situ production of reactive oxygen species (ROS) like the strong oxidant hydroxyl radical ($^{\bullet}OH$), having a standard reduction potential (E^{o}) as high as 2.72 V/SCE. $^{\bullet}OH$ can attack most organic contaminants typically via hydroxylation and dehydrogenation processes up to reaching their mineralization [3,8]. Other potent recently developed procedures involve the emerging sulfate radical ($SO_4^{\bullet-}$)-based AOPs [9]. $SO_4^{\bullet-}$ is another strong oxidant with an $E^{o} = 2.44$ V/SCE, a value comparable to that $^{\bullet}OH$ [5], although it possesses greater selectivity to attack organics via electronic transfer and longer half-life ($\approx$ 40 μs) than $^{\bullet}OH$ ($\approx$ 20 ns) [9]. In this way, sulfate radical-based AOPs have been proposed to possess larger efficiency for the removal and mineralization of organic pollutants. Persulfate ($S_2O_8^{2-}$, PS) is a weak oxidant that needs to be activated to form $SO_4^{\bullet-}$, which can then evolve to $^{\bullet}OH$. The reaction medium plays an important role over the oxidation action of both radicals since it has been reported that $SO_4^{\bullet-}$ prevails at pH < 7 while $^{\bullet}OH$ predominates in alkaline media, thus largely affecting the efficiency of PS-based AOPs [10]. Weaker ROS such as the radical superoxide ion ($O_2^{\bullet-}$) and the non-radical singlet oxygen ($^1O_2$) can be formed as well, depending on the method applied, operation conditions, and aqueous matrix tested [11], thus leading to complex degradation and/or mineralization mechanisms of organics. Recent works have shown the great impact of removing antibiotics by PS activated with different methods, but a comprehensive review deeply analyzing the characteristics of these treatments has not been reported yet in the literature.

This article presents a critical review over the most relevant research published on the PS-based treatments of antibiotics in synthetic and real waters and wastewaters, covering up to June 2023. PS activation with homogeneous and heterogeneous catalytic, UVC, photocatalytic, thermal, dielectric barrier, and electrochemical processes, along with other hybrid methods with 1 activator and combined activation processes, is summarized. The fundamentals and characteristics of all these treatments for antibiotic removal are described with special emphasis over their oxidation power, the effect of operating variables, the generation and identification of radical and non-radical oxidizing agents, the influence of added inorganic anions and natural organic matter (NOM), and the detection of by-products formed. Figures-of-merit are used to analyze their performance. Finally, the overall detoxification or partial loss of toxicity of treated antibiotic solutions during the PS-based AOPs is discussed.

2. Bibliometric analysis

The keyword "Antibiotic and Persulfate" was introduced in the Scopus database to find the scientific papers and reviews that have been published over the remediation of synthetic and real waters and wastewaters contaminated with persulfate up to June 2023. Only articles written in English were selected and those related to book chapters and communications in congresses were directly excluded. The title, authors, and abstract of retrieved publications were listed to be analyzed for their possible acceptance in the present review. Following this way, a total of 9 reviews related to the matter and 148 scientific papers were identified. PS activation with catalysts, UVC, photocatalysts, temperature (thermal), dielectric barrier, electrochemical treatments, other hybrid methods with 1 activator, and combined processes have been considered. These papers reported: (i) the characterization and/or synthesis of catalysts and photocatalysts used for activation, (ii) the effect of operating variables mainly including temperature, pH, content of PS, catalyst and/or photocatalyst, fluence of UVC irradiation, electrolytic cell, and synthetic or real aqueous matrix over antibiotic degradation associated with its concentration decay monitored by high-performance liquid chromatography (HPLC), (iii) the evolution of total organic carbon (TOC) and chemical oxygen demand (COD) abatements related to the antibiotic mineralization, (iv) the assessment of energetic parameters, (v) the identification of the generated radical and non-radical oxidants by means of electron paramagnetic resonance (EPR) or better, by the inhibitory action of selected specific scavengers, (vi) the effect of added inorganic anions, humic or fulvic acid as NOM, and water matrix, (vii) the detection of the by-products formed, usually with techniques of LC-MS/MS, with the proposal of a reaction sequence for the degradation/mineralization of the antibiotic, and (viii) in some cases, the change of solution toxicity in the treatment. The present review briefly describes the fundamentals of the procedures used to activate PS, followed by the analysis of the degradation of selected antibiotics for each method. Great attention has been made over the influence of operating variables, the oxidizing species generated, and the detection of by-products. This review presents 3 tables and 24 figures, especially designed to remark the findings reported in the scientific papers.

At present, seven reviews have partially described the removal of antibiotics by some PS-based processes. So, the application of PS activation by UV-based processes [12,13], cavitation [14,15], electrochemical treatments [1,8], and photocatalysis [16] to degrade several antibiotics has been reported. Li et al. [17] considered a general degradation of fluoroquinolone antibiotics by AOPs. Recently, Honarmandrad et al. [11] detailed the application of several activation methods of PS and peroxymonosulfate (PMS) to the remediation of some antibiotic waters mainly remarking the role of several operating variables, However, our review is much more complete than the latter one because it analyzes the systems used, the action of catalysts, UVC, and photocatalysts, the generation of oxidizing agents, the existence of radical and non-radical mechanisms, the by-products formed, and the change in toxicity of treated wastewaters. The present review then presents a comprehensive work of all these characteristics of the PS-based AOPs, summarizing their usage to degrade antibiotics from synthetic and real waters and wastewaters during all the time that such technologies have been developed up to June 2023.

The bibliometric analysis also allowed identifying 148 scientific papers related to PS-based processes. Fig. 2a depicts that only 29 articles have been published up to 2018, whereas the most important research has been developed in the period of 2022–2023 with 62 publications, demonstrating the current and increasing interest of PS-based AOPs for antibiotic removal. Concerning the kind of PS activation applied. Fig. 2b highlights that homogeneous (5.4%) and heterogeneous catalytic (39.8%) treatments with 67 articles have been the most used methods, followed by 23 articles (16.7%) with UVC, 20 articles (13.5%) with combined activations processes, and 17 articles (11.5%) with photocatalytic treatments. Much less works reported other procedures such as 7 articles (4.7%) with thermal activation, 4 articles (2.7%) with dielectric barrier activation, and 5 articles with electrochemical activation (3.4%) and other hybrid methods with 1 activator (3.4%). Most papers focused the effectiveness of the PS-based AOPs in synthetic wastewaters, with description of the effect of scavengers, inorganics anions, and NOM. The treatment with real matrices including tap water, bottled water, river water, lake water, groundwater, and wastewater (WWTP) effluents has been analyzed in many cases. Comparison with other common AOPs has been reported as well, especially with H_2O_2.

It should be noted that many PS-based AOPs have been developed to remediate wastewaters contaminated with other pharmaceuticals as well. The Scopus database collects a total of 120 publications related to other pharmaceuticals, most of which (64 articles, 53.3%) in the last three years. This demonstrates again the recent interest of these technologies for the treatment of wastewaters with emerging contaminants.

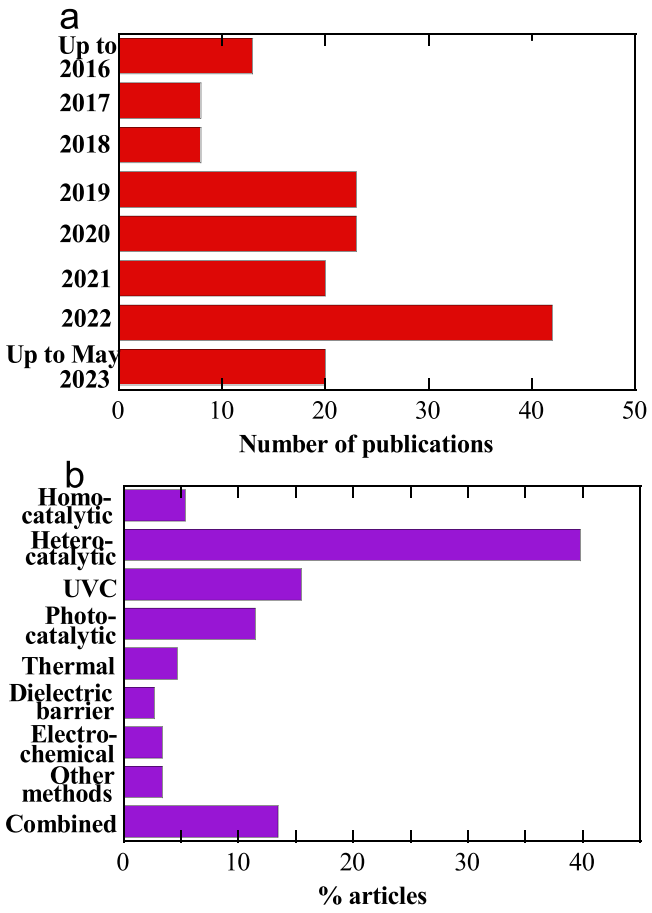

Fig. 2. Bibliometric analysis of the literature for the persulfate activation to remediate antibiotics from synthetic and real water and wastewaters. (a) Number of publications by year. (b) Percentage of articles for each activation method.

3. Persulfate activation for the removal of antibiotics from waters

As pointed out above, PS needs to be activated to produce strong oxidants able to attack and remove antibiotics and their by-products. Several procedures have been developed to do this activation including catalytic, UVC, photocatalytic, thermal, dielectric barrier and electrochemical processes. Other hybrid methods with 1 activator and combined activation processes have been considered as well. This section is devoted to explain the fundamentals of such processes and summarize their main characteristics such as their oxidation power as function of the experimental variables, the identification of oxidizing agents and by-products formed, and the influence of scavengers, inorganics anions. and NOM.

3.1. Catalytic activation

Since the catalytic processes have been the most usual treatments to activate PS, as shown in Fig. 2b, this review begins detailing their performance. Depending on the nature of the catalyst, homogeneous and heterogeneous methods can be distinguished. The homogeneous catalytic activation has been performed with soluble iron ions, whereas the heterogeneous catalytic activation has been developed with a large variety of insoluble solid materials in suspension in the synthetic or real water and wastewater. The characteristics of these catalytic activations are analyzed below. Table 1 summarizes the most relevant results reported remarking the antibiotic tested and the system and experimental conditions used.

3.1.1. Homogeneous catalysis

Homogeneous catalytic processes for PS activation have been made by adding iron ions to the wastewater. Fe^{2+} has been used to remove ciprofloxacin and sulfamethoxazole [18], levofloxacin [19], sulfamethoxazole [20,21], and trimethoprim [22], whereas Fe^{3+} has been tested to degrade sulfamethoxazole [23] and sulfanilamide [24]. Cations such as Zn^{2+}, Cu^{2+}, Fe^{2+}, and Fe^{3+} have been used for sulfadiazine degradation in pure water and a WWTP effluent [25].

When Fe^{2+} catalyst is checked, it reacts with added PS via the electron-transfer reaction (1) to form Fe^{3+} and $SO_4^{\bullet-}$, which then evolves by reactions (2)-(4) and further produces the other strong oxidant $^{\bullet}OH$ by reactions (5) or (6) and its parasitic reactions (7)-(9) [18]:

$$S_2O_8^{2-} + Fe^{2+} \rightarrow Fe^{3+} + SO_4^{\bullet-} + SO_4^{2-} k_2 = 27\ M^{-1}\ s^{-1} \quad (1)$$

$$2SO_4^{\bullet-} \rightarrow S_2O_8^{2-}\ k_2 = 8{\cdot}1 \times 10^8\ M^{-1}\ s^{-1} \quad (2)$$

$$SO_4^{\bullet-} + Fe^{2+} \rightarrow SO_4^{2-} + Fe^{3+}\ k_2 = 3{\cdot}0 \times 10^8\ M^{-1}\ s^{-1} \quad (3)$$

$$SO_4^{\bullet-} + S_2O_8^{2-} \rightarrow SO_4^{2-} + S_2O_8^{\bullet-} k_2 = 6{\cdot}1 \times 10^5\ M^{-1}\ s^{-1} \quad (4)$$

$$SO_4^{\bullet-} + H_2O \rightarrow SO_4^{2-} + {}^{\bullet}OH + H^+\ k_2 = 2{\cdot}0 \times 10^3\ M^{-1}\ s^{-1} \quad (5)$$

$$SO_4^{\bullet-} + OH^- \rightarrow SO_4^{2-} + {}^{\bullet}OH\ k_2 = 6{\cdot}5 \times 10^7\ M^{-1}\ s^{-1} \quad (6)$$

$$2{}^{\bullet}OH \rightarrow H_2O_2\ k_2 = 5{\cdot}5 \times 10^9\ M^{-1}\ s^{-1} \quad (7)$$

$$SO_4^{\bullet-} + {}^{\bullet}OH \rightarrow HSO_4^- + 1/2\ O_2\ k_2 = 1{\cdot}0 \times 10^{10}\ M^{-1}\ s^{-1} \quad (8)$$

$$S_2O_8^{2-} + {}^{\bullet}OH \rightarrow S_2O_8^{\bullet-} + OH^-\ k_2 = 1{\cdot}2 \times 10^7\ M^{-1}\ s^{-1} \quad (9)$$

Ji et al. [18] compared the PS/Fe^{2+} processes of 50 mL of 30 μM of ciprofloxacin (CIP) or sulfamethoxazole (SMX) in pure water at pH = 6.0. After 240 min of treatment, 96% of the former was degraded using 600 μM of PS and Fe^{2+}, whereas only 75% of the latter was removed with higher contents of 2.4 mM of PS and Fe^{2+} (see Table 1). To detect the oxidizing radicals formed, 60 mM ethanol (EtOH) or *tert*-butanol (TBA) were added to the above solutions. It is well-known that these compounds act of scavengers of generated $SO_4^{\bullet-}$ and $^{\bullet}OH$ according to reactions (10)-(13). The small absolute second-order rate constant k_2 of reaction (13) informs that TBA only reacts with $^{\bullet}OH$, whereas EtOH can react with both radicals. This agrees with the decay in the percent of degradation of both antibiotics presented in Fig. 3a and b, since it was reduced to 21% and 10% with EtOH, much largely than 57% and 21% with TBA, respectively. From these data, one can conclude that $SO_4^{\bullet-}$'and $^{\bullet}OH$ oxidized CIP, more rapidly than SMX by $^{\bullet}OH$.

$$EtOH + {}^{\bullet}OH \rightarrow \text{intermediates} k_2 = (1{\cdot}2\text{–}2{\cdot}8) \times 10^9\ M^{-1}\ s^{-1} \quad (10)$$

$$EtOH + SO_4^{\bullet-} \rightarrow \text{intermediates} k_2 = (1{\cdot}6\text{–}7{\cdot}7) \times 10^7\ M^{-1}\ s^{-1} \quad (11)$$

$$TBA + {}^{\bullet}OH \rightarrow \text{intermediates} k_2 = (3{\cdot}8\text{–}7{\cdot}6) \times 10^8\ M^{-1}\ s^{-1} \quad (12)$$

$$TBA + SO_4^{\bullet-} \rightarrow \text{intermediates}\ k_2 = (4{\cdot}0\text{–}9{,}1) \times 10^5\ M^{-1}\ s^{-1} \quad (13)$$

The effect of adding quenchers of Fe^{2+} like citric acid, EDTA (ethylenediaminetetraacetic acid), and EDDS ((*S*,*S*)-ethylenediamine-*N*,*N*'-succinic acid) was investigated. Contradictory results can be observed in Fig. 3c and d for CIP and SMX, respectively. A loss of degradation for 300 μM of PS and Fe^{2+} using the same content of all quenchers can be seen for CIP in Fig. 3c,

as expected by the formation of Fe(II)-complexes that inhibit the amount of soluble Fe^{2+} to oxidize PS from reaction (1). On the contrary, the degradation of analogous solutions of SMX was enhanced in the presence of quenchers (see Fig. 3d), a behavior that cannot be easily interpreted and that requires a deeper study to be clarified. Fig. 3e highlights that the removal of each antibiotic diminished in river water as compared to pure water. This is indicative of a loss of oxidizing radicals by reaction with the scavenger components (inorganic anions and NOM) of the river water. The authors also identified 15 primary by-products of CIP by LC-MS and proposed the reaction sequence of Fig. 4

Table 1
Selected results reported for the removal of antibiotics from different aqueous matrices by catalytic activation of persulfate.

Antibiotic	System	Experimental remarks	Best results	Ref.
Homogeneous catalytic activation				
Ciprofloxacin Sulfamethoxazole	Stirred cylindrical glass reactor with Fe^{2+} catalyst	50 mL of 30 μM of each antibiotic in pure water and river water, from 1:1:1–1:80:80 ratio with PS and Fe^{2+}, pH = 6.0, effect of chelating agents (citric acid, EDTA[a], and EDDS[b]) and scavengers (ethanol and TBA[c]), 240 min	Degradation: 96% with 1:20:20 for ciprofloxacin and 75% with 1:80:80 for sulfamethoxazole, reduced to 21% and 10% with ethanol, and 57% and 21% with TBA. $SO_4^{\bullet-}$ and $^{\bullet}OH$ oxidized the former antibiotic, and predominantly $^{\bullet}OH$ the latter one. Inhibition/acceleration with chelating agents and river water. For ciprofloxacin, 15 primary by-products detected by LC-MS	[18]
Levofloxacin	Stirred cylindrical glass reactor with Fe^{2+} catalyst	400 mL of 75 μM of antibiotic in pure water, from 1:2.5:1–1:40:1 and from 1:20:0.5–1:20:8 ratio with PS and Fe^{2+}, pH = 3.0–9.0, 21 °C, 180 min	Total degradation with 1:20:8 ratio in 90 min, but only 8% TOC removal in 180 min at pH = 3.0–7.0. Lower performance at pH = 9.0. Quicker removal with additional H_2O_2. 6 primary by-products from LC-MS	[19]
Trimethoprim	Bottle in a shaker at 160 rpm with Fenton or PS/Fe^{2+}	100 mL of 0.05 mM antibiotic in pure water and WWTP effluent, 0.5–4.0 mM PS, 0.5–4.0 mM H_2O_2, 0.025–4.0 mM Fe^{2+}, pH = 3.0, 25 °C, 240 min^{-2}	Degradation with Fenton with 1.0 mM H_2O_2: 100% in 30 min with 1.0 mM Fe^{2+} and 87% in 240 min with 0.05 mM Fe^{2+}, corresponding to 53% and 45% TOC decay. For 4.0 mM PS and Fe^{2+}, 82% degradation and 54% TOC reduction. For the WWTP effluent, 35% and 43% abatement for Fenton (0.1 mM Fe^{2+}) and PS/Fe^{2+}. 5 and 6 primary by-products found from Fenton and PS/Fe^{2+} by LC-MS	[22]
Sulfamethoxazole	Stirred tank reactor with Fe^{3+} and sulfite as catalysts	100 mL of 10 μM of antibiotic in pure water, 1.0–3.0 mM PS, 0.25–0.75 mM Fe^{3+}, 0.5–1.5 mM Na_2SO_3, pH = 2.26–6.89, effect of scavengers (methanol and TBA), 15 min	Optimization by response surface methodology: 83% degradation with 2.0 mM PS, 0.50 mM Fe^{3+}, and 1.0 mM Na_2SO_3 at pH = 5.96. Superiority of $^{\bullet}OH$ over $SO_4^{\bullet-}$ as oxidant. Identification of 8 aromatic, 4 heteroaromatic, and 2 aliphatic by-products by LC-MS	[23]
Heterogeneous catalytic activation				
Biochar				
Sulfamethoxazole	Stirred tank reactor with biochar catalyst	250 mL of 125–500 μg L^{-1} of antibiotic in pure water, bottled water, and WWTP effluent, 0–250 mg L^{-1} PS, 90 mg L^{-1} catalyst, natural pH (6.0–8.0), effect of scavengers (methanol, and TBA) and humic acid, room temperature, 90 min	More rapid removal at smaller antibiotic content and greater PS dosage. In pure water, 95% removal for 125 μg L^{-1} antibiotic and 250 mg L^{-1} PS with k_1[d] = 0.029 min^{-1}. 82% removal with bottled water and 80% with WWTP effluent. Little effect of scavengers and negative influence of humic acid	[28]
Tetracycline	Stirred tank reactor with sewage sludge biochar catalyst	50 mL of 10 mg L^{-1} of antibiotic in pure water, 2.0–10 mM PS, 0.2–1.0 g L^{-1} catalyst, pH = 3.0–11.0, effect of scavengers (methanol, TBA, FF[f], and *p*-BQ[g]), anions (Cl^-, HCO_3^-, $H_2PO_4^-$, and SO_4^{2-}), and humic acid, 25 °C, 180 min	87% antibiotic abatement with 10 mM PS, 1.0 g L^{-1} catalyst, and pH = 5.0. $^1O_2$ as dominant oxidant, followed by $^{\bullet}OH$, $O_2^{\bullet-}$, and $SO_4^{\bullet-}$. PS reaction involved with C-O-Fe(II) bridge on the biochar surface<	[33]
Trimethoprim	Stirred cylindrical vessel with biochar catalyst	120 mL of 0.15–0.5 mg L^{-1} of antibiotic in pure water and real waters, 0.1–0.5 g L^{-1} PS, 0.045–0.18 g L^{-1} catalyst, natural pH, effect of scavengers (methanol, TBA, and sodium azide), anions (Cl^-, HCO_3^-, and SO_4^{2-}), and humic acid, room temperature, 120 min	In pure water, total degradation with k_1 = 0.0139 min^{-1} for 0.15 mg L^{-1} antibiotic with 0.5 g L^{-1} PS and 0.09 g L^{-1} catalyst. Using 0.5 mg L^{-1} antibiotic, degradation: pure water without and with all inorganic ions (78%) > bottled water (53%) > WWTP effluent (18%). Strong inhibition up to 25% removal with humic acid. Predominance of non-radical mechanism. 7 heteroaromatic derivatives found by LC-MS	[34]
Modified biochar				
Cephalexin	Flask shaken at 150 rpm with Fe_2O_3/loofah biochar catalyst	50 mL of 10 mg L^{-1} of antibiotic in pure water, 0.1–0.8 g L^{-1} PS, 0.1–0.8 g L^{-1} catalyst, pH = 3.0–9.6, effect of scavengers (ethanol and TBA) and anions (Cl^-, NO_3^-, HCO_3^-, SO_4^{2-}, and $H_2PO_4^-$), 15–45 °C, 200 min	Faster degradation up to 74% with k_1 = 0.0104 $min^{-1}$for 0.1 g L^{-1} PS, 0.4 g L^{-1} catalyst, pH = 4.82, and 30 °C. E_a[e] = 38.76 kJ mol^{-1}. Inhibition at pH = 3.0 and 9.6, and with $H_2PO_4^-$. Oxidation with both $SO_4^{\bullet-}$ and $^{\bullet}OH$. Low reusability after 4 cycles. Identification of 13 aromatic by-products by LC-MS	[35]
Norfloxacin	Tank reactor shaken at 180 rpm with CuO/Fe_3O_4/biochar catalyst	176 mL of 30 mg L^{-1} of antibiotic in pure water, 6.0 mM PS, 0.5 g L^{-1} catalyst, pH = 3.0–11.0, effect of scavengers (methanol, TBA, and L-histidine), 25 °C, 180 min	Quicker antibiotic loss up to 95% at pH = 9.0. Predominance of $^1O_2$ as oxidant (non-radical mechanism). Low reusability with loss of 12% performance in 4 successive cycles. 10 heteroaromatic by-products identified by LC-MS	[37]
Sulfadiazine	Test tube in a multicomposition reactor with Fe/biochar catalyst	50 mL of 10–80 mg L^{-1} of antibiotic in pure water, 0–2.0 mM PS, 0–1.5 g L^{-1} catalyst, pH = 3.1–9.7, effect of scavengers (methanol, TBA, and FF[h]) and anions (Cl^-, HCO_3^-, SO_4^{2-}, and PO_4^{3-}), 25 °C, 60 min	91% of antibiotic decay for 40 mg L^{-1} antibiotic, 1.5 mM PS, 1.0 g L^{-1} catalyst, and pH = 5.2 with k_1 = 0.031 min^{-1}. More oxidative role of $^{\bullet}OH$ than $SO_4^{\bullet-}$ and $^1O_2$. Large negative effect of all the anions. Low reusability after 3 successive steps. Detection of 4 aromatic and 6 heteroaromatic by-products by LC-MS	[38]
Sulfamethoxazole	Stirred tank reactor with Fe_3O_4/biochar catalyst prepared by pyrolysis at 400 and 700 °C	100 mL of 10 mg L^{-1} of antibiotic in pure water and real waters, 2.0 mM PS, 0.5 g L^{-1} catalyst, pH = 3.5,	82% of antibiotic decay for the catalyst prepared at 700 °C with k_1 = 0.031 min^{-1}. Similar trend in the pH range 3.5–9.0. Little inhibition by adding Cl^- and	[39]

(*continued on next page*)

Table 1 (*continued*)

Antibiotic	System	Experimental remarks	Best results	Ref.
		effect of scavengers (ethanol and phenol), Cl^-, and humic acid, 25 °C, 120 min	humic acid. Degradation: pure water > lake water = seawater > piggery wastewater > landfill leachate. Non-radical mechanism with Fe(IV) dominated the catalyst at 400 °C and electron transfer for that ay 700 °C	
Sulfamethoxazole	Conical flask shaken at 180 rpm with N,S,Co/biochar catalyst	100 mL of 20–80 mg L^{-1} of antibiotic in pure water, 5.0 mM PS, 0.025–1.0 g L^{-1} catalyst, pH = 2.0–9.0, effect of scavengers (methanol, TBA, L-histidine, and FF), room temperature, 120 min	93% and 66% degradation for 30 mg L^{-1} catalyst, 1.0 g L^{-1} of catalyst molten with KCl and NaCl, respectively, at pH = 6.0. Predominance of $^1O_2$ over $SO_4^{\bullet-}$ and $^{\bullet}OH$ as oxidant. Techno-economic study for the production of the catalyst with KCl (US$ 2.34 kg^{-1}) and NaCl (US$ 1.72 kg^{-1})	[40]
Sulfamethoxazole	Stirred tank reactor with CeO_2/biochar catalyst	120 mL of 0.5 mg L^{-1} of antibiotic in pure water, bottled water, and WWTP effluent, 200–500 mg L^{-1} PS, 90 mg L^{-1} catalyst, natural pH (6.0–8.0), effect of scavengers (methanol, TBA, and sodium azide), anions (Cl^- and CO_3^{2-}), and humic acid, room temperature, 120 min	In pure water, little effect of PS dosage with 65% degradation and $k_1 = 0.0089$ min^{-1}. Antibiotic removal: 40% with bottled water ($k_1 = 0.0032$ min^{-1}) > 22% with WWTP effluent ($k_1 = 0.0016$ min^{-1}). Little positive effect of Cl^- and inhibition with humic acid, more strongly with CO_3^{2-}. Oxidation with $SO_4^{\bullet-}$,$^{\bullet}OH$, and $^1O_2$	[41]
Sulfapyridine	Bottle shaken at 180 rpm with FeCu/biochar catalyst	200 mL of 20 mg L^{-1} of antibiotic in pure water, 4.0 mM PS, 1.0 g L^{-1} catalyst, pH = 3.0–11.0, 25 °C, 120 min	Degradation at pH = 8.2 (with 10 mM $NaHCO_3$): 99% with FeCu/biochar > 70% with Fe-biochar > 50% with biochar. Using FeCu/biochar, similar removal at pH = 7.0–9.0 and moderate reusability losing 7% performance after 3 consecutive steps by Cu^{2+} lost	[42]
Tetracycline	Conical flask in rotary shaker at 180 rpm with Cu-FeOOH/biochar catalyst	100 mL of 20–80 mg L^{-1} of antibiotic in pure water, 20 mM PS, 0.2 g L^{-1} catalyst, pH = 3.0–11.0, effect of scavengers (ethanol and TBA) and anions, 25 °C, 120 min	98% degradation and 55% and 46% COD and TOC removals, respectively, for 0.5Cu-1FeOOH/biochar at pH = 7.0. Analogous abatement in all the pH interval. Predominance of $SO_4^{\bullet-}$in acidic media and of$^{\bullet}OH$ in alkaline suspensions. Degradation: Pure water > NO_3^- > SO_4^{2-} > PO_4^{3-}> Cl^- > HCO_3^-. Low reusability after 5 consecutive runs, with a loss of 8% of the antibiotic content, 14% of COD and 9% of TOC	[44]
Carbonaceous materials				
Sulfamethoxazole	Flow system with filtration with a N-graphene/rGO[h]/CNTs[i] membrane	Recirculation of 250 mL of 0.5 mg L^{-1} antibiotic in pure water, 2.0–10 mM PS, pH = 4.0–10.0, liquid flow rate = 1.0 mL min^{-1}, effect of Cl^- and fulvic acid, room temperature, 100 min	94% abatement with 8 g m^{-2} of carbon loading and 5.0 mM PS at pH = 7.0. Strong inhibition in the presence of Cl^- and fulvic acid. Good reproducibility after 3 consecutive cycles	[51]
Tetracycline	Stirred tank reactor with S,N-carbon catalyst	250 mL of 0.02 mM of antibiotic in pure water and real waters, 2.0 mM PS, 0.4 g L^{-1} catalyst, pH = 3.0, effect of scavengers (ethanol, sodium azide, and β-carotene), 25 °C, 60 min	81% degradation for the catalyst synthesized at 800 °C. Oxidation dominated by$^1O_2$ and mediated electron transfer (non-radical mechanisms). TOC removal: pure water (43%) > river water (21%) > lake water (16%) > raining water (15%). Identification of 11 aromatic, 1 cyclic, and 3 aliphatic by-products by LC-MS	[54]
Iron and iron compounds				
Chloramphenicol	Tank reactor in a rotary oscillating water bath with nZVI[j] and S-nZVI catalyst	100 mL of 20 mg L^{-1} of antibiotic in pure water, 1.0–10 mM PS, 0.05–0.3 g L^{-1} catalyst, pH = 3.1–9.1, effect of scavengers (ethanol and TBA) and anions (Cl^-, CO_3^{2-}, and SO_4^{2-}), 20 °C, 30 min	Total degradation with 3.0 mM PS and 0.1 g L^{-1} S-nZVI catalyst at pH = 6.9 with $k_1 = 0.2115$ min^{-1}. Faster degradation with more PS dosage, but little influence of catalyst content and pH from 3.1 to 6.9. Slight inhibition with Cl^- and SO_4^{2-}, but very strong with CO_3^{2-}. $SO_4^{\bullet-}$'and$^{\bullet}OH$ as oxidants. Detection of 18 aromatic by-products by LC-MS	[58]
Sulfamethoxazole	Conical flask in rotary shaker with nZVI catalyst	100 mL of 10–40 mg L^{-1} of antibiotic in pure water, 0.5–3.0 mM PS, 0.05–0.30 g L^{-1} catalyst, pH = 3.1–9.3, effect of scavengers (ethanol, and TBA), 25 °C, 120 min	Enhancement of antibiotic abatement with decreasing its content and at higher PS dosage. Little influence of catalyst dosage and pH. 88% degradation and 20% TOC removal for 10 mg L^{-1}, 1.0 mM PS, 0.1 g L^{-1} catalyst and pH = 5–5. Overall removal with 3.0 mM PS. Oxidation by $SO_4^{\bullet-}$ and$^{\bullet}OH$	[62]
Tetracycline	Stirred beaker with γ-Fe_2O_3/CeO_2 catalyst	100 mL of 20 mg L^{-1} of antibiotic in pure water and real waters, 0.5–4.0 mM PS, 0.1–0.8 g L^{-1} catalyst, pH = 2.0–9.0, effect of scavengers (ethanol TBA, *p*-BQ, and phenol), anions (Cl^-, NO_3^-, HCO_3^-, and SO_4^{2-}), and humic acid, room temperature, 120 min	In pure water, 83% degradation for 3.0 mM PS and 0.2 g L^{-1} catalyst. Little influence of pH. Cost of US$ 0.106 m^{-3}. Degradation decayed to 63% with river water and 60% with pond water. Small influence of all anions and humic acid, except a drastic reduction with HCO_3^-. $SO_4^{\bullet-}$and$^{\bullet}OH$ dominated as oxidants in front of $O_2^{\bullet-}$ and$^1O_2$. Low reusability after 5 successive cycles. Detection of 13 aromatic by-products by LC-MS	[65]
Tetracycline	Conical flask in a shaker at 150 rpm with ferrocene/chitosan/Fe_3O_4 catalyst	100 mL of 30 mg L^{-1} of antibiotic in pure water, 0.1–0.5 g L^{-1} PS, 0.1–0.5 g L^{-1} catalyst, pH = 2.0–11.0, effect of scavengers (methanol and TBA), anions (Cl^-, NO_3^-, CO_3^{2-}, and HCO_3^-), and fulvic acid, 25 °C, 60 min	Total degradation in 50 min with 0.4 g L^{-1} PS, 0.4 g L^{-1} catalyst, and pH = 5.0. Little effect of Cl^- and NO_3^- and strong inhibition with CO_3^{2-}, HCO_3^-, and fulvic acid. $SO_4^{\bullet-}$ dominated over$^{\bullet}OH$ as oxidant. Good reproducibility after 5 consecutive steps	[66]
Tetracycline	Stirred tank reactor with Fe,Co, O-g-C_3N_4 catalyst	100 mL of 5–25 mg L^{-1} of antibiotic in pure water and real waters, 1.0–3.0 g L^{-1} PS, 0.2–0.8 g L^{-1} catalyst, pH = 3.0–11.0, effect of scavengers (methanol, TBA, *p*-BQ, FF, and phenol), 40 °C, 120 min	In pure water, faster decay at lower antibiotic content and pH, and higher PS and catalyst dosages. 90% removal with $k_1 = 0.026$ min^{-1} for 15 mg L^{-1} antibiotic, 2.5 g L^{-1} PS, 0.6 g L^{-1} catalyst, and pH = 3.0. Oxidant $O_2^{\bullet-}$ predominated over $SO_4^{\bullet-}$,$^{\bullet}OH$, and$^1O_2$. TOC removal: pure water (68%) > river water	[67]

(*continued on next page*)

Table 1 (*continued*)

Antibiotic	System	Experimental remarks	Best results	Ref.
			(34%) > tap water (19%) > WWTP effluent (6.9%). Moderate reusability after 5 successive runs. LC-MS allowed detecting 11 aromatic 5 cyclic, and 2 aliphatic by-products	
Tetracycline	Stirred tank reactor with FeS catalyst	100 mL of 5.0 mM of antibiotic in pure water, 0.05–4.0 mM PS, 25–200 mg L^{-1} catalyst, pH = 2.0–9.0, effect of scavengers (methanol, TBA, and phenol), 20 °C, 60 min	Quicker abatement with raising PS and catalyst contents and decreasing pH. Total decay in 10 min with a maximum TOC removal of about 50%. $SO_4^{\bullet-}$ and $^{\bullet}OH$ as oxidants. Initial heterogeneous surface process, further passing to homogeneous reaction. Detection of 13 aromatic, 11 cyclic, and 1 aliphatic derivatives by LC-MS	[68]
Non-ferrous metal oxides				
Sulfamethoxazole	Stirred tank reactor with $LaNiO_3$ catalyst	60 mL of 0.25–1.0 mg L^{-1} of antibiotic in pure water, bottled water, and WWTP effluent, 0.05–0.1 g L^{-1} PS, 25–250 mg L^{-1} catalyst, pH = 6.0, effect of scavengers (methanol and TBA), anions (Cl^- and HCO_3^-), and humic acid, room temperature, 20 min	In pure water, higher PS and catalyst dosages enhanced more largely antibiotic removal at lower content. Total degradation in 10 min for 0.5 mg L^{-1} antibiotic, 0.1 g L^{-1} PS, and 250 mg L^{-1} catalyst with $k_1 = 0.2267$ min^{-1}. Strong inhibition at pH = 9.0 and with bottled water and WWTP effluent. Little influence of Cl^-, and large inhibition with HCO_3^- and humic acid. Predominance of $SO_4^{\bullet-}$ over $^{\bullet}OH$ as oxidant. Excellent reusability after 4 successive cycles	[72]
Tetracycline	Stirred conical flask with ZrO_2/$MnFe_2O_4$ catalyst	100 mL of 3.43–65.8 mg L^{-1} of antibiotic in pure water and real waters, 6.0 mM PS, 0.2 g L^{-1} catalyst, pH = 7.1, effect of scavengers (ethanol TBA, and *p*-BQ) and anions (Cl^-, NO_3^-, HCO_3^-, and $H_2PO_4^-$), 25 °C, 120 min	Lower concentration yielded greater removal. 88% degradation for .3.43 mg L^{-1} antibiotic with $k_1 = 0.038$ min^{-1}. It decayed to 73% for lake water > 60% for landfill leachate. $SO_4^{\bullet-}$,$^{\bullet}OH$, and $O_2^{\bullet-}$ acted as oxidants. Inhibition: $H_2PO_4^- > HCO_3^- > NO_3^- > Cl^-$. Low reusability after 5 consecutive steps. 14 aromatic, 1 cyclic, and 3 aliphatic by-products detected by LC-MS	[74]
Tetracycline	Tank reactor with mesoporous ordered MnO_x catalyst	500 mL of 10 mg L^{-1} of antibiotic in pure water and groundwater, 0.48 g L^{-1} PS, 80 mg L^{-1} catalyst, natural pH (about 7.0), effect of scavengers (ethanol and TBA), room temperature, 360 min	In pure water, 88% abatement and 87% TOC removal. In groundwater, 69% and 81% degradations with 0.6 and 1.8 g L^{-1} catalyst, respectively. $SO_4^{\bullet-}$and $^{\bullet}OH$ as oxidants in both media. Excellent reusability in groundwater after 4 successive cycles	[75]
Other catalysts				
Chloramphenicol	Tank reactor in an ultrasonic bath with Al-MIL catalyst	50 mL of 0.25 mM of antibiotic in pure water, 10 mM PS, 0.25 g L^{-1} catalyst, pH = 4.1–10.8, effect of scavengers (ethanol and TBA), 28–50 °C, 120 min	At pH = 5.3 and 40 °C, 71% TOC reduction.$^{\bullet}OH$ as predominant oxidant. Moderate reusability with loss of 11% of TOC reduction after 5 consecutive steps	[76]
Sulfamethazine	Erlenmeyer flask in a rotating speed at 180 rpm with 4 commercial tourmalines catalysts	100 mL of 5.0 mg L^{-1} of antibiotic in pure water, 0–4.0 mM PS, 5.0 g L^{-1} catalyst, pH = 2.0–10.0, effect of scavengers (methanol, TBA, L-histidine, and sodium oxalate), 25 °C, 150 min	Overall degradation in 120 min at pH = 2.0 and 150 min at pH = 5.0 for the best tourmaline catalyst.$^{\bullet}OH$, $SO_4^{\bullet-}$,$^1O_2$, and holes detected as oxidants. Preferential action of the two latter agents for the best tourmaline	[81]
Sulfamethoxazole	Stirred tank reactor with Cu_3P catalyst	120 mL of 0.5–4.1 mg L^{-1} of antibiotic in pure water, bottled water, and WWTP effluent, 0.05–1.0 g L^{-1} PS, 20–80 mg L^{-1} catalyst, natural pH, effect of scavengers (methanol and TBA), room temperature, 30 min	Faster removal at lower antibiotic concentration and higher PS and catalyst dosages. For 0.5 mg L^{-1} antibiotic in pure water with 0.1 g L^{-1} PS and 40 mg L^{-1} catalyst, total degradation in 15 min with $k_1 = 0.226$ min^{-1}. For bottled water, $k_1 = 0.027$ min^{-1}.and for WWTP effluent, $k_1 = 0.017$ min^{-1}. $SO_4^{\bullet-}$ as dominant oxidant	[82]

[a] EDTA: Ethylenediaminetetraacetic acid.
[b] EDDS: (*S*,*S*)-Ethylenediamine-*N*,*N*′-succinic acid.
[c] TBA: *tert*-Butylalcohol.
[d] k_1: Pseudo-first-order rate constant for antibiotic degradation.
[e] E_a: Activation energy.
[f] FF: Furfuryl alcohol.
[g] *p*-BQ: *p*-Benzoquinone.
[h] r-GO: Reduced graphene oxide.
[i] CNTs; Carbon nanotubes.
[j] nZVI: Nanoscaled zero-valent iron.

considering that $^{\bullet}OH$ is the preferent oxidant respect to $SO_4^{\bullet-}$. The CIP (**1**) degradation is initiated by 3 parallel ways involving: (i) the piperazine ring cleavage to form **2**; (ii) the hydroxylation of the pyridine ring yielding **3**; and (iii) the defluorination of the benzenic ring originating **4**. The subsequent oxidation of the residual piperazine group de **2** leads to the compounds **5**-**10**, and finally, the amino derivative **11**. Defluorination of **3** gives rise to **12**, which is also formed from the hydroxylation of the benzenic ring of **4**. Hydroxylation of the benzenic ring of **12** yields **13**, which is further decarboxylated to **14** followed by its pyridine ring cleavage to give **15**. Finally, the piperazine ring cleavage of **4** leads to **16**.

Other work related to the treatment of levofloxacin with PS/Fe^{2+} was carried out with 400 mL of 75 μM of the antibiotic in pure water at pH = 3.0–9.0 using a stirred cylindrical reactor [19]. A good degradation performance was found by adding 1.5 mM PS and 0.6 mM Fe^{2+} at pH = 3.0–7.0 with total abatement in 90 min. In contrast, the by-products formed were so recalcitrant that only 8% of TOC was removed in 180 min (see Table 1). The performance at pH = 9.0 decayed strongly due to the precipitation of $Fe(OH)_2$, meaning that this method can be only run in acidic medium. Wang and Wang [22] used a bottle in a shaker at 160 rpm to compare the Fenton and PS/Fe^{2+} processes of 100 mL of 0.05 mM trimethoprim in pure water at pH = 3.0.

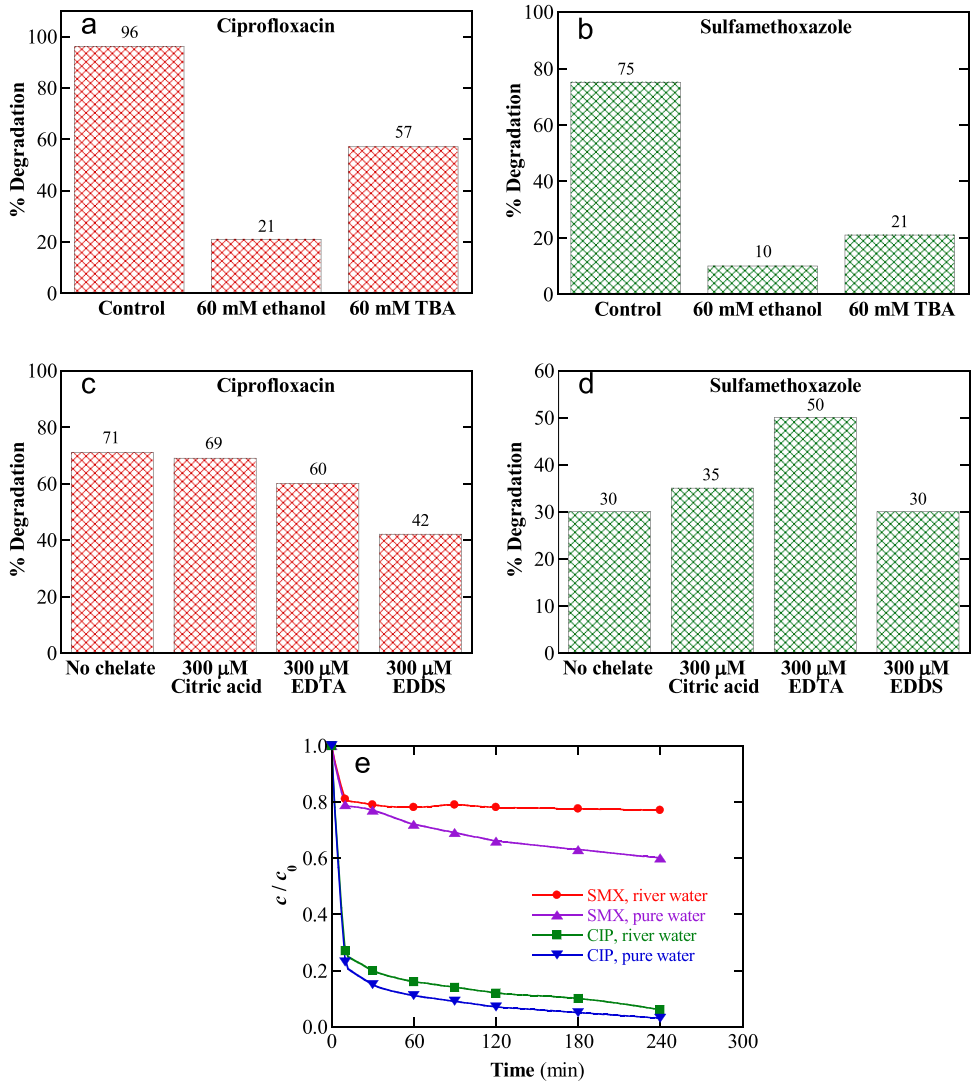

Fig. 3. Percentage of degradation after 240 min of the PS/Fe^{2+} treatment of 50 mL of 30 μM of (a) ciprofloxacin (CIP) with 600 μM PS and 600 μM Fe^{2+} and (b) sulfamehoxazole (SMX) with 2.4 mM PS and 2.4 mM Fe^{2+} at pH = 6.0. In both cases, the effect of 60 mM ethanol or *tert*-butanol (TBA) as scavengers is given. Effect of 300 μM of PS, Fe^{2+}, and various quenchers on the percentage of degradation of (c) CIP and (d) SMX. (e) Normalized antibiotic concentration with time for CIP and SMX with 600 μM PS and 600 μM Fe^{2+} in pure water and river water.
Adapted from ref. [18].

The Fenton process with 1.0 mM H_2O_2 and Fe^{2+} to originate $^{\bullet}OH$ yielded overall removal in 30 min and 53% TOC decay in 240 min. Worse results were found for the degradation by PS/Fe^{2+} with 4.0 mM PS and Fe^{2+} since only 83% of trimethoprim was abated, although a similar value of 54% of TOC was reduced in 240 min. For a WWTP effluent, a smaller degradation of 43% was obtained by PS/Fe^{2+} due to the scavenging effect of the components of the aqueous matrix, whereas less decay of 35% was determined by Fenton using 0.1 mM Fe^{2+} (see Table 1). These findings allow concluding that the PS/Fe^{2+} is preferable respect to Fenton for trimethoprim removal.

Yuan et al. [23] explored the use of Fe^{3+} as homogeneous catalyst on PS-based AOPs. Since this ion does not activate PS, they added sulfite (SO_3^{2-}) to the medium to generate Fe^{2+} as activator from the following reaction:

$$Fe^{3+} + SO_3^{2-} \rightarrow Fe^{2+} + SO_3^{\bullet-} \quad (14)$$

The authors used the response surface methodology to optimize the treatment of 100 mL of 10 μM of sulfamethoxazole by PS/Fe^{3+}/SO_3^{2-} with a stirred tank reactor. The best conditions were found with 83% of degradation with 2.0 mM PS, 0.50 mM Fe^{3+}, and 1.0 mM Na_2SO_3 at pH = 5.96 (see Table 1). Using methanol (scavenger of $SO_4^{\bullet-}$ and $^{\bullet}OH$) and TBA (scavenger of $^{\bullet}OH$), it was established a major action of $^{\bullet}OH$ over $SO_4^{\bullet-}$'as oxidant. Moreover, the LC-MS analysis of the optimized treated solution revealed the production of 8 aromatic, 4 heteroaromatic, and 2 aliphatic by-products.

It should be noted that homogeneous catalyst is not useful for antibiotic remediation in practice because the transition metallic ions added remain in the treated solution, needing an expensive post-treatment for their removal to water reuse. For this reason, heterogeneous catalysts easily separable from the aqueous matrix have been more extensively developed, representing a top research area for PS-based AOPs, as exposed in the next subsection.

3.1.2. *Heterogeneous catalysis*

The catalytic behavior of solid materials to activate PS depends on the composition and structure of their surfaces. According to these properties, they can be classified as biochar, modified biochar, carbonaceous materials, iron and iron compounds, non-ferrous metal oxides, and other catalysts. Table 1 collects some relevant examples for each of these materials.

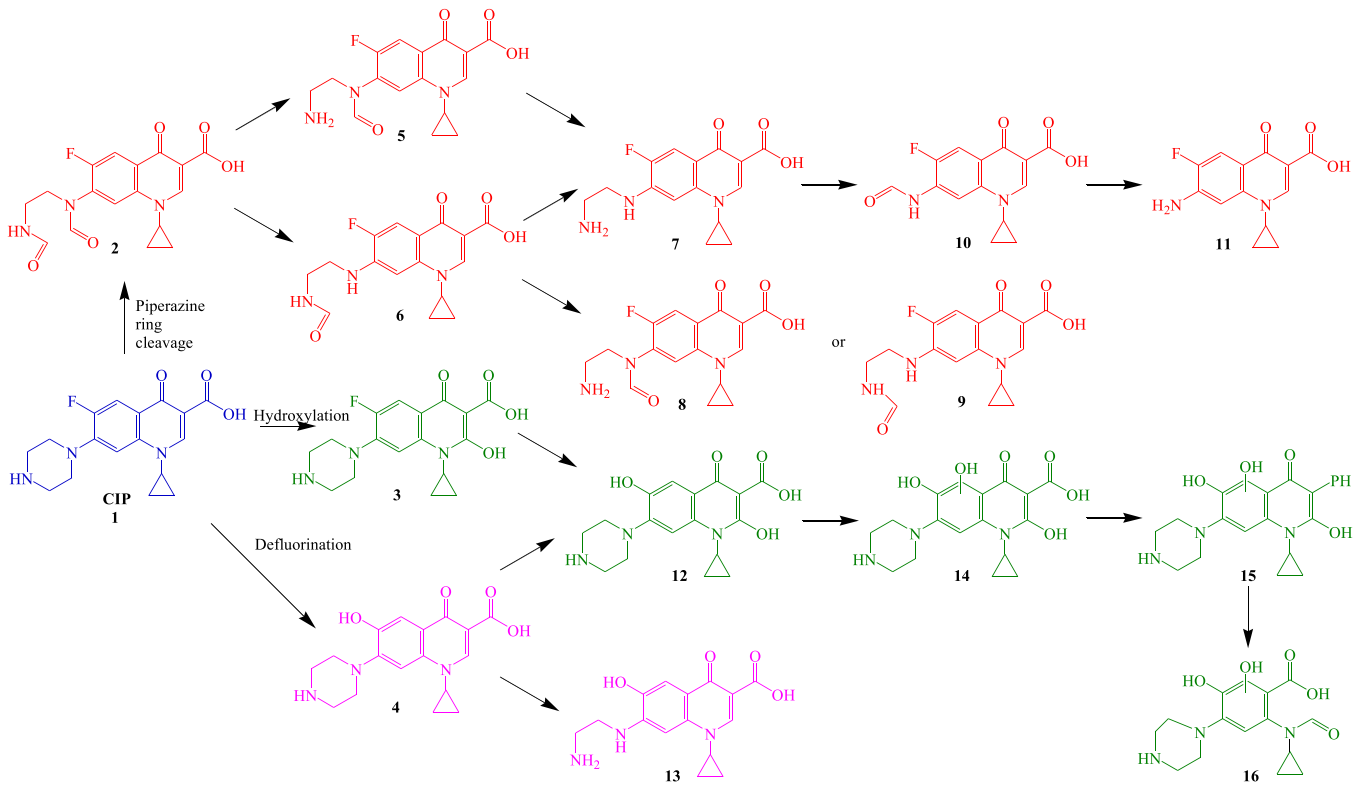

Fig. 4. Reaction sequence proposed for the initial degradation of ciprofloxacin by PS catalyzed with homogeneous Fe^{2+}. The main oxidizing agent was $^{\bullet}OH$ respect to $SO_4^{\bullet-}$.
Adapted from ref. [18] with permission 5644801130110 from Elsevier.

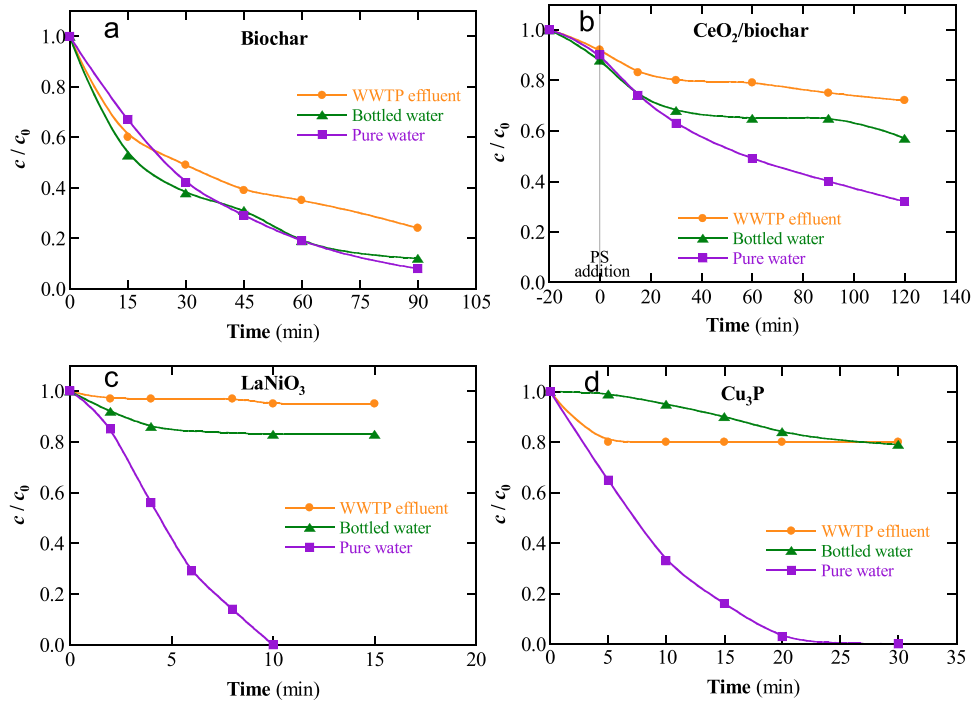

Fig. 5. Variation of normalized sulfamethoxazole concentration with time for the PS treatment with different catalysts in pure water, bottled water, and WWTP effluent at natural pH using a stirred tank reactor: (a) 250 mL of 250 μg L^{-1} antibiotic with 250 mg L^{-1} PS and 90 mg L^{-1} biochar catalyst. (b) 120 mL of 500 μg L^{-1} antibiotic with 200 mg L^{-1} PS and 90 mg L^{-1} CeO_2/biochar catalyst (c) 60 mL of 500 μg L^{-1} antibiotic with 100 mg L^{-1} PS and 250 mg L^{-1} $LaNiO_3$ catalyst. (d) 120 mL of 500 μg L^{-1} antibiotic with 100 mg L^{-1} PS and 40 mg L^{-1} Cu_3P catalyst.
(a) (adapted from ref. [28]) (b) (adapted from ref. [41]). (c) (adapted from ref. [72]). (d) (adapted from ref. [82]).

3.1.2.1. Biochar. The works using biochar as catalyst treated chlortetracycline [26], quinolones [27], sulfamethoxazole [28], tetracycline [29–33], and trimethoprim [34]. Biochar is a low-cost carbon-containing material that is thermally prepared from waste biomass in the absence of O_2. It presents a high porosity and an excellent adsorption of a wide array of organic pollutants, thus promoting waste valorization. Kemmou et al. [28] synthesized biochar by heating spent malt rootlets at 900 ºC. Scanning electron microscopy (SEM) images of the as-material revealed the presence of < 5% of minerals on its surface with an irregular distribution of inorganic oxides of Fe and Zn (< 0.01%), whereas its FTIR spectra showed the presence of surface -OH groups in phenolic structures that conferred positive or negative charges depending of pH (zero potential charge = 8.4). From these findings, they proposed the oxidation of surface -OH groups by PS to originate the oxidant $SO_4^{\bullet-}$ from reaction (15), producing the oxidant $^{\bullet}OH$ from reactions (5) or (6). Adsorbed organics were then degradeed by both oxidants onto the biochar surface.

$$\text{Biochar-OH} + S_2O_8^{2-} \rightarrow \text{Biochar-O}^{\bullet} + SO_4^{\bullet-} + HSO_4^- \quad (15)$$

The study was centered in the treatment of suspensions of 250 mL of 125–500 μg L^{-1} of sulfamethoxazole, up to 250 mg L^{-1} PS, and 90 mg L^{-1} of biochar catalyst in pure water at natural pH using a stirred tank reactor. The degradation of the antibiotic always obeyed a pseudo-first-order kinetics. It was quicker degraded at smaller antibiotic content due to the faster degradation of less organic matter with similar amounts of oxidants generated, as well as at higher PS dosage because of the greater production of oxidants. For 125 μg L^{-1} of antibiotic and 250 mg L^{-1} of PS, a 95% removal was found in 90 min with k_1 = 0.029 min^{-1} (see Table 1). Similar assays were performed with bottled water and a WWTP effluent, yielding lower removals of 82% and 80%, respectively, owing the scavenging effect of their components. This trend can be observed in Fig. 5a that shows the comparative normalized sulfamethoxazole content vs. time for the three aqueous matrices tested for 250 μg L^{-1} of antibiotic. Under these conditions, less antibiotic was removed (92%) from pure water in 90 min as compared to 95% for 125 μg L^{-1} due to its higher concentration. A negative influence on the abatement was also found by adding humic acid as NOM component in pure water.

It is interesting to remark the recent work of Kang et al. [33] who prepared a biochar with a very high Fe content (16.8%) from a sewage sludge. Using 1.0 g L^{-1} of this catalyst, 50 mL of 10 mg L^{-1} of tetracycline in pure water with 10 mM PS at pH = 5.0 in a stirred tank reactor were slowly degraded, achieving a 87% of antibiotic abatement in 180 min (see Table 1). Several scavengers were used to identify the generated oxidants, like methanol for $SO_4^{\bullet-}$ and $^{\bullet}OH$, TBA for $^{\bullet}OH$, *p*-benzoquinone (*p*-BQ) for superoxide radical ($O_2^{\bullet-}$), and furfuryl alcohol (FF) for singlet oxygen $^1O_2$. From the physical analysis of the biochar, it was established that Fe(II) was linked to -C-OH groups, so that, the resulting -C-O-Fe(II) bridge reduced PS via reaction (16) giving rise to $SO_4^{\bullet-}$ that evolved to $^{\bullet}OH$. The π electrons on the biochar layer then promoted the reduction of the -C-O-Fe(III) bridge to the -C-O-Fe(II) one. Apart from these oxidants, $O_2^{\bullet-}$ was proposed to be formed from hydrolysis of PS onto the biochar defects via reaction (17), whereas the oxidation of this radical, e.g., with $^{\bullet}OH$, originated $^1O_2$ from reaction (18). The existence of all these oxidizing agents was confirmed by EPR analysis of treated suspensions by adding DMPO and TEMP. In this way, two routes for tetracycline removal were envisaged, a radical mechanism involving the reactions with $SO_4^{\bullet-}$, $^{\bullet}OH$, and/or $O_2^{\bullet-}$ and a non-radical mechanism related to $^1O_2$, which can run in parallel or overlapped depending on the chemical nature of the intermediates formed. In this way, Grilla et al. [36] using a biochar from a spent malt rootlets showed the preponderance of the non-radical mechanism with $^1O_2$ for the degradation of trimethoprim from the stronger scavenging effect found with sodium azide for this species respect to methanol and TBA (see Table 1).

$$\text{-C-O-Fe(II)} + S_2O_8^{2-} \rightarrow \text{-C-O-Fe(III)} + SO_4^{\bullet-} + SO_4^{2-} \quad (16)$$

$$3S_2O_8^{2-} + 4\,H_2O \rightarrow 6SO_4^{2-} + 2\,O_2^{\bullet-} + 8\,H^+ \quad (17)$$

$$O_2^{\bullet-} + {}^{\bullet}OH \rightarrow {}^1O_2 + OH^- \quad (18)$$

Although biochar is an effective PS activator, its reusability in consecutive cycles needs to be studied to know its applicability at industrial level.

3.1.2.2. Modified biochar. Many composites of biochar coated with metals or their oxides have been used to remove antibiotics like cephalexin with Fe_2O_3/loofah biochar [35], doxycycline with Co/N-biochar [36], norfloxacin with CuO/Fe_3O_4/biochar [37], sulfadiazine [38] and sulfamethoxazole [39] with Fe/biochar, sulfamethoxazole with N,S, Co/biochar [40] and CeO_2/biochar [41], sulfapyridine with FeCu/-biochar [42], and tetracycline with Cu-Fe_3O_4/biochar [43], Cu-FeOOH/biochar [44], nanoscaled zero-valent iron (nZVI)/biochar [45], red mud/biochar [46], and N-Fe/biochar [47]. These composites enhanced the oxidation power of PS activated with biochar alone, promoting the non-radical mechanism.

Fig. 6 exemplifies the results obtained for treating 50 mL of 40 mg L^{-1} sulfadiazine in pure water with 1.5 mM PS and 1.0 g L^{-1} of Fe/biochar at pH = 5.2 using a tube test. Fig. 6a schematizes the different species present at the catalyst surface including Fe^0, iron oxides, and carboxylic acid and hydroxyl groups, which decompose PS to form $SO_4^{\bullet-}$, $^{\bullet}OH$, and $^1O_2$ as main oxidants. Note that soluble O_2 can be reduced to $O_2^{\bullet-}$ by Fe^0 that is oxidized to Fe^{2+}, and further, $O_2^{\bullet-}$ can react with $^{\bullet}OH$ to form $^1O_2$ from reaction (18).

Fig. 6b depicts that the PS/Fe/biochar process yielded 91% of sulfadiazine decay in 60 min with k_1 = 0.031 min^{-1} (see Table 1), generating much more oxidizing species than the corresponding PS/biochar one that only degraded 20% of the antibiotic. Moreover, it can be seen that the former PS treatment was much more potent than the analogous Fenton process with 1.5 mM H_2O_2 and 1.0 g L^{-1} Fe^{2+} giving 48% of sulfadiazine decay. Addition of 10 mM of inorganic anions instead of 1 mM inhibited more largely the PS/Fe/biochar degradation un the order HCO_3^- < PO_4^{3-} < Cl^- < SO_4^{2-}, as can be deduced from Fig. 6c by the corresponding lower k_1-value. This trend can be related to the loss of generated $SO_4^{\bullet-}$ and $^{\bullet}OH$ by reaction with the three first anions.

producing $CO_3^{\bullet-}$, $PO_4^{\bullet 2-}$, and $Cl^{\bullet}$, respectively. For SO_4^{2-}, its adsorption onto the catalyst blocked part of their active centers and caused lesser production of oxidants. The generation of $SO_4^{\bullet-}$, $^{\bullet}OH$, and $^1O_2$ was confirmed by specific scavengers as methanol, TBA, and FF. Fig. 6d makes evident the decay of k_1-value for these assays, and from these data, it was established a more oxidative role of $^{\bullet}OH$ than $SO_4^{\bullet-}$ and $^1O_2$. Despite the good results obtained for the PS/Fe/biochar process, the 3 consecutive treatments shown in Fig. 6e highlight a rapid loss of the degradation efficiency related to the solubilization of the Fe coating, indicating a low reusability for long-time experiments and making it not useful in practice.

Liang et al. [39] described two other non-radical mechanisms using Fe_3O_4/biochar catalysts synthesized at 400 and 700 ºC to treat 100 mL of 10 mg L^{-1} of sulfamethoxazole in pure water with 2.0 mM PS and 0.5 g L^{-1} catalyst at pH = 3.5 lasting 120 min. The best degradations were found for the catalyst prepared at 700 ºC, which yielded 82% of antibiotic decay with k_1 = 0.031 min^{-1}, as shown in Fig. 7a. The process was inhibited with ethanol addition (scavenger of $SO_4^{\bullet-}$ and $^{\bullet}OH$), but much largely using phenol (scavenger of radical and non-radical species). Fig. 7b makes evident that the degradation was quite similar in the pH range 3.5–9.0. Under these conditions, Fig. 7c depicts a decrease of the degradation in real waters in the sequence: pure water > lake water = seawater > piggery wastewater > landfill leachate, according to the larger presence of their scavenging constituents. From electrochemical and Raman spectroscopy studies, it was established the preferent oxidation of the adsorbed antibiotic onto the catalyst by direct

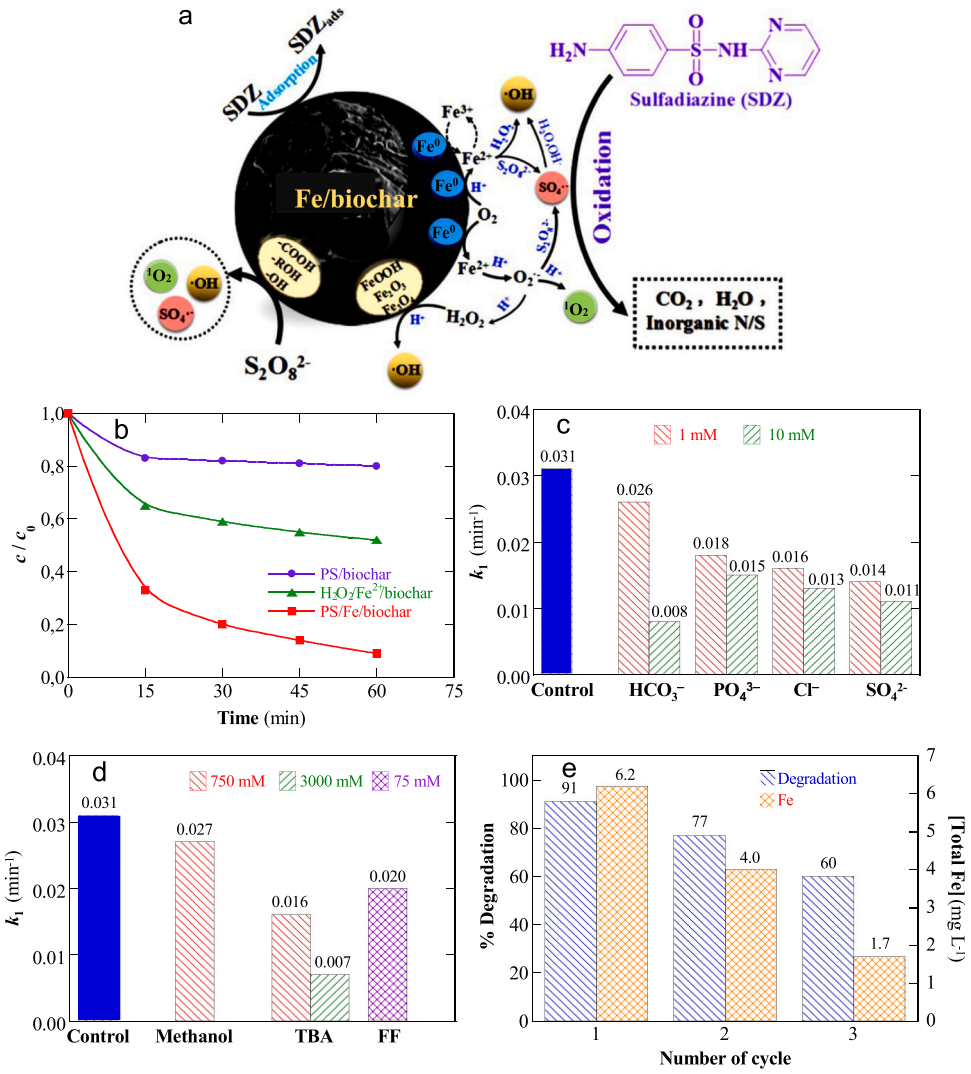

Fig. 6. (a) Mechanism proposed for the generation of oxidizing agents by a Fe/biochar catalyst for sulfadiazine (SDZ) removal. (b) Normalized sulfadiazine content vs. time for the degradation of 50 mL of 40 mg L^{-1} antibiotic with 1.5 mM of PS or H_2O_2 and 1.0 g L^{-1} of biochar, Fe/biochar or Fe^{2+} catalyst at pH = 5.2 using a test tube. (c) Effect of inorganic anions at 1 and 10 mM in the above PS/Fe/biochar process (control) over the pseudo-first-order rate constant for sulfadiazine decay. (d) Change of the pseudo-first-order rate constant for the Fe^{2+}/biochar process with scavengers like methanol, TBA, and furfuryl alcohol (FF). (e) Percentage of degradation and total Fe in suspensions for the same Fe^{2+}/biochar process in 3 successive cycles.
Adapted from ref. [38]. Mechanism (a) with permission 5644810424349 from Elsevier.

electron-transfer with surface PS as non-radical mechanism. For the catalyst prepared at 400 ºC, the authors determined that the main oxidant of organics was Fe(IV) formed from the two-electron transfer of surface Fe^{2+} to PS. This was confirmed from the capture of generated Fe (IV) by the quenching methylphenyl sulfoxide (PMSO) (see Fig. 7d) along with Mossbauer and in situ Raman spectroscopy analysis.

The results listed in Table 1 for modified biochar show the production of different oxidizing agents depending on the composite used. For cephalexin with Fe_2O_3/loofah biochar, it is explained that only both $SO_4^{\bullet-}$and $^{\bullet}OH$ acted as oxidants [35], whereas for tetracycline with Cu-FeOOH/biochar, it is specified the predominance of $SO_4^{\bullet-}$ as oxidant in acidic media and of $^{\bullet}OH$ in alkaline suspensions by the acceleration of reaction (6) [44]. The oxidation of sulfamethoxazole with $SO_4^{\bullet-}$, $^{\bullet}OH$, and $^1O_2$ has been described using CeO_2/biochar [41]. The predominance of the non-radical mechanism with $^1O_2$ over the radical mechanism with $SO_4^{\bullet-}$ and $^{\bullet}OH$ has been reported for CuO/Fe_3O_4/biochar [37] and N,S,Co/biochar [40]. It is noteworthy that operating under similar conditions, poorer performance was found with CeO_2/biochar than with biochar alone, as can be deduced from the comparison of Fig. 5a and b. Fig. 5b makes evident the adsorption of the antibiotic during 20 min before the PS addition. For both catalysts, the degradation in different aqueous matrices diminished in the order: pure water > bottled water > WWTP effluent, but it was much higher only using biochar. This means that the oxidation ability of a PS process is a function not only of the kind of oxidizing species generated, but also of their reactive concentration.

Finally, it is remarkable the low reusability determined for many modified biochars, except FeCu/biochar (see Table 1), due to the progressive loss of the metal coating. Better stable composites should be synthesized to show their possible usage in practice.

3.1.2.3. Carbonaceous materials. Treatments with other carbonaceous materials have been performed for aztreonam with g-C_3N_4 [48], metronidazole with activated carbon [49], sulfachloropyridazine with carbocatalytic activation [50], sulfamethoxazole with N-graphene/reduced graphene oxide (rGO)/carbon nanotubes (CNTs) membrane [51], N-carbon [52], and N-rGO [53], and tetracycline with S,N-carbon [54] and graphene/Fe@N-doped carbon [55].

Qian et al. [51] studied the PS process of 250 mL of 0.5 mg L^{-1} of sulfamethoxazole in pure water with a N-graphene/rGO/CNTs catalyst

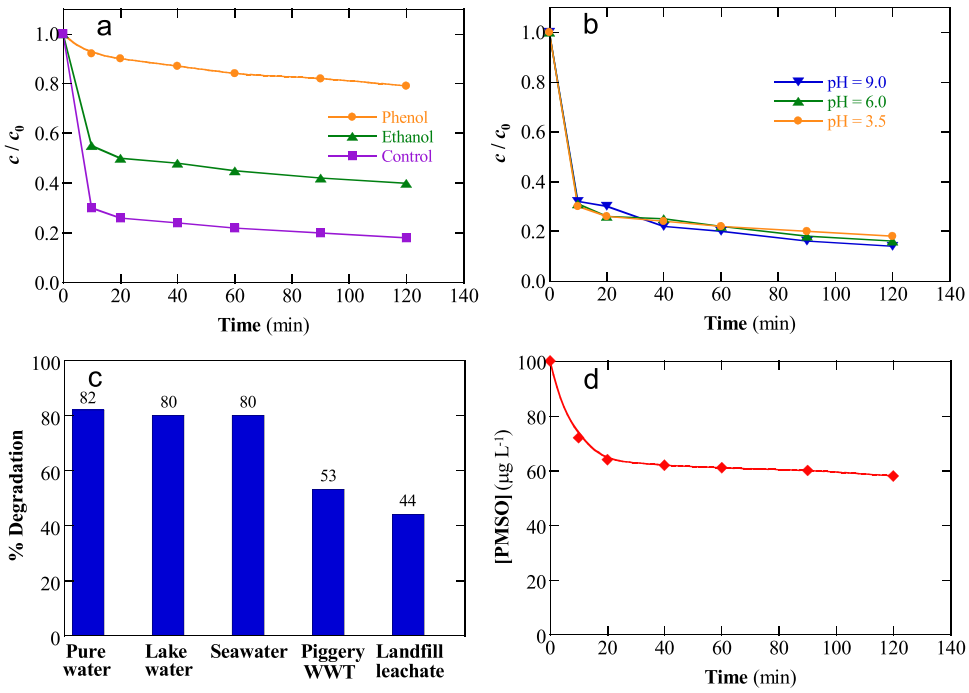

Fig. 7. (a) Effect of scavengers over the time course of the normalized sulfamethoxazole concentration of 100 mL of 10 mg L^{-1} of antibiotic in pure water treated with 2.0 mM PS, 0.5 g L^{-1} of Fe/biochar catalyst pyrolyzed at 700 °C, 2 M ethanol, and 0.04 M phenol at pH = 3.5 and 25 °C using a stirred tank reactor. (b) Effect of pH on the normalized antibiotic decay. (c) Percentage of sulfamethoxazole degradation in several aqueous matrices upon the same conditions at pH = 3.5. (d) Change of 100 μM methyl phenyl sulfoxide (PMSO) content with time with 2.0 mM PS and 0.5 g L^{-1} of Fe/biochar catalyst synthesized at 400 °C and at pH = 3.5. Adapted from ref. [39].

at pH between 5.0 and 10.0 using a flow system with filtration at liquid flow rate of 1.0 mL min^{-1}. After 100 min of treatment with 8 g m^{-2} of carbon loading and 5.0 mM PS at neutral pH = 7.0, an excellent loss of 94% of the antibiotic was determined, with a good reproducibility after 3 successive runs (see Table 1). However, the authors did not identify the oxidants generated and only reported a strong inhibition in the presence of Cl^- and fulvic acid, as expected by their competitive consumption of oxidants removing less amount of sulfamethoxazole.

It is remarkable the work of Huo et al. [54] who used a stirred tank reactor to treat a suspension of 250 mL of 0.02 mM of tetracycline in pure water with 2.0 mM PS and 0.4 g L^{-1} of S,N-carbon catalyst synthesized at 800 °C at pH = 3.0 (see Table 1). Fig. 8a shows the two non-radical mechanisms proposed as dominant for the antibiotic removal. It is established that the S and N doping create catalytic points for: (i) the mediated electron transfer of tetracycline (TC) to PS that is decomposed to SO_4^{2-} and (ii) the strong binding ability of defects to form reactive PS complexes that generate $^1O_2$. The existence of these processes was evidenced from scavengers. Fig. 8b depicts that the above tetracycline concentration was reduced by 81% under the conditions tested in 60 min, which was slightly inhibited in the presence of ethanol (scavenger of $SO_4^{\bullet-}$ and $^\bullet OH$) but at much larger extent by adding sodium azide and β-carotene, both scavengers of $^1O_2$. Additionally, the $^1O_2$ production was confirmed by bubbling O_2 up to saturation because the degradation raised up to 90% (see Fig. 8b) due to the formation of $O_2^{\bullet-}$ that is then oxidized to $^1O_2$ via reaction (18). Fig. 8c makes evident that the maximum degradation and TOC removal were reached in pure water, being the process less efficient in real waters in the sequence: river water > lake water > raining water, by the scavenging effect of their components. On the other hand, the authors also identified 11 aromatic, 1 cyclic, and 3 aliphatic by-products by LC-MS. Fig. 9 presents the reaction sequence of the degradation/mineralization of TC (**1**) proposed from such derivatives assuming the above two non-radical mechanisms. The process is initiated by 3 parallel routes of **1**: (i) its hydroxylation to **2**; (ii) its N-demethylation to **3**; and (iii) its dehydration to **4**. The ring opening of **2** yields **5**, which is further oxidized to a mixture of **6** and **7**. The ring opening of **3** leads to **8**, followed by oxidation to form **9**. The N-demethylation of **4** and subsequent ring opening give **10** and **11**, respectively, being the latter further oxidized to **12**. Finally, the intermediates **7**, **8**, and **12** are oxidized to produce the cyclic compound **13** and the aliphatic by-products **14-16**, which can be further mineralized to CO_2 and H_2O.

Carbonaceous materials doped with non-metals are very effective to activate PS and present good reproducibility. This research area should be more explored in the future.

3.1.2.4. Iron and iron compounds. Using iron and iron compounds, the remediation of aqueous suspensions of amoxicillin with Fe_3O_4/GO [56], chloramphenicol with α-FeOOH [57] and nZVI and S-nZVI [58], erythromycin with iron powder-H_2O_2 [59], levofloxacin and oxytetracycline with Fe/Mn [60], sulfadimethoxine with ZVI [61], sulfamethoxazole with nZVI [62], S-nZVI [63], and Fe_3O_4 [64], and tetracycline with γ-Fe_2O_3/CeO_2 [65], ferrocene/chitosan/Fe_3O_4 [66], Fe,Co,O-g-C_3N_4 [67], FeS [68], and $FeSe_2$-based [69], has been studied.

Wu et al. [58] studied the surface structure of nZVI and S-nZVI to explain their catalytic activation over PS. From XPS spectroscopy, surface Fe(II) ($\equiv Fe^{2+}$) as FeOOH and surface Fe(III) ($\equiv Fe^{3+}$) as Fe_2O_3 were found onto nZVI, whereas Fe^0 and FeS were pre-eminently present onto the sulfurized nZVI. PS can then react with surface Fe(II) to form $SO_4^{\bullet-}$ by reaction (19) and Fe^0 can be oxidized or decompose PS to soluble Fe^{2+} and $^\bullet OH$ from reactions (20) or (21), respectively. Moreover, the soluble Fe^{2+} can activate PS to $SO_4^{\bullet-}$ via reaction (1), which can be partially transformed into $^\bullet OH$ by reactions (5) or (6).

$$\equiv Fe^{2+} + S_2O_8^{2-} \rightarrow \equiv Fe^{3+} + SO_4^{\bullet-} + SO_4^{2-} \quad (19)$$

$$Fe^0 + O_2 + 2\,H^+ \rightarrow Fe^{2+} + {}^\bullet OH + OH^- \quad (20)$$

$$Fe^0 + S_2O_8^{2-} + 2\,H_2O \rightarrow Fe^{2+} + 2{}^\bullet OH + 2SO_4^{2-} + 2\,H^+ \quad (21)$$

These authors used a tank reactor in a rotary oscillating water bath

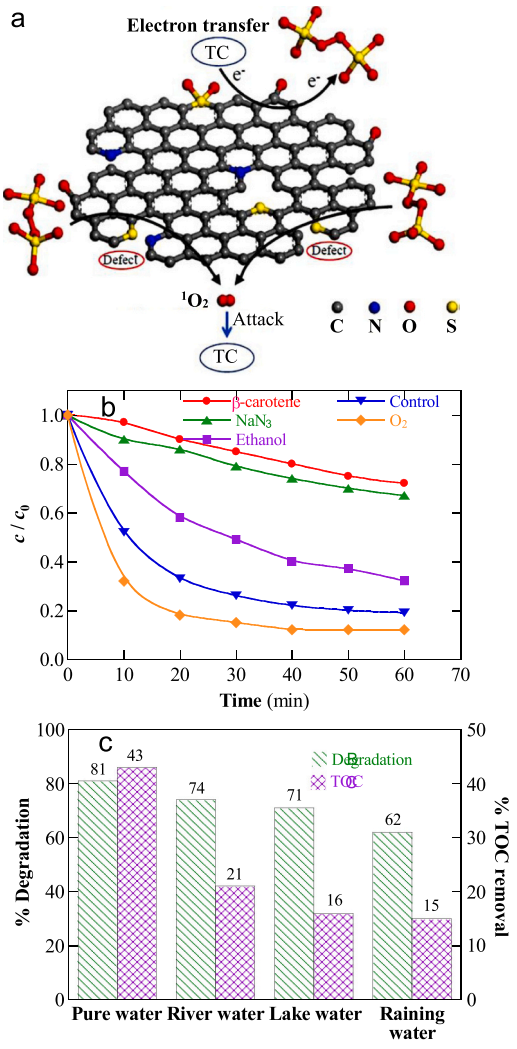

Fig. 8. (a) Non-radical mechanisms proposed for the degradation of tetracycline by PS with a S,N-carbon catalyst. (b) Effect of scavengers and O_2 bubbling over the normalized antibiotic concentration with time for the treatment of 250 mL of 0.02 mM tetracycline in pure water with 2.0 mM PS, 0.4 g L^{-1} of S, N-carbon catalyst synthesized at 700 °C, 1 M ethanol, 10 mM sodium azide, and 20 mg L^{-1} β-carotene at pH = 3.0 and 25 °C using a stirred tank reactor, (c) Percentages of degradation and TOC removal after 60 min of the PS processes in several aqueous matrices upon the above conditions.
Adapted from ref. [54]. Fig. 8a with permission 5644810982649 from Elsevier.

for treating 100 mL of 20 mg L^{-1} of chloramphenicol in pure water with 1.0–10 mM PS and 0.05–0.3 g L^{-1} of nZVI or S-nZVI catalyst at pH = 3.1–9.1 for 30 min. For 3.0 mM PS and 0.1 g L^{-1} S-nZVI catalyst at pH = 6.9, a fast total degradation was determined with $k_1 = 0.2115$ min^{-1} (see Table 1). This process was quicker than using nZVI that only yielded 95% removal, which was ascribed to the larger production of more oxidants from the faster rate of reaction (20) than (19), i.e., yielding more Fe^{2+} and $^{\bullet}OH$ from Fe^0 oxidation because of its higher content onto the S-nZVI surface. For this catalyst, Fig. 10a depicts greater antibiotic decay with raising the PS content from 1.0 to 3.0 mM due to its larger decomposition from reactions (1), (5), and (20) to form the oxidants $SO_4^{\bullet-}$ and $^{\bullet}OH$. A slightly higher degradation can be observed for 10 mM PS since the excess the oxidizing species is consumed by parasitic reactions like (2)-(4) and (7)-(9). A little enhancement can also be seen in Fig. 10b with increasing the S-nZVI dosage from 0.05 to 0.3 g L^{-1} and decreasing the pH from 9.1 to 3.1. While the former effect can be related to the fast acceleration of parasitic reactions that inhibit the action of more catalyst, the change of the slow reaction (21) in alkaline medium.

by the faster reaction (20) in acidic one can explain the latter effect. The scavenging effect of 1–100 mM of several inorganic ions is presented in Fig. 10c, being much stronger with CO_3^{2-} than with Cl^- and SO_4^{2-}. Under these conditions, the use of scavengers like ethanol and TBA allowed determining the percent of oxidants generated, as shown in Fig. 10d. As can be seen, $SO_4^{\bullet-}$ dominated on $^{\bullet}OH$ for both PS/nZVI and PS/S-nZVI processes at pH = 6.9 in the absence of added anions, whereas the percent of the latter radical was more strongly inhibited at higher anion concentration indicating a quicker reaction of $^{\bullet}OH$ with such species. Finally, 18 aromatic by-products were identified by LC-MS, but no consecutive runs were made to assess the reusability of the S-nZVI catalyst, as needed to show its feasible applicability in practice.

Table 1 summarizes the excellent results obtained for the degradation of tetracycline in pure water with several PS processes activated with iron and iron compounds [65–68]. It is noticeable the article of Wu et al. [67] that reported the remediation of 100 mL of 5–25 mg L^{-1} of antibiotic in pure water by adding 1.0–3.0 g L^{-1} of PS and 0.2–0.8 g L^{-1} of Fe,Co,O-g-C_3N_4 catalyst at pH = 3.0–11.0 and 40 °C lasting 120 min with a stirred tank reactor. The surface of this catalyst contained Fe (II)/Co(II) species linked to O that can be oxidized to Fe(III)/Co(III) ones by PS to yield $SO_4^{\bullet-}$ in heterogeneous reactions similar to (19). $^{\bullet}OH$ was further generated from reactions (5) or (6), as well as $O_2^{\bullet-}$ from reaction (17) and $^1O_2$ from reaction (18). The generation of all these oxidants caused a faster decay at lower tetracycline content and pH, and higher PS and catalyst dosages, by the reasons pointed out above. Up to 90% abatement with $k_1 = 0.026$ min^{-1} was obtained for 15 mg L^{-1} antibiotic with 2.5 g L^{-1} PS and 0.6 g L^{-1} catalyst at the best pH = 3.0 (see Table 1). Fig. 11a shows the increasing k_1-value obtained for different processes at pH = 5.0 with raising the content of generated oxidants, which is maximal for the Fe,Co,O-g-C_3N_4. Fig. 11b depicts the gradual decrease of k_1 when pH grew from 3.0 to 11.0, as expected by the progressive loss of $SO_4^{\bullet-}$ concentration as reaction (5) is being replaced by reaction (6). The influence of several scavengers on the PS/ Fe,Co, O-g-C_3N_4 treatment at pH = 3.0 is presented in.

Fig. 11c, revealing that $O_2^{\bullet-}$ scavenged by *p*-BQ is the main oxidant, followed by $^1O_2$ scavenged by FF and being less significant $SO_4^{\bullet-}$ and $^{\bullet}OH$ scavenged by methanol and TBA. The production of these 4 oxidants was confirmed by the EPR spectra of their adducts with DMPO or TEMP shown in Fig. 11d-f. Several real waters were mineralized with this process as well and it was found a decreasing TOC reduction in 120 min as: pure water (68%) > river water (34%) > tap water (19%) > WWTP effluent (6.9%), according to the increasing loss of oxidants from their.

scavenging agents (inorganic anions and NOM, preferentially). However, a moderate reusability was determined after 5 successive steps in pure water, suggesting the need of a deeper assessment of the Fe,Co, O- g-C_3N_4 treatments in real waters to know their possible practical application. This should also be assessed for each iron and iron compound used due to the easy removal of iron ions, mainly in acidic conditions, inducing their loss of reproducibility and the poisoning of the medium.

3.1.2.5. Non-ferrous metal oxides. Suspensions with non-ferrous metal oxides have been applied to degrade amoxicillin, cephalexin, ofloxacin, and sulfamethoxazole with CuO [70], ciprofloxacin with NiO/Mg-Al layered double hydroxide [71], sulfamethoxazole with $LaNiO_3$ [72] and $La_{0.8}Sr_{0.2}CoO_3$-δ [73], and tetracycline with $ZrO_2/MnFe_2O_4$ [74] and mesoporous ordered MnO_x [75].

Good performance can be seen in Table 1 for these treatments in pure water showing the generation of $SO_4^{\bullet-}$ and $^{\bullet}OH$ and in some cases $O_2^{\bullet-}$ as well as an excellent reusability for $LaNiO_3$ [72] and MnO_x [75]. Petala et al. [72] reported the larger effectiveness of $LaNiO_3$ to activate PS than other catalysts. They examined the behavior of 60 mL of 0.25–1.0 mg L^{-1} of sulfamethoxazole in pure water with 0.05–0.1 g L^{-1} PS and 25–250 mg L^{-1} catalyst at pH = 6.0 using a stirred tank reactor.

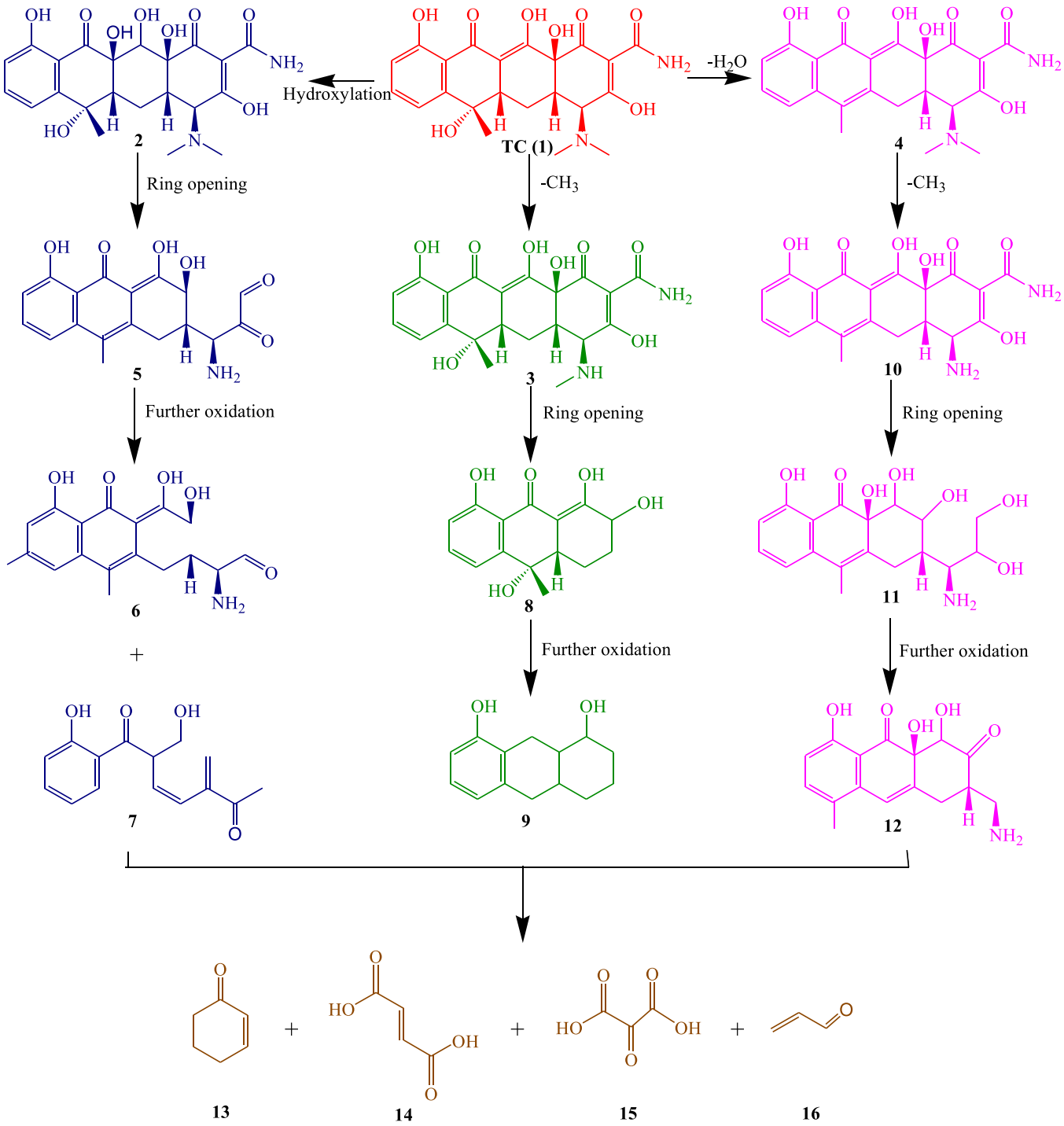

Fig. 9. Reaction pathway for the degradation/mineralization of tetracycline (TC, 1) by PS with a S,N-carbon catalyst. The oxidation mainly occurred through non-radical mechanisms involving $^1O_2$ and mediated electron transfer between TC and PS at the carbon surface.
Adapted from [54] with permission 5644810982649 from Elsevier.

As expected, higher PS and catalyst dosages enhanced more largely the antibiotic removal at its lower concentration. Fig. 5c shows that overall abatement was rapidly attained in only 10 min with $k_1 = 0.2267$ min^{-1} for 0.5 mg L^{-1} of sulfamethoxazole with 0.1 g L^{-1} PS and 250 mg L^{-1} catalyst. This process was much faster than that found by the same group using biochar (see Fig. 5a), CeO_2/biochar (see Fig. 5b), and Cu_3P (see Fig. 5d) under similar conditions. Unfortunately, the removal with $LaNiO_3$ catalyst was strongly inhibited in bottled water and WWTP effluent (see Fig. 5c), a fact that was attributed to the presence of HCO_3^- and NOM in the real aqueous matrix. Despite the very efficient degradation determined in pure water, the $LaNiO_3$ catalyst does not seem useful for the treatment of real waters and wastewaters, being preferable the simple use of biochar, as can be seen in Fig. 5a.

3.1.2.6. Other catalysts. Other catalysts used for PS activation considered the degradation of chloramphenicol with Al-MIL [76], ciprofloxacin with zero-valent Al [77], norfloxacin with C-$ZnFe_2O_4$ [78], oxytetracycline with V_2O_5/rGO/Pt [79], sulfachloropyridazine with Ni/N-graphene [80], sulfamethazine with 4 commercial tourmalines [81], sulfamethoxazole with Cu_3P [82] and red mud [83], and

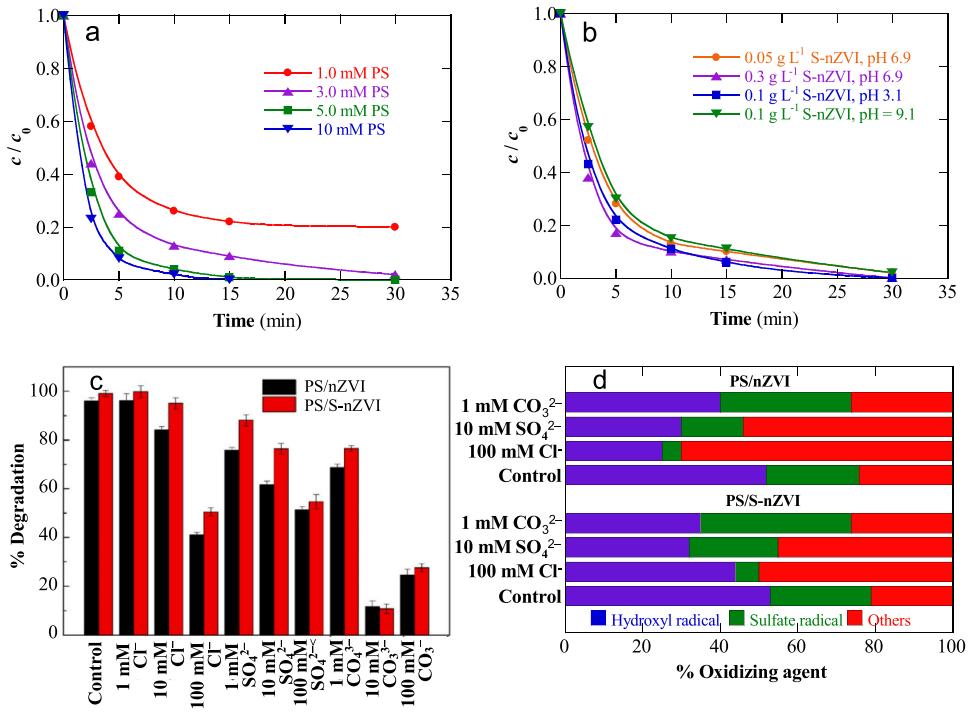

Fig. 10. (a) Effect of PS concentration on the normalized chloramphenicol concentration with time for 100 mL of 20 mg L^{-1} of antibiotic in pure water with 0.1 g S-nZVI catalyst at pH = 6.9 and 20 °C using a tank reactor in a rotary oscillating water bath at 250 rpm. (b) Influence of S-nZVI dosage and pH in the above assays. (c) Percentage of degradation after 30 min of the PS/nZVI and PS/S-nZVI processes made with 0.1 g S-nZVI of each catalyst at pH = 6.9, alone and in the presence of various inorganic anions concentrations. (d) Percentage of oxidizing agent detected in the above assays. Adapted from ref. [58].

tetracycline with Cu-doped C/SiO_2 nanofibrous membranes [84].

An aluminum-based metal organic framework (Al-MIL) was applied to remove chloramphenicol by activating PS [76]. The assays were made with a tank reactor in an ultrasonic bath filled with 50 mL of 0.25 mM of antibiotic in pure water containing 10 mM PS and 0.25 g L^{-1} catalyst at pH = 4.1–10.8 and 28–50 °C lasting 120 min. It was found a good 71% TOC abatement at pH = 5.3 and 40 °C. being $^{\bullet}OH$ the predominant oxidant, as determined by using ethanol and TBA as scavengers (see Table 1). The drawback of using this catalyst was its moderate reusability after 5 consecutive cycles with 11% TOC reduction. Jiao et al. [81] used 4 commercial tourmalines for the degradation of sulfamethazine with PS. Tourmaline is a mesoporous silicate mineral with BO_3 and metallic ions like Fe^{2+}, Fe^{3+}, and Al^{3+}, and can activate PS producing $^{\bullet}OH$, $SO_4^{\bullet-}$, $^1O_2$, and holes, as detected from scavengers (see Table 1). The best tourmaline catalyst of PS presented a good oxidation ability yielding total antibiotic degradation in 120 min at pH = 2.0 and 150 min at pH = 5.0 for the treatment of 100 mL of 5.0 mg L^{-1} of antibiotic in pure water with 4.0 mM PS and 5.0 g L^{-1} catalyst. Alexopoulou et al. [82] degraded 120 mL of 0.5–4.1 mg L^{-1} of sulfamethoxazole in pure water, bottled water, and WWTP effluent by adding 0.05–1.0 g L^{-1} of PS and 20–80 mg L^{-1} of Cu_3P catalyst at natural pH. Fig. 5d shows the fast removal obtained for 0.5 mg L^{-1} of the antibiotic in pure water with 0.1 g L^{-1} PS and 40 mg L^{-1} catalyst, with total disappearance in 15 min with $k_1 = 0.226$ min^{-1}. However, the process decayed for bottled water with $k_1 = 0.027$ min^{-1}.and for WWTP effluent with $k_1 = 0.017$ min^{-1} (see Table 1), meaning that the catalyst cannot be applied to the treatment of real waters and wastewaters. The use of scavengers revealed the predominance of $SO_4^{\bullet-}$ as oxidant.

3.2. UVC activation

The remediation of antibiotic solutions with UVC/PS has been explored for amoxicillin [85], cefixime [86], ceftriaxone [87], cephalexin, norfloxacin, and ofloxacin [88], chloramphenicol [89,90], ciprofloxacin [91–94], erythromycin [95], florfenicol [96], β-lactams [97], levofloxacin and ofloxacin [98], oxytetracycline [99], sulfamethoxazole [100], sulfadiazine, sulfamerazine, sulfamethoxazole, and sulfathiazole [101], sulfaquinoxaline [102], tetracycline [103], tylosin [104], and a mixture of antibiotics [105]. Other authors irradiated with sunlight to degrade azithromycin [106] and sulfamethoxazole [107]. However, no techno-economical studies were made in these works to show the possible beneficial of this process respect to other conventional treatments for the remediation of waters and wastewaters contaminated with antibiotics.

Table 2 summarizes the most relevant results reported for this treatment, where PS was energetically activated under UVC light for λ < 280 nm from reaction (22) to be homolytically dissociated into $SO_4^{\bullet-}$ [87,92]. This radical can then evolve to $^{\bullet}OH$ from reactions (5) or (6).

$$S_2O_8^{2-} + h\nu \rightarrow 2SO_4^{\bullet-} \quad (22)$$

In some works, the PS/UVC process has been compared with UVC/ClO^- and UVC/H_2O_2 ones where oxidants such as $Cl^{\bullet}$ and $^{\bullet}OH$ are formed as follows [87,92]:

Kattel et al. [85] studied the degradation of 1 L of 40 μM of amoxicillin in several waters at natural pH with 40–800 μM PS using a stirred cylindrical photoreactor upon a 11 W UVC light. The antibiotic abatement increased with raising PS dosage due to the progressive generation of more oxidants. For 400 μM PS, the k_1 for degradation and the percent of TOC removal decreased with the matrix tested in the order: pure water > groundwater > WWTP effluent > drinking water, according to the increasing scavenging of their components (see Table 2). The addition of scavengers (ethanol and TBA) to the solution in pure water revealed that $SO_4^{\bullet-}$. dominated over $^{\bullet}OH$ as oxidant. Moreover, 6 aromatic by-products were identified by LC-MS. In the case of cefixime, a good 72% loss of 20 mg L^{-1} of the antibiotic in 500 mL of pure water with 800 mg L^{-1} PS at pH = 3.0 and 70 °C was found in 60 min using a

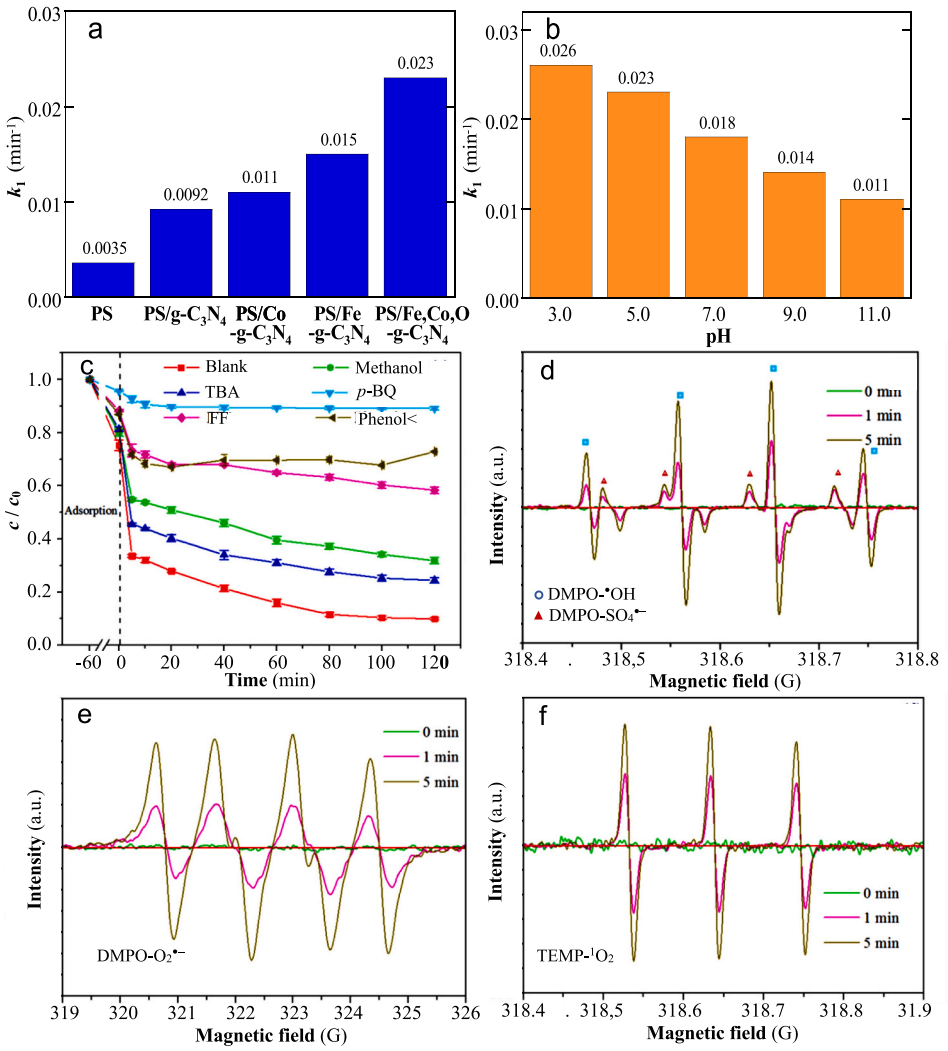

Fig. 11. (a) Pseudo-first-order rate constant for tetracycline decay obtained for PS processes of 100 mL of 15 mg L^{-1} antibiotic with 2.5 g L^{-1} PS and 0.6 g L^{-1} of each catalyst at pH = 5.0 and 40 °C using a stirred tank reactor. (b) Effect of pH on the pseudo-first-order rate constant for the PS/Fe,Co,O-g-C_3N_4 process. (c) Influence of several scavengers like methanol, TBA, FF, *p*-benzoquinone (*p*-BQ), and phenol over the pseudo-first-order rate constant for the PS/Fe,Co,O-g-C_3N_4 process. EPR spectra for: (d) DMPO-$^{\bullet}$OH and DMPO-$SO_4^{\bullet-}$, (e) DMPO-$O_2^{\bullet-}$, and (f) TEMP-$^1O_2$.
Adapted from ref. [67]. Fig. 11c, d, e, and f with permission 5644821296395 from Elsevier.

stirred tank photoreactor with a 16 W UVC light [86] (see Table 2). Better results have been reported for 400 mL of 33 μM ceftriaxone in pure water with 3.0 mM PS filling a flow-through photoreactor with a 23 W KrCl excilamp of λ = 222 nm, where total abatement with k_1 = 0.3791 min^{-1} was achieved in 20 min and 83% TOC reduction was obtained in 60 min [87] (see Table 2). The presence of less organic load with 16.5 μM antibiotic yielded 98% mineralization with only 0.5 mM PS. Similar performance was obtained with tap water because surprisingly, anions like Cl^-, NO_3^-, SO_4^{2-}, and HCO_3^- slightly accelerated the degradation process. It is noticeable that the authors showed a better performance for UVC/PS than UVC/H_2O_2. In the latter case, 33 μM of antibiotic were degraded with 3.0 mM H_2O_2 giving a lower k_1 = 0.0599 min^{-1} and less mineralization, only 23%, in 60 min

Fig. 12a shows the scheme of the flow set-up with two connected stirred photoreactors containing 4.9 W UVC lamp each that was used by Ghauch et al. [90] for the treatment of 600 mL of 31 μM of chloramphenicol (CAP) in pure water with 0.25–5.0 mM PS at pH = 4.0–11.0 at 20 °C lasting 60 min. It was found that the CAP degradation was enhanced with increasing the UVC.

fluence due to the acceleration of reaction (22). Fig. 12b highlights that at natural pH and UVC fluence of 330 J, 85% of antibiotic abatement was reached from 1.0 mM PS, whereas 70% mineralization was attained for 5.0 mM PS. Better performance was obtained for pH = 9.0 with overall abatement with k_1 = 0.038 min^{-1} for 0.25 mM PS, as can be seen in Fig. 12c. Fig. 12d shows the high impact of direct UVC over CAP removal with 52% degradation in 60 min, which was largely overpassed by adding 1.0 mM PS. This process was strongly decelerated by adding 400 mM methanol, at much larger extent than 400 mM TBA, indicating the preferential oxidation with $SO_4^{\bullet-}$ over $^{\bullet}$OH in the UVC/PS treatment (see Table 2). Addition of common anions yielded a positive effect on degradation at small contents, but a high inhibition was found at higher contents. The presence of humic and fulvic acids as NOM components also decelerated the CAP loss. This behavior justifies the degradation decay in different matrices in the sequence: pure water > river water> WWTP effluent. The LC-MS analysis of treated solution revealed the formation of 9 primary aromatic by-products.

An interesting work of Yang et al. [92] used the stirred cylindrical photoreactor with an inner 10 W UVC lamp schematized in Fig. 13a to comparatively treat 1 L of 1 μM of ciprofloxacin in tap water and reclaimed water with 1.0 mM PS at pH = 7.4 by several UVC methods. Fig. 13b makes evident that in both aqueous waters the k_1-value for antibiotic removal decreased as: UV/PS > UV/ClO^- > UV/H_2O_2.

Table 2
Selected results obtained for the degradation of antibiotics from different aqueous matrices by UVC and photocatalytic activation of persulfate.

Antibiotic	System	Experimental remarks	Best results	Ref.
UVC activation				
Amoxicillin	Stirred cylindrical photoreactor with a 11 W UVC lamp	1 L of 40 μM of antibiotic in pure water, drinking water, groundwater, and WWTP effluent, 40–800 μM PS, natural pH (7.4–8.1), effect of scavengers (ethanol and TBA), 22 °C, 120 min	Faster degradation at higher PS dosage. For 400 μM PS, k_1 (min^{-1}) for degradation and % TOC removal: pure water (0.216, 63) > groundwater (0.132, 50) > WWTP effluent (0.123, 14) > drinking water (0.119, 18). $SO_4^{\bullet-}$. dominated over $^{\bullet}OH$. 6 aromatic by-products identified by LC-MS	[85]
Cefixime	Stirred tank photoreactor with a 16 W UVC lamp	500 mL of 5–30 mg L^{-1} of antibiotic in pure water, 200–1000 mg L^{-1} PS, pH = 3.0–11.0, effect of anions (Cl^-, and HCO_3^-) and humic acid, 40–70 °C, 60 min	Better removal of 72% for 20 mg L^{-1} of antibiotic, 800 mg L^{-1} PS, pH = 3.0, and 70 °C. Inhibitory effect of inorganic anions and humic acid	[86]
Ceftriaxone	Flow-through photoreactor with a 23 W KrCl excilamp (λ = 222 nm)	400 mL of 16.5–66 μM of antibiotic in pure water and tap water, 0–3.0 mM PS, pH = 5.6, effect of anions (Cl^-, NO_3^-, SO_4^{2-}, and HCO_3^-), room temperature, 60 min	In pure water, for 33 μM antibiotic and 3.0 mM PS, overall abatement with k_1 = 0.3791 min^{-1} in 20 min and 83% TOC reduction in 60 min, whereas 98% mineralization was attained for 16.5 μM antibiotic and 0.5 mM PS. Similar performance with tap water. All the anions slightly accelerated the degradation process. Using 33 μM antibiotic and 3.0 mM H_2O_2, lower k_1 = 0.0599 min^{-1} and 23% mineralization	[87]
Chloramphenicol	Two connected flow stirred photoreactors with 4.9 W UVC lamp each	600 mL of 31 μM of antibiotic in pure water and real waters, 0.25–5.0 mM PS, pH = 4.0–11.0, effect of scavengers (methanol and TBA), anions (Cl^-, NO_3^-, NO_2^-, SO_4^{2-}, and HCO_3^-), and humic and fulvic acids, 20 °C, 60 min	Increasing degradation and TOC decay at higher UVC fluence and PS dosage at pH = 9.0. Total degradation with k_1 = 0.038 min^{-1} for 0.25 mM PS at this pH. Lower abatement with river water > WWTP effluent. Positive effect for small anions contents, but inhibition at higher contents and with humic and fulvic acids. Predominance of $SO_4^{\bullet-}$ over $^{\bullet}OH$. Detection of 9 aromatic by-products by LC-MS	[90]
Ciprofloxacin	Stirred cylindrical photoreactor with a 10 W UVC lamp	1 L of 1 μM of antibiotic in tap water and reclaimed water, 1.0 mM PS, pH = 7.4, effect of anions (Cl^- and HCO_3^-) and humic acid, 25 °C, 12 min	In tap water, complete degradation in 1 min with k_1 = 6.31 min^{-1}. Slower removal with UV/ClO^- (k_1 = 5.71 min^{-1}) > UV/H_2O_2 (k_1 = 1.38 min^{-1}) with the same oxidant dosage. Slower abatement with inorganic anions, enhanced with humic acid. For reclaimed water under the same conditions, total degradation in 8 min with k_1 = 0.7012 min^{-1} and E_{EO}[a] = 0.76 kWh m^{-3} $order^{-1}$	[92]
Erythromycin	Stirred cylindrical photoreactor with a 9 W UVC lamp	600 mL of 100 μg L^{-1} of antibiotic in pure water, bottled water, and WWTP effluent, 0–50 mg L^{-1} PS, pH = 3.0–8.0, effect of scavengers (ethanol and TBA) and humic acid, 22 °C, 90 min	Larger antibiotic removal with increasing PS dosage and pH. For 10 mg L^{-1} PS at pH = 8.0, total degradation (min) and k_1 (min^{-1}): pure water (30, 0.55) > bottled water (60, 0.26) > 10 mg L^{-1} humic acid solution (90, 0.06) > WWTP effluent (90, 0.03). Predominance of $SO_4^{\bullet-}$ (63%) over $^{\bullet}OH$ (37%). 9 transformation by-products detected by LC-MS	[95]
Florfenicol	Two parallel stirred dishes photoreactor submitted to a 75 W UVC light	20 μM of antibiotic in pure water and real waters, 2.0 mM PS, pH = 6.8, effect of anions (Cl^-, NO_3^-, and HCO_3^-) and humic acid, room temperature, 60 min	Overall removal with k_1 = 0.0561 min^{-1}, E_{EO} = 415.58 kWh m^{-3} $order^{-1}$, and 22.3% TOC decay. Using 2.0 mM H_2O_2, 0.0325 min^{-1}, 886.15 kWh m^{-3} $order^{-1}$, and 5.6%, respectively. Inhibition with humic acid and HCO_3^- > NO_3^- > Cl^-. Degradation decayed with river waters < WWTP effluent. $SO_4^{\bullet-}$ and $^{\bullet}OH$ as oxidants	[96]
Levofloxacin Ofloxacin	Stirred cylindrical photoreactor with a 25 W UVC lamp	50 mL of 5.0 mg L^{-1} of each antibiotic in pure water, 50–300 μM PS or H_2O_2, pH = 3.0–11.0, effect of scavengers (ethanol, TBA, and sodium azide), anions (Cl^-, SO_4^{2-}, and HCO_3^-), and NOM, 25 °C, 30 min	Faster decay of both antibiotics with greater amount of each oxidant and smaller pH. Total degradation achieved with all systems at pH = 3.0, more rapidly for levofloxacin. Negative effect of all anions and NOM. TOC decay near 35% for ofloxacin and 50% for levofloxacin with 150 μM of both oxidants. Oxidative contribution of $SO_4^{\bullet-}$ > $^{\bullet}OH$ > $^1O_2$ using PS.	[97]
Sulfamethoxazole	Continuous flow quartz photoreactor with a sunlight-focusing system coupled to a sunlight tracker	3 L of 5.0 mg L^{-1} of each antibiotic in pure water, 50 mg L^{-1} PS, pH = 7.0, liquid flow rate = 6.54 mL min^{-1}, 45 °C, residence time = 60 min	Detection of 10 primary intermediates by LC-MS Maximum 73% loss of insecticide after 205 min of continuous treatment	[99]
Sulfadiazine Sulfamerazine Sulfamethoxazole Sulfathiazole	Stirred dish with an 8 W UVC light	100 mL of 10 mg L^{-1} of each antibiotic in pure water and real waters, 300 mg L^{-1} PS, natural pH, effect of anions (Cl^-, NO_3^-, SO_4^{2-}, HCO_3^-, and $H_2PO_4^-$) and humic acid, room temperature, 60 min	In pure water, > 90% removal of all antibiotics. Little effect of anions and slight deceleration with humic acid. Slower degradation with tap water < river water	[101]
Tetracycline	Stirred cylindrical photoreactor with a 40 W UVC lamp	200 mL of 5.0 mg L^{-1} of antibiotic in mariculture wastewater, 0–50 mg L^{-1} PS, pH = 6.9, effect of scavengers (ethanol, TBA, and isopropanol) and anions (Cl^- and Br^-), room temperature, 30 min	96% degradation with k_1 = 0.10 min^{-1} and without practical TOC reduction for the optimum 30 mg L^{-1} PS. The abatement was enhanced by adding Cl^- and more largely with Br^-. Detection of	[103]

(*continued on next page*)

Table 2 (*continued*)

Antibiotic	System	Experimental remarks	Best results	Ref.
			$SO_4^{\bullet-}$ and $^{\bullet}OH$, along with $Cl^{\bullet}$ and $Cl_2^{\bullet-}$ in the presence of Cl^-. Identification of 16 aromatic by-products by LC-MS	
Photocatalytic activation				
Amiloride	Stirred tank photoreactor with Pd/$BiVO_4$ photocatalyst and a 300 W Xe lamp	100 mL of 20 mg L^{-1} of antibiotic in pure water and real waters, 1.68 mM PS, 0.2 g L^{-1} photocatalyst, natural pH, effect of scavengers (methanol, TBA, *p*-BQ, and EDTA-2Na), anions (Cl^-, NO_3^-, SO_4^{2-}, CO_3^{2-}, HCO_3^-, and $H_2PO_4^-$), and humic acid, room temperature, 30 min	Total degradation with $k_1 = 0.1231$ min^{-1} and 75% TOC removal. Inhibition from 5.0 mg L^{-1} humic acid and with all the anions, more largely with CO_3^{2-} and HCO_3^-. Oxidation by holes, $O_2^{\bullet-}$, $SO_4^{\bullet-}$, and $^{\bullet}OH$	[108]
Ciprofloxacin	Stirred tank photoreactor with MIL-101 (Fe)− 1-(4-(methyl)phenyl)urea photocatalyst and a 35 W LED lamp (λ = 400–830 nm)	20 mL of 3.02 μM of antibiotic in pure water, 5.0 mM PS, 0.5 g L^{-1} photocatalyst, pH = 3.0–11.0, 25 °C, 120 min	Overall antibiotic decay with $k_1 = 0.0396$ min^{-1} and 41% TOC removal at optimum pH = 3.0, Both $SO_4^{\bullet-}$, and $^{\bullet}OH$ acted as oxidants. Poor reusability after 3 consecutive cycles of 60 min with 24% of loss of degradation.	[111]
Ciprofloxacin	Stirred tank photoreactor with carbonyl modified g-C_3N_4 photocatalyst and LED lamp (λ = 400–700 nm)	20 mg L^{-1} of antibiotic in pure water and real waters, 1.0 mM PS, 0.3 g L^{-1} photocatalyst, pH = 3.0–11.0, effect of scavengers (methanol, TBA, *p*-BQ, and EDTA-2Na), anions (Cl^-, NO_3^-, SO_4^{2-}, HCO_3^-, and $H_2PO_4^-$), and humic acid, room temperature, 90 min	96% degradation with $k_1 = 0.0365$ min^{-1} and 53% TOC removal at optimum pH = 7.0. $SO_4^{\bullet-}$,$^{\bullet}OH$, and $^1O_2$ as oxidants. Low influence of all the anions, except a strong inhibition with HCO_3^- and humic acid. Similar degradation with tap water and WWTP effluent. Moderate reusability after 5 consecutive cycles losing 7% of degradation. Identified 10 heteroaromatic by-products by LC-MS	[112]
Chloramphenicol	Stirred tank photoreactor with 4:1 graphene foam @FeS_2/α-Fe_2O_3 photocatalyst and a 120 W LED lamp (λ > 400 nm)	100 mL of 20 mg L^{-1} of antibiotic in pure water, 1.0 mM PS, 1.0 g L^{-1} photocatalyst, pH = 3.0–8.6, effect of scavengers (methanol, ethanol, hydroquinone, and EDTA), anions (Cl^-, NO_3^-, SO_4^{2-}, CO_3^{2-}, HCO_3^-, and $H_2PO_4^-$), and humic acid, 25 °C, 180 min	Total abatement in 50 min with 64% TOC reduction at pH = 8.6. 95% degradation in 180 min with $k_1 = 0.0159$ min^{-1} and $E_{EO} = 4.3$ kWh m^{-3} $order^{-1}$ at pH 5.8. Main oxidants $SO_4^{\bullet-}$ and $^{\bullet}OH$, followed by $O_2^{\bullet-}$ and holes. Good reusability after 5 consecutive steps of 180 min at pH = 8.6. Detection of 10 aromatic by-products by LC-MS	[113
Oxytetracycline	Helicoidal plug flow photoreactor with α-Fe_2O_3/ZnO/rGO photocatalyst and an external 24 W LED lamp (λ = 460–470 nm)	70 mL of 20 mg L^{-1} of antibiotic in pure water, 1.0–5.0 mM PS, 0.1–0.5 g L^{-1} photocatalyst, pH = 4.0–10.0, effect of scavengers (methanol, TBA, ascorbic acid, and EDTA-2Na), room temperature, 90 min	Optimum conditions by response surface methodology: 98% degradation with $k_1 = 0.1248$ min^{-1}, 2.06 mM PS, 0.37 g L^{-1} photocatalyst, and pH = 4.0. Oxidant: $SO_4^{\bullet-}$ (37%) > holes (36%) > $O_2^{\bullet-}$ (16%) > $^{\bullet}OH$ (11%)	[114]
Sulfamethoxazole	Stirred tank photoreactor with 0.75% CuO_x/$BiVO_4$ photocatalyst and a 100 W Xe lamp	120 mL of 0.5 mg L^{-1} of antibiotic in pure water, bottled water, and WWTP effluent, 100 mg L^{-1} PS, 0.5 g L^{-1} photocatalyst, natural pH (6.5–8.0), effect of scavengers (methanol, TBA, and EDTA-2Na), room temperature, 120 min	Degradation and k_1: complete at 30 min and 0.1133 min^{-1} in pure water < complete at 60 min and 0.0433 min^{-1} in bottled water < 53% at 120 min and 0.0067 min^{-1} in WWTP effluent. Predominance of holes as oxidant, followed by $SO_4^{\bullet-}$ and low influence of $^{\bullet}OH$	[116]
Tetracycline	Stirred tank photoreactor with $ZnFe_2O_4$/Ag photocatalyst and a 30 W LED lamp (λ = 450–460 nm)	100 mL of 20 mg L^{-1} of antibiotic in pure water and real waters, 1.5 g L^{-1} PS, 0.3 g L^{-1} photocatalyst, pH = 3.0–11.0, effect of scavengers (ethanol, TBA, *p*-BQ, and ammonium oxalate), anions (Cl^-, NO_3^-, HCO_3^-, and PO_4^{3-}), and humic acid, 25 °C, 80 min	90% of antibiotic abatement at pH = 3.0. Little influence of PS dosage between 1.0 and 2.0 g L^{-1}. $O_2^{\bullet-}$,$^1O_2$, and holes as main oxidants. Inhibition by adding Cl^- and more large influence with PO_4^{3-} and humic acid. Lesser degradation with tap water, river water, and WWTP effluent. Rapid loss of 50% performance after 3 successive runs. Detection of 9 aromatic, 7 cyclic, and 1 aliphatic derivatives by LC-MS	[120]
Trimethoprim	Pilot flow plant with a solar CPC[b] photoreactor, TiO_2 photocatalyst, and under sunlight irradiation	39 L of 1.0 mg L^{-1} of antibiotic in natural water, well water, and WWTP effluent, 0–0.5 mM PS, 0.2 g L^{-1} photocatalyst, pH = 7.3–8.1, room temperature, 50 min	In natural water, quicker total removal in about 20 min with energy consumption of 3 kJ L^{-1} for 0.25 mM PS. In well water, total decay was achieved in 30 min with energy consumption of 5 kJ L^{-1}, but in the WWTP effluent, only 42% abatement was attained in 50 min. Using 0.25 mM H_2O_2 as alternative oxidant in natural water, a longer time of about 30 min was required for total degradation	[121]

[a] E_{EO}: Electrical energy consumption per order.
[b] CPC: Compound parabolic collector.

$$ClO^- + H_2O + h\nu \rightarrow Cl^{\bullet} + {}^{\bullet}OH + OH^- \quad (23)$$

$$H_2O_2 + h\nu \rightarrow 2{}^{\bullet}OH \quad (24)$$

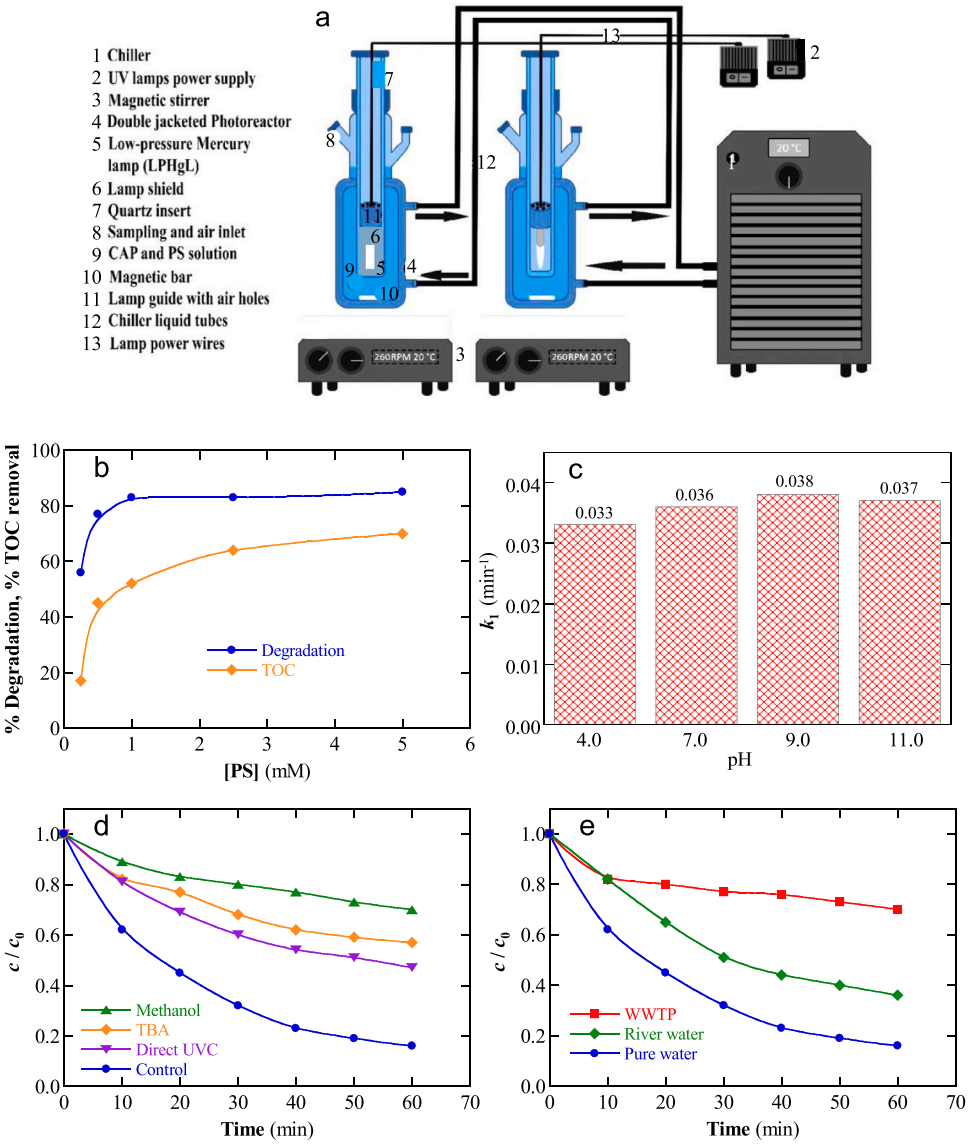

Fig. 12. (a) Sketch of the flow set-up with two connected stirred photoreactors containing 4.9 W UVC lamp each used for the PS treatment of chloramphenicol (CAP) solutions. (b) Percentages of degradation and TOC removal vs. the PS dosage after 60 min of treating 600 mL of 31 μM of CAP in pure water at natural pH under an UVC fluence of 330 J. (c) Effect of pH over the rate constant of the process with 0.25 mM PS using 10 mM phosphate buffer. (d) Influence of 400 mM methanol or TBA on the time course of normalized antibiotic concentration upon the above conditions at natural pH (control), along with that found under direct UVC irradiation. (e) Normalized concentration removal under the same conditions using several aqueous matrices.
Adapted from ref. [90]. The sketch (a) with permission 5644830277642 from Elsevier.

Reactions (22)-(24) account for by the generation of oxidizing radicals in these systems. The more powerful UV/PS process was so rapid that ciprofloxacin was completely abated in only 1 min in tap water. In contrast, this treatment was much slower in reclaimed water, being required up to 8 min for achieving total degradation with an electric energy consumption per order (E_{EO}) of 0.76 kWh m^{-3} order^{-1} (see Table 2). To explain this behavior, Fig. 13c depicts the strong degradation inhibition found when humic acid was added to the tap water, whereas the addition of Cl^- and HCO_3^- only yielded a little smaller abatement. This means that NOM was the main component that scavenged the oxidizing radicals in the reclaimed water.

A similar behavior has been reported by Gao et al. [96] for the treatment of 20 μM of florfenicol in pure water and real waters with the two parallel stirred dishes photoreactor submitted to a 75 W UVC light schematized in Fig. 14a. Fig. 14b shows the normalized concentrations of the antibiotic and TOC with time for the assay with 2.0 mM PS or H_2O_2 at pH = 6.8. The UVC/PS process yielded total removal in 20 min with k_1 = 0.0561 min^{-1}, a high E_{EO} = 415.58 kWh m^{-3} order^{-1}, and a low 22.3% of TOC decay. It was shown that both, $SO_4^{\bullet-}$ and $^{\bullet}OH$ acted as oxidants. The analogous UVC/H_2O_2 treatment was much slower giving 87% of loss of antibiotic with smaller k_1 = 0.0325 min^{-1}, an enormous E_{EO} = 886.15 kWh m^{-3} order^{-1}, and 5.6% TOC abatement (see Table 2). Addition of inorganic anions caused a deceleration of the UVC/PS process in the sequence: $HCO_3^- > NO_3^- > Cl^-$, which was also very strong with humic acid. According to this, Fig. 14c highlights the drop in k_1 as: pure water> river water > finished water > WWRP effluent.

It is also remarkable the study of He et al. [97] on the remediation of 50 mL of 5.0 mg L^{-1} of levofloxacin or ofloxacin in pure water with a stirred cylindrical photoreactor with a 25 W UVC lamp. The trials were performed with 50–300 μM PS or H_2O_2 at pH = 3.0–11.0 and 25 °C. A faster decay of both antibiotics was obtained with greater amount of each oxidant and smaller pH by the greater production of oxidizing radicals from reactions (22) or (24). All the systems were very efficient and total degradation was achieved in 30 min operating at pH = 3.0,

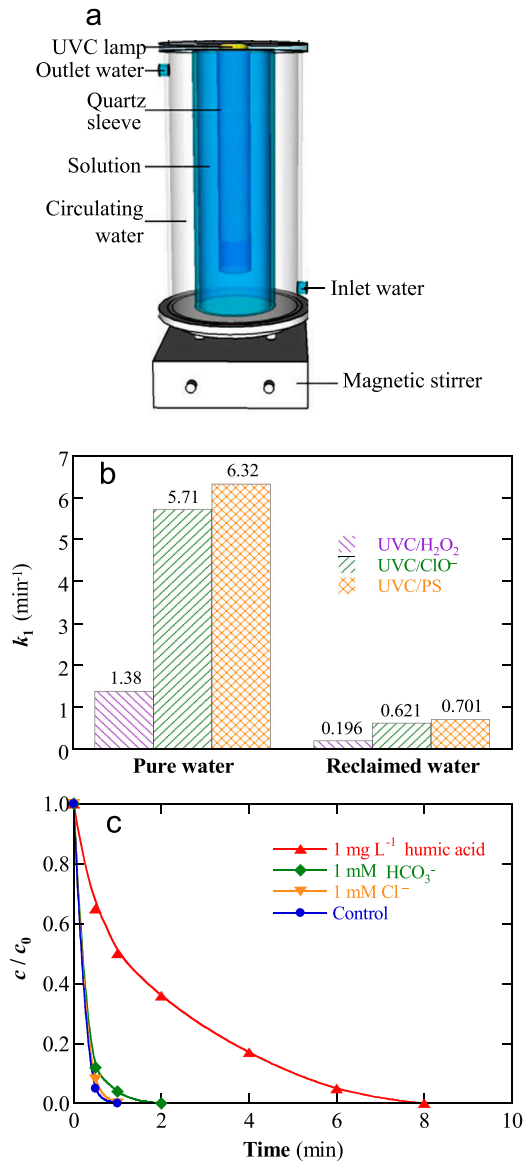

Fig. 13. (a) Scheme of the stirred cylindrical photoreactor with an inner 10 W UVC lamp used to oxidize ciprofloxacin with PS. (b) Pseudo-first-order rate constant for ciprofloxacin removal for the UVC/H_2O_2, UVC/ClO^- and UVC/PS processes of 1 μM antibiotic in tap water and reclaimed water with 1.0 mM of each oxidant at pH = 7.4 and 25 °C. (c) Time course of the normalized antibiotic concentration using the above UVC/PS treatment (control) and with the addition of several scavengers and humic acid in tap water.
Adapted from ref. [92]. Scheme (a) with permission 5644830798692 from Wiley.

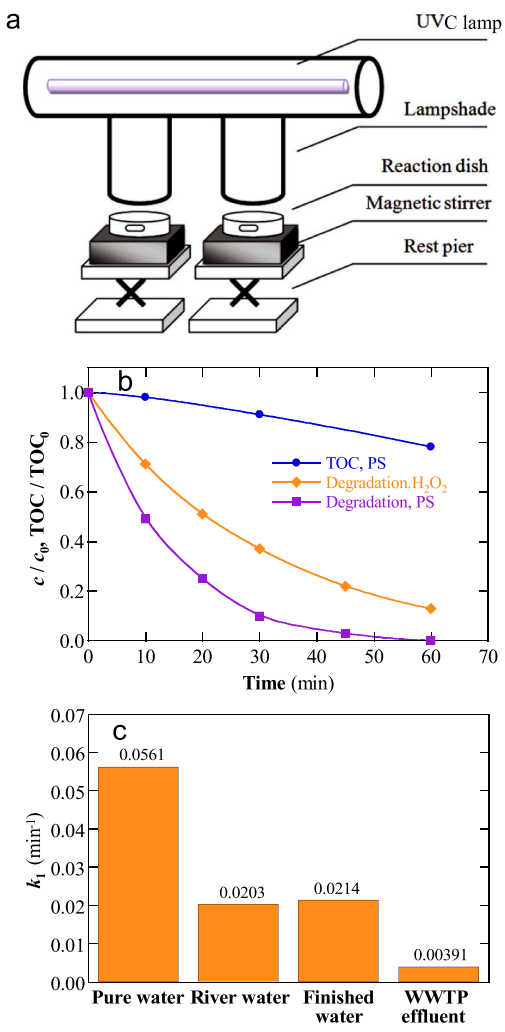

Fig. 14. (a) Sketch of two parallel stirred dishes photoreactor submitted to a 75 W UVC light and used for the PS treatment of florfenicol solutions. (b) Normalized antibiotic and TOC concentrations with time for the processes of 20 μM of antibiotic in pure water with 2.0 mM PS or H_2O_2 at pH = 6.8. (c) Pseudo-first-order rate constant determined for the UVC/PS treatment in several aqueous matrices upon the same conditions.
Adapted from ref. [96].

being more rapid for levofloxacin. Under these conditions, TOC was reduced by 35% for ofloxacin and 50% for levofloxacin with 150 μM of both oxidants (see Table 2). The authors used ethanol, TBA, and sodium azide as scavengers in the UVC/PS system to demonstrate the decreasing oxidative action of $SO_4^{\bullet-}$ > $^{\bullet}OH$ > $^1O_2$. The formation of $^1O_2$ from reactions (17) and (18) is thus confirmed during the UVC/PS treatment, a fact not shown by other authors. This opens the doors to consider non-radical mechanisms in this process.

For tetracycline, the study centered with 200 mL of 5.0 mg L^{-1} of antibiotic in mariculture wastewater of pH = 6.9 was made with a stirred cylindrical photoreactor under a 40 W UVC light [103]. The degradation process was fast and 96% of the antibiotic was removed in 30 min with k_1 = 0.10 min^{-1} (see Table 2). However, TOC was not practically reduced. It was found that this was improved by adding Cl^- and more largely with Br^- to the wastewater. This was explained by the generation of other strong oxidizing agents. So, using specific scavengers with Cl^-, the expected $SO_4^{\bullet-}$ and $^{\bullet}OH$ oxidants were detected, along with additional $Cl^{\bullet}$ and $Cl_2^{\bullet-}$ radicals. Moreover, 16 primary aromatic by-products were identified by LC-MS.

All these works clearly showed the superiority of UVC to activate PS over H_2O_2 and ClO^-. However, the applicability of the UVC/PS treatment can be limited by the expensive cost of the UVC lamp. This can be solved by illuminating the solution with sunlight using suitable photocatalysts, as described in the next subsection.

3.3. Photocatalytic activation

The activation of PS by photocatalysis has been devoted to the removal of amiloride with Pd/$BiVO_4$ [108], ciprofloxacin with TiO_2/-Fe_2O_3/zeolite [109], Fe-ZnO [110], MIL-101(Fe)– 1-(4-(methyl) phenyl)urea [111], and carbonyl modified g-C_3N_4 [112], chloramphenicol with 1:4 graphene foam@FeS_2/α-Fe_2O_3 [113], oxytetracycline with α-Fe_2O_3/ZnO/rGO [114], penicillin G [115], sulfamethoxazole with 0.75% CuO_x/$BiVO_4$ [116] and $FeMoO_4$ [117], tetracycline with $CaTiO_3$/carbon fiber [118], CuO/Fe_3O_4/GO [119], and $ZnFe_2O_4$/Ag

[120], trimethoprim with TiO_2 [121] and GO/CuFe [122]. Table 2 lists relevant results reported in selected works. They were made in the laboratory and the required sunlight as energy source (λ = 300–800 nm) was, in most cases, simulated with a Xe lamp, Light emitting díodes (LED) lamps were also used to provide visible light with λ > 400 nm.

In photocatalysis, a semiconductor material so-called photocatalyst is suspended into the polluted solution being illuminated to promote an electron e^-_{CB} of its valence band (VB) up to its conduction band (CB) giving a hole h^+_{VB} in the VB by reaction (25) [123]. The band gap energy (E_{bg}) of the semiconductor has to be equal or lower than the energy of the incident photons and so, the charges can be separated yielding the e^-_{CB}/h^+_{VB} pair. Typical photocatalysts like TiO_2 and ZnO become effective under UVA light, and for this reason, new materials sensible to visible light have been synthesized to profit the overall wavelength of solar irradiation. The photogenerated h^+_{VB} can directly oxidize the organics or react with water or OH^- to form the oxidant $^\bullet OH$ by reactions (26) or (27), respectively. The e^-_{CB} reduces O_2 to $O_2^{\bullet-}$, H_2O_2 to $^\bullet OH$, and $S_2O_8^{2-}$ to $SO_4^{\bullet-}$ from reactions (28) to (30). However, the effectiveness of the process is limited by the rapid recombination of the photoproduced h^+_{VB} and e^-_{CB} by reaction (31).

$$\text{Semiconductor} + h\nu \rightarrow h^+_{VB} + e^-_{CB} \quad (25)$$

$$h^+_{VB} + H_2O \rightarrow {}^\bullet OH + H^+ \quad (26)$$

$$h^+_{VB} + OH^- \rightarrow {}^\bullet OH \quad (27)$$

$$O_2 + e^-_{CB} \rightarrow O_2^{\bullet-} \quad (28)$$

$$H_2O_2 + e^-_{CB} \rightarrow {}^\bullet OH + OH^- \quad (29)$$

$$S_2O_8^{2-} + e^-_{CB} \rightarrow SO_4^{\bullet-} + SO_4^{2-} \quad (30)$$

$$h^+_{VB} + e^-_{CB} \rightarrow \text{semiconductor} + \text{heat} \quad (31)$$

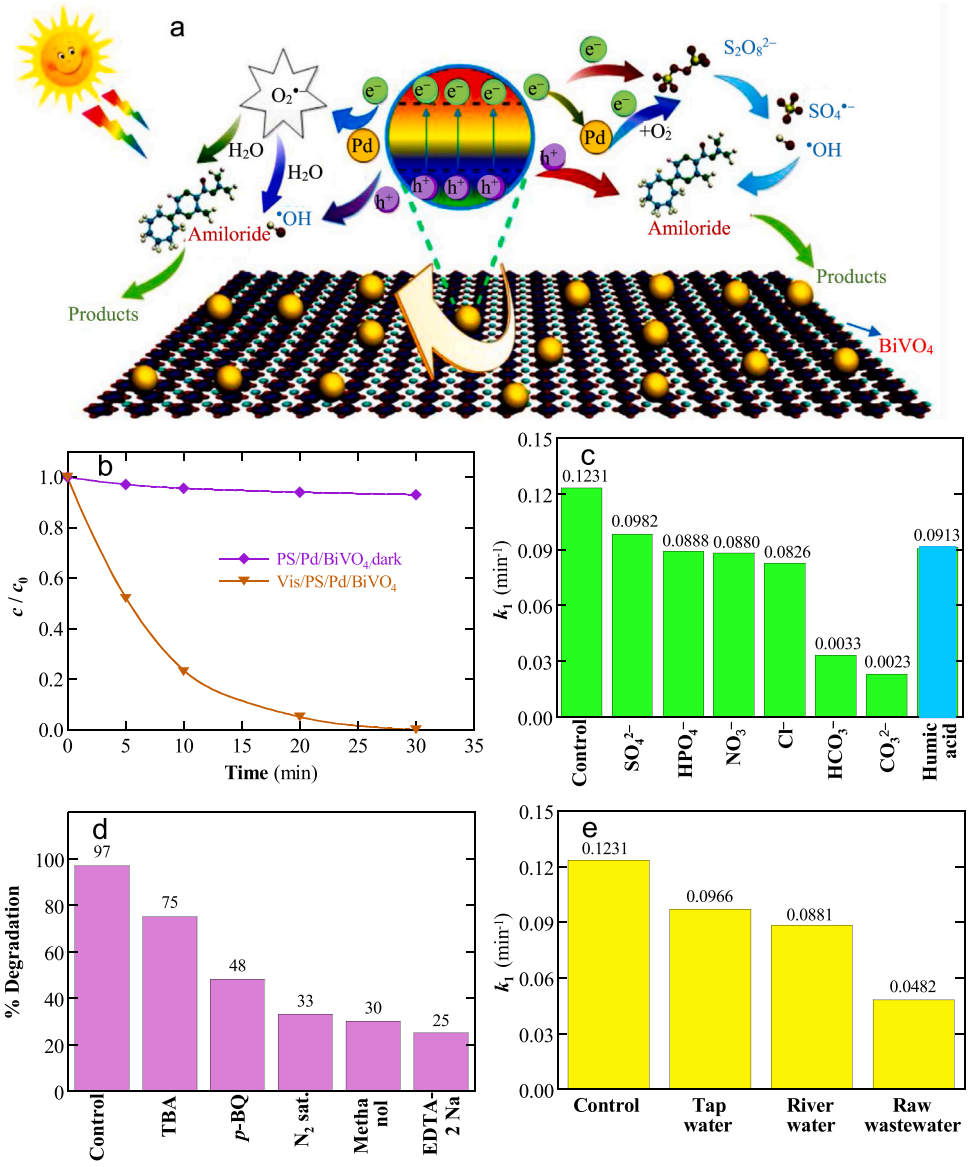

Fig. 15. (a) Mechanism proposed for the oxidation of amiloride with PS activated with a Pd/$BiVO_4$ photocatalyst using a stirred tank photoreactor exposed to an external 300 W Xe lamp (simulated sunlight). (b) Change of normalized antibiotic concentration with time for such PS process in the dark and under illumination using 100 mL of 20 mg L^{-1} amiloride in pure water with 1.68 mM PS and 0.2 g L^{-1} photocatalyst at natural pH. (c) Effect of 10 mM of inorganic ions and 10 mg L^{-1} humic acid on the pseudo-first-order-rate constant of the Vis/PS/Pd/$BiVO_4$ process (control). (d) Effect of scavengers (40 mM TBA and methanol, 1 mM p-BQ and EDTA- 2Na) on the percent of degradation after 30 min of the same process. (e) Pseudo-first-order rate constant for several aqueous matrices.
Adapted from ref. [108]. Mechanism (a) with permission 5644840424057 from Elsevier.

Fig. 15a shows a sketch of the mechanism proposed for the generation of oxidizing radicals from the above reactions to oxidize amiloride with PS activated with a Pd/$BiVO_4$ photocatalyst. A stirred tank photoreactor exposed to an external 300 W Xe lamp to simulate sunlight was used for treating 100 mL of 20 mg L^{-1} of antibiotic in pure water after adding 1.68 mM PS and 0.2 g L^{-1} photocatalyst at natural pH. Fig. 15b depicts the total degradation achieved by amiloride in 30 min with k_1 = 0.1231 min^{-1} when PS was activated under photocatalyst illumination, also attaining 75% of TOC abatement (see Table 2). In contrast, the antibiotic content was only reduced by 7% in the dark indicating that the photogenerated e^-_{CB}/h^+_{VB} pair upon light irradiation.

originated the oxidizing agents. The inhibitory effect of added inorganic ions and humic acid can be observed in Fig. 15c from the decay of the corresponding k_1-values. HCO_3^- and CO_3^{2-} anions gave the highest inhibition of the antibiotic removal. The use of specific scavengers disclosed the oxidizing agents produced. Fig. 15d highlights that the percent of degradation decreased in the sequence: control > TBA (scavenger of $^{\bullet}OH$) > *p*-BQ (scavenger of $O_2^{\bullet-}$) >methanol (scavenger of $SO_4^{\bullet-}$ and $^{\bullet}OH$) > EDTA-2Na (scavenger of h^+_{VB}). The generation of $O_2^{\bullet-}$ was also confirmed from the strong scavenging found under N_2 saturation of the suspension to remove the soluble O_2, as can be seen in Fig. 15d. The production of all these oxidants is highlighted in Fig. 15a. The study was extended to real waters and wastewaters to demonstrate the effectiveness of the method despite the scavenger effect of their components. Fig. 15e shows that the k_1-value of the process decreased as: control > tap water > river water > raw wastewater.

Table 2 shows the total or almost abatement achieved by 3.02 μM [111] and 20 mg L^{-1} [112] of ciprofloxacin in pure water with MIL-101 (Fe)– 1-(4-(methyl)phenyl)urea and carbonyl modified g-C_3N_4 photocatalysts, respectively, under visible LED light. It is remarkable that in the latter work, the detection of $SO_4^{\bullet-}$, $^{\bullet}OH$, and $^1O_2$ as oxidants, pointing to the existence of radical and non-radical mechanisms for the antibiotic removal. The main drawback of these systems was the low reusability of the photocatalysts in few consecutive cycles, probably by the strong adsorption of the by-products formed over their active centers inhibiting their photocatalytic power. In contrast, a good reusability has

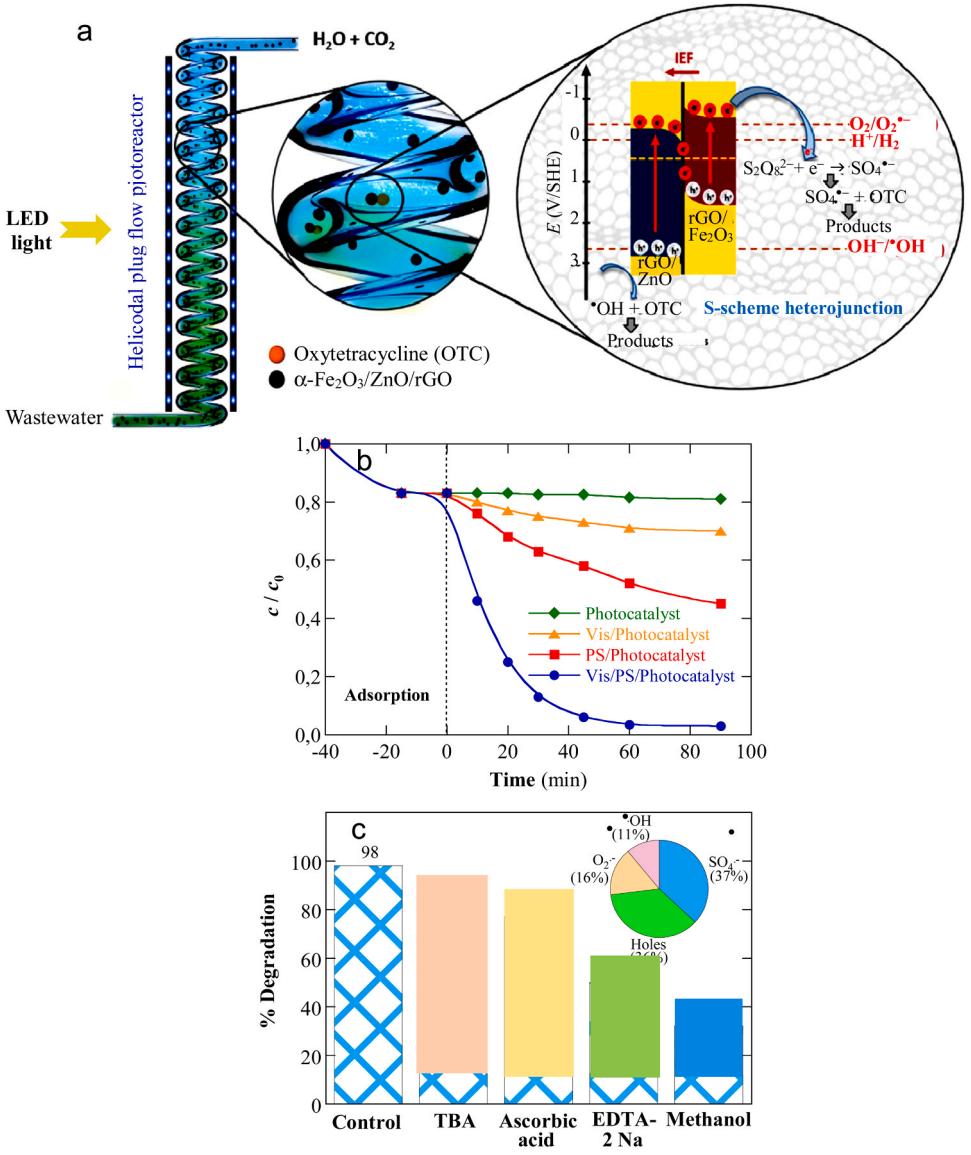

Fig. 16. (a) Photosystem setup and S-scheme mechanism proposed for the oxidation of oxytetracycline (OTC) with PS activated with α-Fe_2O_3/ZnO/rGO photocatalyst upon an external 24 W LED lamp (λ = 460–470 nm). (b) Normalized OTC content vs. time for several processes of 70 mL of 20 mg L^{-1} of antibiotic in pure water with 2.06 mM PS and 0.37 g L^{-1} photocatalyst at pH = 4.0. (c) Percent of degradation after 90 min of the same Vis/PS/photocatalyst process (control) with scavengers and percent of oxidizing agent detected (inset).
Adapted from ref. [114]. Fig. 16a with permission 5644841048323 from Elsevier.

been reported for 1.0 g L^{-1} of 4:1 graphene foam @FeS_2/α-Fe_2O_3 photocatalyst used to degrade 20 mg L^{-1} of chloramphenicol in 100 mL of pure water with 1.0 mM PS at pH = 3.0–8.6 upon a 120 W LED lamp [113]. Total abatement in 50 min with 64% TOC reduction was achieved at the best pH = 8.6. $SO_4^{\bullet-}$ and $^{\bullet}OH$ as main oxidants, followed by $O_2^{\bullet-}$ and holes, were also detected from specific scavengers.

In the case of oxytetracycline (OTC), a helicoidal plug flow photoreactor was used to remediate 70 mL of 20 mg L^{-1} of antibiotic in pure water after adding 1.0–5.0 mM of PS and 0.1-

0.5 g L^{-1} of α-Fe_2O_3/ZnO/rGO photocatalyst at pH = 4.0–10.0 upon an external 24 W LED lamp (λ = 460–470 nm) [114]. Fig. 16a schematizes the photosystem setup used and the S-scheme mechanism proposed for the production of oxidants to oxidize OTC. The holes at the VB of the rGO/ZnO heterojunction acted as oxidant, whereas its e_{CB}^- were transferred into the holes of the VB of the rGO/α-Fe_2O_3 heterojunction, and so, the e_{CB}^- of the CB of this latter composite recombination rate of reaction (31) was strongly diminished, enhancing the oxidation ability of the photocatalytic system. Fig. 16b depicts that under the optimum conditions determined by response surface methodology, 98% degradation with k_1 = 0.1248 min^{-1} was attained using 2.06 mM PS and 0.37 g L^{-1} photocatalyst at pH = 4.0. The photocatalytic activation was much more powerful than using the photocatalyst alone, under visible light and with PS. The use of specific scavengers allowed identifying the oxidants generated, as can be seen in Fig. 16c. From the analysis of these data, it was obtained a drop of the percentage of each oxidant in the order: $SO_4^{\bullet-}$ (37%) > holes (36%) > $O_2^{\bullet-}$ (16%) > $^{\bullet}OH$ (11%) (see inset of Fig. 16c and Table 2).

Kouvelis et al. [116] reported the benefits of CuO_x/$BiVO_4$ photocatalyst for the activated PS process of 120 mL of sulfamethoxazole suspensions with a stirred tank photoreactor under an external 100 W Xe lamp. Fig. 17a shows the effectiveness of the activated process for different aqueous matrices with 0.5 mg L^{-1} antibiotic, 100 mg L^{-1} of PS and 0.5 g L^{-1} of photocatalyst at natural pH, highlighting a drop in performance as: pure water > bottled water > WWTP effluent, as expected from the increasing scavenging of their components. The corresponding decrease of the k_1-value is presented in Fig. 17b. The degradation loss with specific scavengers depicted in Fig. 17c make evident the predominance of holes as oxidant due to the larger inhibition of its scavenger EDTA-2Na, being less important the action of $SO_4^{\bullet-}$ and with a low influence of $^{\bullet}OH$ (see Table 2). These findings reflect again the importance of the nature of the photocatalyst in the oxidation process where the photogenerated holes play a significant role, in some cases, even superior to the $SO_4^{\bullet-}$ formed from PS reduction by reaction (30).

It is worth mentioning the work of Grilla et al. [121] over the treatment of 39 L of 1.0 mg L^{-1} trimethoprim suspensions in a pilot flow plant with a solar compound parabolic collector (CPC). The assays were made with 0.2 g L^{-1} of a conventional TiO_2 photocatalyst at natural pH upon direct sunlight illumination and the quicker total removal was attained in about 20 min with an energy consumption of 3 kJ L^{-1} for natural water with 0.25 mM PS (see Table 2). When well water was used as aqueous matrix, the parallel degradation of its constituents decelerated the antibiotic removal and its total decay was achieved at a longer time of 30 min with greater energy consumption of 5 kJ L^{-1}. However, only 42% of abatement was reached in 50 min for a WWTP effluent due to the higher content of its scavenging components. The authors also confirmed a lower effectiveness with 0.25 mM H_2O_2 as alternative oxidant in natural water, since a longer time close to 30 min was required for total trimethoprim degradation.

The use of pilot flow plants for treating large volumes of antibiotic waters and wastewaters by PS with novel photocatalysts should be largely studied in the next future to clearly know their oxidation power and characteristics for their possible scaled-up at industrial level. In these assays, direct sunlight instead of UV, visible, or LED lamps should be used for illumination to obtain more cost-effective treatments. Comparison with other photoactivated processes with H_2O_2, ClO^-, etc., along with techno-economic studies, can help to confirm the applicability of this process for the remediation of antibiotics.

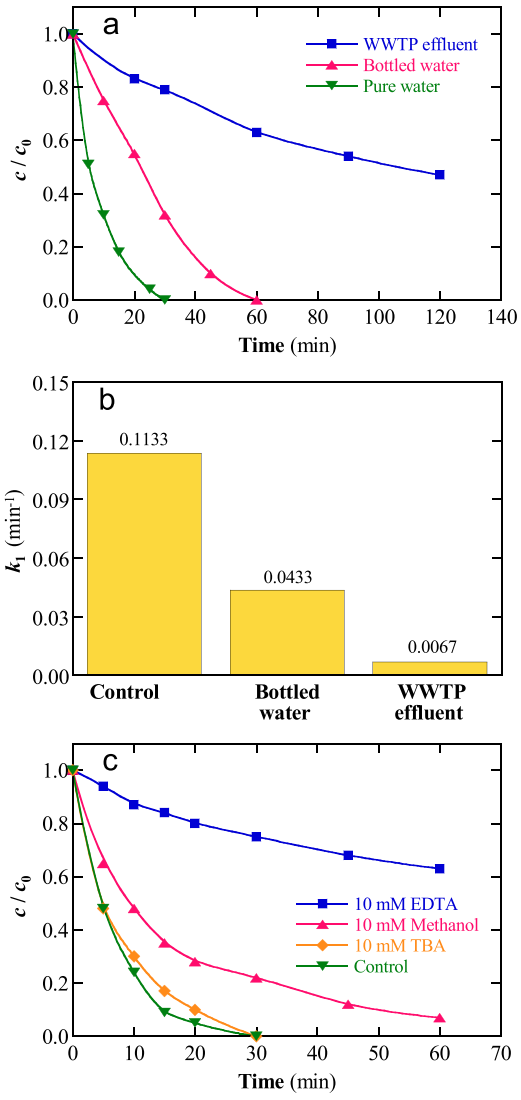

Fig. 17. (a) Variation of the normalized sulfamethoxazole concentration with time for the degradation of 120 mL of 0.5 mg L^{-1} antibiotic in pure water, bottled water, and WWTP effluent containing 100 mg L^{-1} of PS and 0.5 g L^{-1} of 0.75% CuO_x/$BiVO_4$ photocatalyst at natural pH (6.5–8.0) using a stirred tank photoreactor under an external 100 W Xe lamp. (b) The pseudo-first-order rate constant for the above processes. (c) Effect of different scavengers over the degradation treatment in pure water (control).
Adapted from ref. [116]

3.4. Other activation methods

A little number of papers have reported the degradation of antibiotics by PS under thermal, dielectric barrier, and electrochemical activations. Other hybrid methods with 1 activator and many combined activation processes have also been described. All these procedures are discussed in this subsection and their selected results are summarized in Table 3.

3.4.1. Thermal activation

The thermal activation of PS has been applied to the removal of ampicillin [124], cephalexin [125], cephalosporin [126], ciprofloxacin [127], metronidazole [128], sulfachloropyridazine [129], and trimethoprim [130]. The PS/heat method is a simple hybrid process in which

Table 3
Selected results reported for the removal of antibiotics from different aqueous matrices by persulfate activated with other single and combined methods.

Antibiotic	System	Experimental remarks	Best results	Ref.
Thermal activation				
Ampicillin	Stirred double-walled cylindrical reactor thermostated with recirculating water	120 mL of 0.25–2.5 mg L^{-1} of antibiotic in pure water, bottled water, and river water, 0–250 mg L^{-1} PS, pH = 3.0, 6.4, and 10.0, effect of scavengers (methanol and TBA), anions (Cl^- and HCO_3^-), and humic acid, 40–60 °C, 60 min	Removal enhancement at lower antibiotic content and pH and at higher PS dosage and temperature. In pure water, total degradation in 45 min with k_1 = 0.0565 min^{-1} for 0.5 mg L^{-1} antibiotic, 50 mg L^{-1} PS, pH = 6.4, and 50 °C. Inhibition by adding anions and humic acid. k_1: 0.0251 min^{-1} for bottled water > 0.0156 min^{-1} for river water. $SO_4^{\bullet-}$ dominated over $^{\bullet}OH$ as oxidant. Detection of 7 transformation by-products by LC-MS	[124]
Ciprofloxacin	Cylindrical vial in a thermostated water bath	20 mL of 30 μM of antibiotic in pure water and real waters, 2.0 mM PS, pH = 2.0–11.0, 20–70 °C, 480 min	Lower pH and higher temperature enhanced the antibiotic removal. 92% abatement in 180 min at pH = 7.0 and 60 °C. E_a = 67.8 kJ mol^{-1}. Degradation rate: pure water > groundwater > seawater > lake water. Identified 15 primary intermediates by LC-MS/MS	[127]
Metronidazole	Tank reactor in a stirred water bath	60 mL of 100 mg L^{-1} of antibiotic in pure water, 10–50 mM PS, pH = 5.0–11.0, effect of scavengers (methanol and TBA), 50–80 °C, 180 min	Scarce influence of pH on antibiotic abatement, which raised at higher PS content and temperature. 97% degradation with k_1 = 0.0237 min^{-1} for 20 mM PS and 60 °C at natural pH. E_a = 23.9 kcal mol^{-1}. 97% TOC reduction in 600 min. Predominance of $SO_4^{\bullet-}$ over $^{\bullet}OH$ as oxidant	[128]
Trimethoprim	Cylindrical vial in a thermostated water bath	20 mL of 30 μM of antibiotic in pure water and simulated waters, 2.0 mM PS, pH = 3.0–10.5, 50–65 °C, 480 min	Faster removal at pH = 3.0 and 7.0 and at higher temperature. E_a = 177.8 kJ mol^{-1}. Total abatement with k_1 = 0.0121 min^{-1} at pH = 7.0 and 55 °C. At 60 °C, overall degradation: simulated seawater (120 min) < pure water (180 min) < simulated river water (240 min). Identification of 5 heteroaromatic by-products by LC-MS	[130]
Dielectric barrier activation				
Metronidazole	Coaxial immersed DBD plasma (12–27 W) with air bubbling	140 mL of 10–50 mg L^{-1} of antibiotic in pure water, 0.25–2.5 g L^{-1} PS, natural pH, air flow rate = 100–250 mL min^{-1}, effect of scavengers (methanol and TBA), room temperature, 45 min	Greater decay at lower antibiotic content and input power and greater PS dosage and air flow rate. 95% removal with k_1 = 0.0512 min^{-1} for 10 mg L^{-1} antibiotic, 2.5 g L^{-1} PS, 12 W, and 150 mL min^{-1} of air flow. $^{\bullet}OH$ (47%) dominated over $SO_4^{\bullet-}$ (30%) as oxidant. 6 heteroaromatic derivatives detected by LC-MS	[132]
Sulfamethoxazole	Flow system with a coaxial immersed DBD plasma (24–28 kV or 3.5–7.1 W)	200 mL of 0.8 mg L^{-1} of antibiotic in pure water, 0–4.0 mM PS, pH = 2.0–10.0, liquid flow rate = 200 mL min^{-1}, effect of scavengers (ethanol. TBA, and *p*-BQ), room temperature, 30 min	Increasing PS content, pH, and pulse voltage raised antibiotic decay. 68% removal with k_1 = 0.0553 min^{-1} in 15 min for 0.8 mM PS, pH = 8.0, and 26 kV. Production of O_3 and H_2O_2. $SO_4^{\bullet-}$, $^{\bullet}OH$, $O_2^{\bullet-}$, and $^1O_2$ acted as oxidants	[133]
Electrochemical activation				
Cephalexin	Stirred undivided cell with a SnO_2/Ni@N-CNTs anode and a Ni@N-CNTs cathode	150 mL of 100 mg L^{-1} of antibiotic in pure water, 0.050 M Na_2SO_4, 0.2–1.5 mM PS, pH = 6.8, j[a] = 10–25 mA cm^{-2}, effect of scavengers (methanol and TBA), 20 °C, 240 min	Improvement of > 20% degradation with PS. Overall removal in 45 min with 1.0 mM PS and j = 20 mA cm^{-2}, 94% and 78% of COD and TOC reductions in 240 min. Radical oxidation with $SO_4^{\bullet-}$ and $^{\bullet}OH$ and non-radical oxidation. Low reusability after 5 consecutive cycles with loss of 14% of TOC decay. Identification of 6 aromatic and 5 heterocyclic derivatives by LC-MS. Using ion chromatography, malic, oxalic, and oxalic acids, along with released NH_4^+ and NO_3^-,were detected	[136]
Ciprofloxacin	Stirred undivided cell with 2 pairs of Al anodes and cathodes	600 mL of 10–60 mg L^{-1} of antibiotic in pure water and hospital wastewater, 0.050 M Na_2SO_4, 0.42–1.68 mM PS, pH = 3.0–9.0, j = 0.9–4.25 mA cm^{-2}, effect of scavengers (methanol and TBA), room temperature, 40 min	Better removal conditions: 90% for 20 mg L^{-1} antibiotic, 0.84 mM PS, pH = 7.0, and j = 2.75 mA cm^{-2}. 81% reduction of 3.5 mg L^{-1} antibiotic in hospital wastewater. Following a second-order kinetics. $^{\bullet}OH$ dominated over $SO_4^{\bullet-}$ at the initial time, but further high amount of $Al(OH)_3$ precipitate coagulated the antibiotic	[137]
Ciprofloxacin	Stirred undivided cell with 2 pairs of Fe anodes and cathodes	600 mL of 10–40 mg L^{-1} of antibiotic in pure water, 0.050 M Na_2SO_4, 0.42–1.26 mM PS, pH = 3.0–9.0, j = 0.75–2.3 mA cm^{-2}, effect of scavengers (methanol and TBA), room temperature, 75 min	Better removal conditions: 94% for 10 mg L^{-1} antibiotic, 0.42 mM PS, pH = 5.0, and j = 1.45 mA cm^{-2}. Following a second-order kinetics. $^{\bullet}OH$ dominated over $SO_4^{\bullet-}$ at the initial time, but at longer time, the precipitation of high amount of $Fe(OH)_3$ coagulated the antibiotic	[138]
Other hybrid methods with 1 activator				
Erythromycin	Tube submitted to gamma (^{60}Co) irradiation at 0.2–10 kGy dose	40 mL of 0.1 mM of antibiotic in pure water, groundwater, and WWTP effluent, 1.0 mM PS, pH = 8.5–9.5, effect of scavengers (methanol and TBA), glucose, and peptone, 20–22 °C	In pure water, overall antibiotic and PS consumption with 50% TOC reduction at 2 kGy dose. Similar results found with groundwater, but a higher 6 kGy dose was needed for the WWTP effluent. Removal enhanced by adding glucose and peptone. $SO_4^{\bullet-}$	[141]

(*continued on next page*)

Table 3 (*continued*)

Antibiotic	System	Experimental remarks	Best results	Ref.
			and $^{\bullet}OH$ contributed to the oxidation. Formic and acetic acids detected by ion chromatography	
Sulfamethoxazole Trimethoprim	Semi-continuous bubble column with an O_3 diffuser	80 μM of each antibiotic alone or mixed, 80–400 μM PS or H_2O_2, pH = 7.7 and 10.9, 2.2 mg L^{-1} O_3 at 2.5 L min^{-1}, 22 °C, 120 min	Faster removal at pH = 10.9 with total removal of each antibiotic in 17 min, regardless the oxidant and PS dosage. k_1 for each antibiotic, alone: 0.30–0.35 min^{-1} and in the mixture: 0.24–0.30 min^{-1}. TOC decay for the mixture with 400 μM oxidant: 36% for PS and 29% for H_2O_2. 8 and 9 intermediates detected for sulfamethoxazole and trimethoprim by LC-MS	[142]
Tetracycline	Microwave digestion tank (500–700 W power)	10 mL of 10–30 mg L^{-1} of antibiotic in pure water, 5.0–25 mM PS, pH = 6.5, effect of scavengers (methanol and TBA), room temperature, 5 min	Complete degradation in 5 min for 20 mg L^{-1} antibiotic and 6.0 mM PS at 500 W. Faster removal at lower antibiotic content and higher PS dosage and power. $SO_4^{\bullet-}$ predominated over $^{\bullet}OH$ as oxidant. 9 aromatic and 4 cyclic by-products found by LC-MS	[144]
Combined activation processes				
Amoxicillin	Stirred undivided cell with a Fe anode, a graphite cathode, and a 6 W UVC lamp and a US[b] bath at 37 kHz	100 mL of 0.5–100 mg L^{-1} of antibiotic in pure water, 20–80 mM PS, 0.050 M Na_2SO_4, pH = 4.0, I[c] = 10–80 mA, effect of scavengers (ethanol and TBA) and anions (Cl^- and CO_3^{2-}), room temperature, 60 min	Removal: 73% with k_1 = 0.022 min^{-1} for PS/electrolysis < 83% for US/PS/electrolysis < 95% for UVC/PS/electrolysis using 50 mg L^{-1} antibiotic, 80 mM PS, and I = 30 mA. $SO_4^{\bullet-}$ and $^{\bullet}OH$ as oxidants. Enhancement with decreasing electrolyte concentration	[145]
Ciprofloxacin	Erlenmeyer flask with Fe_3O_4 catalyst in a US bath at 60 kHz	100 mL of 50–250 mg L^{-1} of antibiotic in pure water, 0.01–1.2 mM PS, 0.01–0.08 g L^{-1} catalyst, pH = 3.0–8.0, room temperature, 120 min	98% abatement in 45 min for 200 mg L^{-1} antibiotic, 0.15 mM PS, 0.01 g L^{-1} catalyst, and pH = 5.0	[151]
Ciprofloxacin	Stirred undivided cell with a Ti/RuO_2/IrO_2 anode, an ACF[d] cathode, and two 6 W UVC lights	500 mL of 100–300 mg L^{-1} of antibiotic in pure water, 5.0–20 mM PS, pH = 3.0–11.0, cell voltage = 2.0–6.0 V, effect of scavengers (methanol, ethanol, TBA, and L-histidine) and anions (Cl^-, NO_3^-, SO_4^{2-}, HCO_3^-, and $H_2PO_4^-$), room temperature, 120 min	Little effect of pH < 9.0 and cell voltage > 4.0 V on abatement, which was improved at lower antibiotic concentration and greater PS dosage. Overall degradation with k_1 = 0.03799 min^{-1} for 100 mg L^{-1} antibiotic, 20 mM PS, pH = 7.0, and 4.0 V cell voltage. Inhibitory effect of all added anions. $^1O_2$ as major oxidant than $SO_4^{\bullet-}$ and $^{\bullet}OH$. Identified 9 primary by-products by LC-MS	[153]
Erythromycin	Conical flask in a shaker at 150 rpm with H_2O_2 and ZVI catalyst	150 mL of 1.0 mg L^{-1} of antibiotic in pure water, 0.07 mM PS, 0.03 mM H_2O_2, 22.4 mg L^{-1} catalyst, pH = 5.0, effect of scavengers (*n*-butyl alcohol and TBA), anions (Cl^-, SO_4^{2-}, CO_3^{2-}, and HCO_3^-), and humic acid, 25 °C, 240 min	98% removal with k_1 = 0.018 min^{-1}. Positive influence of Cl^- and SO_4^{2-} at low contents, and strong inhibition with CO_3^{2-}, HCO_3^-, and humic acid. $^{\bullet}OH$ as predominant oxidant. Slower degradation without H_2O_2, acting $SO_4^{\bullet-}$ and $^{\bullet}OH$ as oxidants. 9 primary by-products detected by LC-MS	[155]
Sulfamethoxazole	Quartz dish for photothermal activation with carbon black under a 300 W Xe light	25 mL of 2.0 mg L^{-1} of antibiotic in pure water and river water, 1.0 mM PS, 0.1 g L^{-1} carbon black, pH = 7.0, effect of scavengers (methanol, TBA, and sodium azide) and NOM, 40–70 °C, 180 min	The carbon black allowed achieving about 60°C in 30 min. Overall abatement in 90 min with k_1 = 0.050 min^{-1} controlling at 70 °C < 180 min with k_1 = 0.0214 min^{-1} at 60 °C. Lower degradation rate by adding NOM or by using river water. Predominance of oxidants $SO_4^{\bullet-}$ and $^{\bullet}OH$ over $^1O_2$. Strong deactivation of the carbon black losing 35% performance after 4 successive runs of 180 min at 60 °C	[157]
Tetracycline	Stirred dish with Fe^{3+} and 75 W UVC light	5.0 mg L^{-1} of antibiotic in pure water, 0.4 mM PS, 0.4 mM Fe^{3+}, pH = 3.0–7.0, effect of scavengers (methanol, TBA, chloroform, and methyl phenyl sulfone), anions (Cl^-, NO_3^-, CO_3^{2-}, and HCO_3^-), and humic acid, 22 °C, UV fluence = 220 mJ cm^{-2}	Total removal with k_1 = 0.0222 cm^2 mJ^{-1} at pH = 3.0. Decreasing abatement with raising pH. Degradation was enhanced with Cl^-, but inhibited with the other anions and humic acid. $SO_4^{\bullet-}$, $^{\bullet}OH$, $O_2^{\bullet-}$, and Fe(IV) as oxidants. 9 aromatic and 2 aliphatic by-products identified by LC-MS	[159]
Tetracycline	Conical flask in a shaker at 200 rpm with nano-Fe_3O_4, coupled to biodegradation with microbes	250 mL of 20 mg L^{-1} of antibiotic in pure water, 0.1 mM PS, 1.0–10 g L^{-1} nano-Fe_3O_4, pH = 3.0 or 6.0, effect of anions (Cl^-, NO_3^-, HCO_3^-, and $H_2PO_4^-$) and humic acid, 25 °C, 360 min	Degradation: PS (30%) < biological (47%) < PS/nano-Fe_3O_4 (77%, pH = 3.0) < PS/nano-Fe_3O_4 - biological (95%, pH = 6.0). Little inhibition with NO_3^- and $H_2PO_4^-$, which largely raised with Cl^-, HCO_3^-, and humic acid. Identified 12 aromatic and 3 aliphatic by-products by LC-MS	[160]

[a] j: Current density.
[b] US: Ultrasound.
[c] I: Current.
[d] ACF: Activated carbon fiber.

the molecule of PS is energetically activated to be decomposed into two $SO_4^{\bullet-}$ radicals from reaction (32) [124,128,129]. Subsequently, the oxidant $^{\bullet}OH$ can be formed from reactions (5) or (6). Only these two kinds of oxidizing radicals have been reported for this method (see Table 3).

$$S_2O_8^{2-} + \text{heat} \rightarrow 2SO_4^{\bullet-} \quad (32)$$

Lalas et al. [124] used a stirred double-walled cylindrical reactor for treating 120 mL of 0.25–2.5 mg L^{-1} of ampicillin in several aqueous matrices with 0–250 mg L^{-1} of PS at pH = 3.0, 6.4, and 10.0 operating between 40 and 60 °C. The action of generated oxidants became more effective at lower antibiotic concentration and pH and at higher PS

dosage and temperature. The k_1-values decreased in the sequence: pure water (0.0565 min^{-1}) > bottled water (0.0251 min^{-1}) > river water (> 0.0156 min^{-1}) for 0.5 mg L^{-1} antibiotic, 50 mg L^{-1} PS, pH = 6.4, and 50 °C (see Table 3). This trend was confirmed by the inhibition observed in pure water by addition of Cl^-. HCO_3^-, and humic acid, present in the other natural waters. The work was completed by the identification of 7 transformation by-products by LC-MS. Similar effects of pH, PS content, and temperature have been described for the PS/heat process of ciprofloxacin [127] and metronidazole [128], In the former case, 92% of abatement was found after 180 min of treatment of 30 μM of antibiotic in a 20 mL solution with 2.0 mM PS at pH = 7.0 and 60 °C. An activation energy (E_a) of 67.8 kJ mol^{-1} was determined between 20 and 70 °C. It was reported that ciprofloxacin degradation also dropped in the order: pure water > groundwater > seawater > lake water (see Table 3). For metronidazole, it was obtained a 97% of degradation with k_1 = 0.0237 min^{-1} for the treatment of 260 mL of 100 mg L^{-1} antibiotic in pure water with 20 mM PS at natural pH and 60 °C, with an.

E_a = 23.9 kcal mol^{-1} calculated between 50 and 80 °C (see Table 3). After 600 min, a 97% of TOC reduction was found, demonstrating a good power oxidation of the procedure.

Fig. 18a shows the rapid enhancement of trimethoprim degradation with raising the temperature from 50 to 65 °C for 20 mL of 30 μM of antibiotic in pure water by adding 2.0 mM PS at pH = 7.0 and using a cylindrical vial in a thermostated water bath [130]. Overall abatement

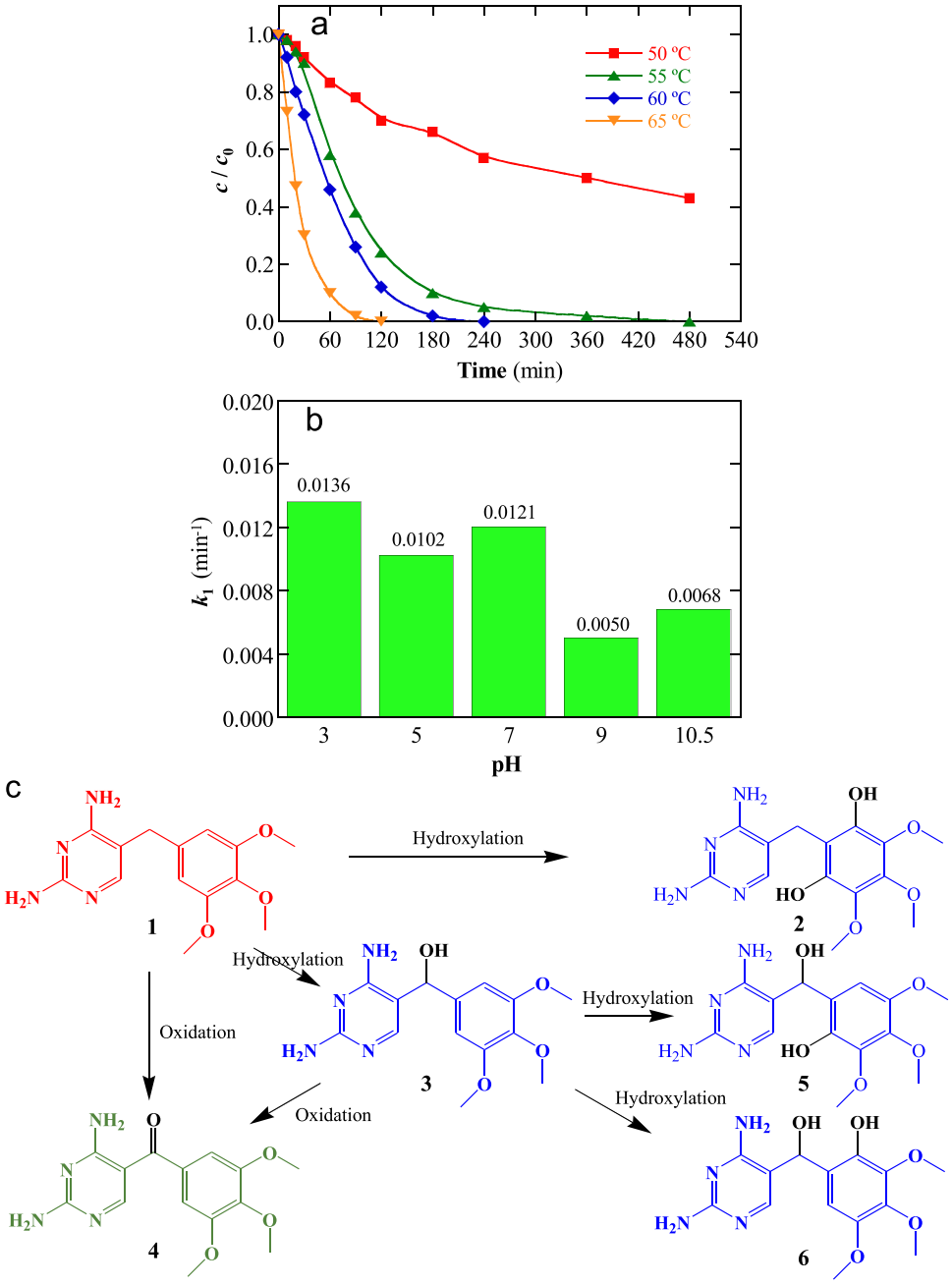

Fig. 18. (a) Effect of temperature on the change of normalized trimethoprim concentration with time for the degradation of 20 mL of 30 μM of antibiotic in pure water with 2.0 mM PS at pH = 7.0, using a cylindrical vial in a thermostated water bath. (b) Influence of pH for the assay performed at 55 °C. (c) Reaction sequence for the initial degradation of trimethoprim (1) under the above conditions.
Adapted from ref. [130]. Fig. 18c with permission 5644850235581 from Elsevier.

was obtained in 120 min at 65 ºC and a high E_a = 177.8 kJ mol^{-1} was determined within this temperature interval (see Table 3). Fig. 18b highlights the change of k_1 with pH for the above assays at 55 ºC. As can be seen, the best pH values for the PS/heat process were 3.0 and 7.0. From the 5 primary by-products detected by LC-MS, the reaction sequence of Fig. 18c was proposed for trimethoprim degradation. The parent molecule (**1**) is hydroxylated to **2** and **3**, as well as oxidized to **4**. Further oxidation of **3** yields **4**, and its hydroxylation gives **5** and **6**.

It is noticeable that thermal activation has been combined with previous PS activators, also enhancing the degradation rate of antibiotic at higher temperature. The heating in PS-AOPs processes can be widely used in further work, although techno-economic studies are required to confirm whether can be useful in practice.

3.4.2. Dielectric barrier activation

The dielectric barrier discharge (DBD) has been used for the hybrid activation of PS for treating ciprofloxacin [131], metronidazole [132], sulfamethoxazole [133], and tetracycline [134]. The DBD reactor consists of two electrodes immersed into the contaminated solution with PS and by applying a sinusoidal high pulse voltage of near 30 kV at high frequency of the order of 10^4 hertz between them. This originates a plasma that can produce oxidants such as H_2O_2, O_3, and $^{\bullet}$OH from water dissociation, as well as UV irradiation, local high temperature, and local vibration wave that can decompose PS to $SO_4^{\bullet-}$ from an energetic reaction similar to (32). Note that the high energetic requirements of the DBD system limits its actual application to large water volumes in practice.

Wang et al. [132] used a coaxial immersed DBD plasma of 12–27 W with air bubbling for the degradation of 10–50 mg L^{-1} of metronidazole in pure water with 0.25–2.5 g L^{-1} of PS at natural pH and an air flow rate = 100–250 mL min^{-1}. They found that the antibiotic abatement was raised with lower content, decreasing the input power of the reactor, and increasing the PS dosage and air flow rate. The best degradation of 95% removal in 45 min with k_1 = 0.0512 min^{-1} was determined for 10 mg L^{-1} of metronidazole, 2.5 g L^{-1} of PS, 12 W of input power, and 150 mL min^{-1} of air flow rate (see Table 3). From the addition of methanol and TBA as scavengers, it was calculated that $^{\bullet}$OH (47%) was the pre-eminent oxidant over $SO_4^{\bullet-}$ (30%). Moreover, 6 heteroaromatic derivatives were identified by LC-MS. In another work, Shang et al. [133] explored the characteristics of a flow system with a coaxial immersed DBD plasma of 24–28 kV or 3.5–7.1 W for the treatment of 200 mL of 0.8 mg L^{-1} of sulfamethoxazole in pure water at a liquid flow rate of 200 mL min^{-1}. The antibiotic was more rapidly abated with increasing the PS content up to 4.0 mM, the pH from 2.0 to 10.0, and the pulse voltage. After 15 min, a 68% of sulfamethoxazole removal with k_1 = 0.0553 min^{-1} was reached using 0.8 mM PS, pH = 8.0, and 26 kV (see Table 3). From scavengers such as ethanol. TBA, and *p*-BQ, the generation of many oxidants like O_3, H_2O_2. $SO_4^{\bullet-}$, $^{\bullet}$OH, $O_2^{\bullet-}$, and $^1O_2$ were detected.

3.4.3. Electrochemical activation

Several hybrid electrochemical treatments have been proposed to degrade cefotaxime [135], cephalexin [136], ciprofloxacin [137,138], and florfenicol [139] by activating PS. These electrolytic systems involve the reduction of the PS molecule at the cathode via reaction (33) [136]. In addition, in a sulfate medium with an undivided cell, the SO_4^{2-} ion can be oxidized at the anode to $S_2O_8^{2-}$ by reaction (34), enhancing the concentration of this compound, whereas organics can be directly oxidized at the anode M or by physisorbed $^{\bullet}$OH (M($^{\bullet}$OH)), from water discharge by reaction (35) [136]. This latter possibility corresponds to the so-called electrochemical oxidation (EO) process. Another possibility is the use of electrocoagulation (EC) with sacrificial anodes of Al of Fe, which are dissolved to Al^{3+} or Fe^{2+}ions, respectively, precipitating as Al/OH)$_3$ or iron hydroxides with coagulation of organic pollutants. These procedures have been explored with good results by Malakootian and Ahmadian [137,138] for the removal of ciprofloxacin from pure water and hospital wastewater (see Table 3).

$$S_2O_8^{2-} + e^- \rightarrow SO_4^{\bullet-} + SO_4^{2-} \quad (33)$$

$$2SO_4^{2-} \rightarrow S_2O_8^{2-} + 2e^- \quad (34)$$

$$M + H_2O \rightarrow M(^{\bullet}OH) + H^+ + 2e^- \quad (35)$$

Another exciting possibility of EO process has been recently by published by Duan et al. [136] with a SnO_2/Ni@N-CNTs anode for cephalexin removal. These authors found that this anodic material was also able to activate PS by chemical reaction with the hydroxyl group of its surface via reaction (36), and so, the antibiotic could be anodically degradeed by direct oxidation or mediated oxidation with M($^{\bullet}$OH) or $SO_4^{\bullet-}$, as schematized in Fig. 19b.

$$M\text{-}OH + S_2O_8^{2-} \rightarrow M\text{-}O^{\bullet} + SO_4^{\bullet-} + HSO_4^- \quad (36)$$

The assays were carried out with a stirred undivided cell equipped with such anode and a Ni@N-CNTs cathode and filled with 150 mL of 100 mg L^{-1} of cephalexin in pure water with 0.050 M Na_2SO_4 as supporting electrolyte and 0.2–1.5 mM PS at pH = 6.8 and by applying a current density (*j*) from 10 to 25 mA cm^{-2}. Fig. 19b depicts that at j = 20 mA cm^{-2} with 1.0 mM PS, the PS/EO process yielded overall removal, being much faster than simple EO or PS alone. The same tendency can be observed in Fig. 19c for the TOC removal that was reduced by 78% by EO/PS in 240 min in front of 48% by EO and 8% by PS alone. The significant mineralization achieved by EO along with the large inhibition obtained by PS/EO in the presence of 1 mM TBA and 1 mM methanol (see Fig. 19d) allowed establishing the existence of a radical mechanism with $SO_4^{\bullet-}$ and $^{\bullet}$OH as oxidants and a non-radical mechanism to degrade the antibiotic. However, the anode had as main drawback its fast loss of electroactivity upon reuse after 5 consecutive.

steps of 240 min (see Table 3). The authors identified 6 aromatic and 5 heterocyclic derivatives by LC-MS, as well 3 final carboxylic acids and released nitrogenated ions by ion chromatography. Fig. 19e highlights the high concentration of malic, formic, and pre-eminently oxalic acids accumulated in the treated solution that prevented the total mineralization of the antibiotic. Moreover, more NH_4^+ than NO_3^- ion was released, preferentially during the first 240 min of electrolysis, suggesting that at such time, most nitrogenated compounds were removed.

An advantage of the electrochemical processes is the low energetic cost as compared to the very high energy input required by artificial lights in photoactivated processes. The treatment of antibiotic waters should be assessed with pilot flow plants equipped with a filter-press electrolytic reactor to show their practical suitability, This requires the preparation of novel electroactive anodes and cathodes and the study of the influence of the current, liquid flow rate, and composition of the aqueous matrix to optimize the oxidation process.

3.4.4. Other hybrid methods with 1 activator

Other hybrid methods for PS activation with 1 activator have been used for the treatment of ampicillin by photothermal process [140], erythromycin by gamma radiolysis [141], sulfamethoxazole and trimethoprim by ozone [142], sulfamethoxazole by CaO_2 [143], and tetracycline by microwave [144]. The photothermal activation is based on the PS decomposition by near-IR, whereas CaO_2 originates H_2O_2 that converts PS into $SO_4^{\bullet-}$. Better results were obtained using the isotope ^{60}Co as activator. This gamma radiation excites energetically the PS molecule for its homolytic transformation into $SO_4^{\bullet-}$, similarly to reaction (32). Chu et al. [141] irradiated ^{60}Co into a tube at 0.2–10 kGy dose, which contained 40 mL of 0.1 mM erythromycin and 1.0 mM PS at pH = 8.5–9.5 and 20–22 ºC. In pure water, the antibiotic and PS contents were completely consumed with 50% TOC reduction after providing a 2 kGy dose of irradiation (see Table 3). For groundwater, similar results were obtained but after applying a higher 6 kGy dose because of the parallel consumption of oxidants by their components, The irradiation dose was even much greater for a WWTP effluent with more

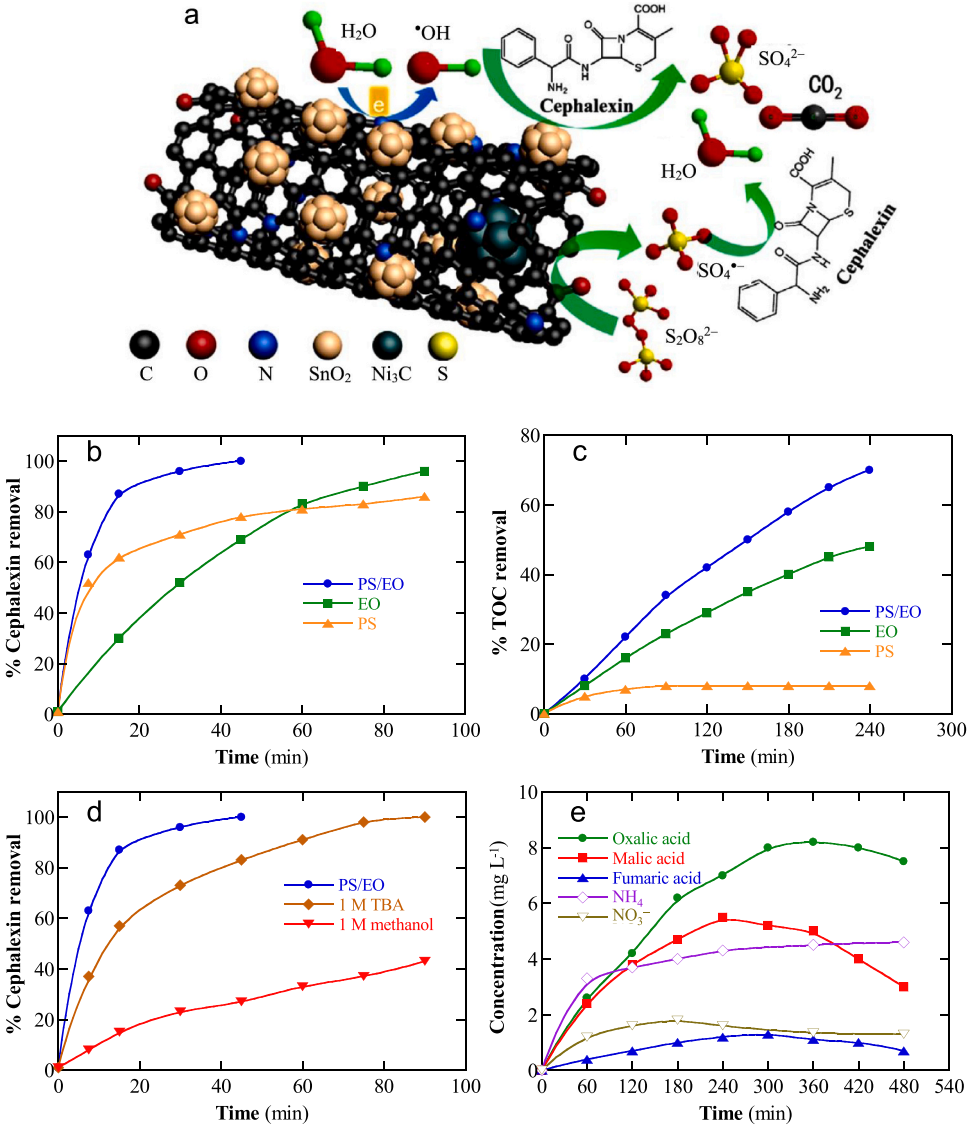

Fig. 19. (a) Mechanism proposed for the production of oxidizing agents from PS activation with an electrochemical oxidation (EO) system equipped with a SnO_2/Ni@N-CNTs anode and a Ni@N-CNTs cathode in a stirred undivided cell. Percentage of (b) cephalexin and (c) TOC removals for several treatments of 150 mL of 100 mg L^{-1} of antibiotic in pure water with 0.050 M Na_2SO_4 and 1.0 mM PS at pH = 6.8 and 25 °C by applying a j = 20 mA cm^{-2}. (d) Effect of scavengers on the PS/EO process. (e) Evolution of the concentration of final carboxylic acids and released inorganic ions for the same process.
Adapted from ref. [136]. Mechanism (a) with permission 5644850769011 from Elsevier.

contaminants. Glucose and peptone acted as PS activators to $SO_4^{\bullet-}$ and their addition to the solution enhanced the antibiotic removal. Specific scavenger revealed the contribution of $SO_4^{\bullet-}$ and $^{\bullet}OH$ to the oxidation process. Final carboxylic acids like formic and acetic were detected by ion chromatography.

It is well-known that in alkaline medium, O_3 yields the hydroperoxide ion (HO_2^-) and O_2 by reaction (37) [142]. HO_2^- is the basic form of H_2O_2 at pH > 11.75 and can react with PS and O_3 via reactions (38) and (39), which take place in the PS/O_3 and H_2O_2/O_3 processes, respectively. The oxidation power of these procedures was checked by Adil et al. [142] for 80 μM of sulfamethoxazole and trimethoprim, alone or mixed, in pure water with 80–400 μM PS or H_2O_2 at pH = 7.7 and 10.9 by putting the solution in a semi-continuous bubble column upon injection of 2.2 mg L^{-1} O_3 gas at 2.5 L min^{-1}. For each antibiotic, total removal was achieved in 17 min at pH = 10.9 with k_1 = 0.30–0.35 min^{-1} in all cases. This excellent result was also obtained for the mixture of antibiotics, but with a lower 0.24–0.30 min^{-1} by the presence of more organic load (see Table 3). A different behavior was found for the TOC removal with 400 μM of each oxidant, which was 36% for PS/O_3 higher than 29% for H_2O_2/O_3, confirming the superiority of the former process, although much more work with real waters is needed for ensuring its possible application.

$$S_2O_8^{2-} + HO_2^- \rightarrow SO_4^{\bullet-} + HSO_4^- + O_2^{\bullet-} \quad (38)$$

$$O_3 + HO_2^- \rightarrow {}^{\bullet}OH + O_2^{\bullet-} + O_2 \quad (39)$$

It is also note worthing the use of a microwave irradiation to energetically excite PS to $SO_4^{\bullet}$ in a similar way to reaction (32). Fig. 20a shows the very rapid and total degradation in about 5 min attained for 20 mg L^{-1} of tetracycline in 10 mL of pure water with 6.0 mM PS using a microwave digestion tank with a power of 500–700 W. Longer time for complete disappearance was found with increasing the antibiotic concentration with 6.0 mM PS and 500 W power due to the slower degradation of mote organic matter (see Fig. 20b). Quicker antibiotic removal can be seen in Fig. 20c when the PS content was raised from 5 to 10 mM PS concentration for 20 mg L^{-1} antibiotic at 500 W power by the progressive production of higher amounts of oxidizing agents. At higher PS

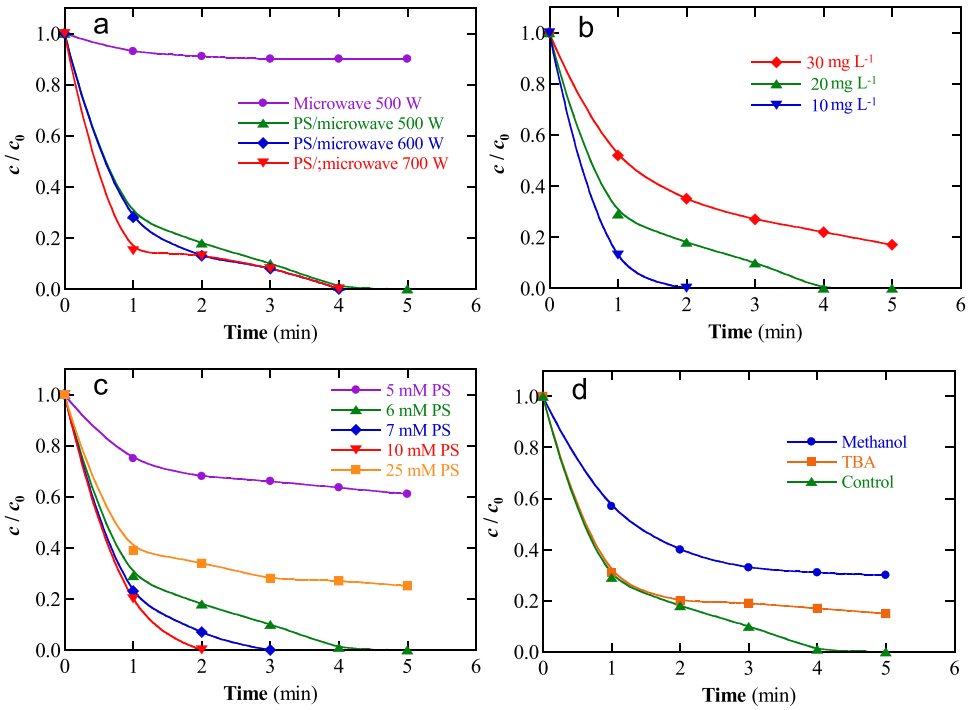

Fig. 20. Effect of (a) microwave power on the normalized tetracycline abatement vs. time for the treatment of 10 mL of 20 mg L^{-1} of antibiotic in pure water with 6.0 mM PS at pH = 6.5 using a microwave digestion tank, (b) antibiotic concentration with 6.0 mM PS at 500 W power, (c) PS concentration for 20 mg L^{-1} antibiotic at 500 W power, and (d) methanol and TBA as scavengers for the treatment upon the conditions of graphic (a) at 500 W power. Adapted from ref. [144].

dosage, the degradation was decelerated as result of the greater increase in rate of parasitic reactions of oxidants like (2), (4), and (7)-(9). The much faster degradation inhibition by adding methanol in front of TBA shown in Fig. 20d indicated the predominance of $SO_4^{\bullet-}$ over $^{\bullet}OH$ as oxidant. The LC-MS analysis of degraded solutions allowed identifying 9 aromatic and 4 cyclic primary by-products (see Table 3). Although this procedure was very effective for tetracycline removal, its application to treat large water volumes is inviable.

3.5. Combined activation processes

Some combined processes with PS activation have been proposed for the remediation of amoxicillin by photoelectrochemical process [145], carbamazepine [146], ceftriaxone [147] and cephalexin [148] by Fe and UV, carbendazim by solar photo-Fenton [149], ciprofloxacin by Zn and US [150], Fe_3O_4 and US [151], Fe^{2+} and US [152], and photoelectrochemical process [153,154], erythromycin by H_2O_2 and ZVI [155], sulfamethazine by Fe and US [156], sulfamethoxazole by photothermal activation with carbon black [157], and tetracycline by ZnO and US [158]. Fe^{3+} and UVC light [159], and nano-Fe_3O_4 coupled to biodegradation [160]. The removal of some antibiotics by photocatalysis and ozone has been described as well [161]. The combined processes facilitate the degradation of antibiotics, but with greater energetic requirements than the individual ones. Table 3 collects the best results reported by selected papers and Figs. 21–23 detail examples of them.

Sepyani et al. [145] treated 100 mL of 0.5–100 mg L^{-1} of amoxicillin in pure water with 0.050 M Na_2SO_4 as supporting electrolyte and 20–80 mM PS at pH= 4.0 in stirred undivided cell with a Fe anode and a graphite cathode. In this way, PS can be activated by its reduction at the cathode by reaction (33) and by Fe^{2+} formed from Fe dissolution by reaction (1). During electrocoagulation, magnetite (Fe_3O_4) was formed from the high contents of iron hydroxide ions originated, as confirmed from the SEM and XRD analysis of the precipitate collected, as shown.

in Fig. 21a and b, respectively. The surface $\equiv Fe^{2+}$ of magnetite can also activate PS from reaction (19). The authors combined this EC process either by irradiating the solution with a 6 W UVC light for additional PS activation by reaction (22) or with an ultrasound (US) bath at 37 kHz to energetically decompose PS by a reaction similar to (32). Operating with 50 mg L^{-1} antibiotic, 80 mM PS, and I = 30 mA, Fig. 21c depicts the low amoxicillin concentration decay with EC and PS alone, whereas it was reduced by 73%, 83%, and 95% for PS/EC, US/PS/EC and UVC/PS/EC, respectively. The combined UVC/PS/EC process was then the more powerful treatment. The effect of scavengers was further studied under PS/EC conditions. Fig. 21d shows the little effect of adding Cl^- and CO_3^{2-} to the medium, probably because they were adsorbed onto the magnetite precipitate, but the degradation was more rapidly inhibited with ethanol than with TBA. This is indicative of the action of $SO_4^{\bullet-}$ and $^{\bullet}OH$ as oxidants (see Table 3). Fig. 21e depicts the expected increase in degradation rate with raising I from 10 to 80 mA, as result of the gradual enhancement of PS activations from reactions (1), (19), and (33). On the other hand, Fig. 21f highlights the curious loss of antibiotic abatement at higher Na_2SO_4 concentration, which can be explained by the rise in the formation of Fe^{2+}-SO_4^{2-} complexes that causes a loss of free Fe^{2+} content with the consequent deceleration of reaction (1).

A stirred undivided cell with a Ti/RuO_2/IrO_2 anode, an activated carbon felt (ACF) cathode, and two inner UVC lamps providing a 6 W light, schematized in Fig. 22a, has been used for the UVC/PS/EO remediation of ciprofloxacin solutions [153]. In this case, PS can be activated at the cathode from reaction (33) and by UVC irradiation from reaction (22). Moreover, the pollutants can be directly oxidized at the anode or by the physisorbed M($^{\bullet}OH$) produced by reaction (35). Fig. 22b shows the percentage of antibiotic degradation determined after 120 min of different processes for 500 mL of 100 mg L^{-1} of ciprofloxacin in pure water with 20 mM PS at pH = 7.0 and a cell voltage of 4.0 V. As can be seen, the process became more efficient as: PS < UVC/PS < PS/EO < UVC/PS/EO. For the latter treatment, total abatement with k_1 = 0.03799 min^{-1} was achieved (see Table 3). Fig. 22c highlights the inhibition caused by added inorganic ions as scavengers of the oxidizing

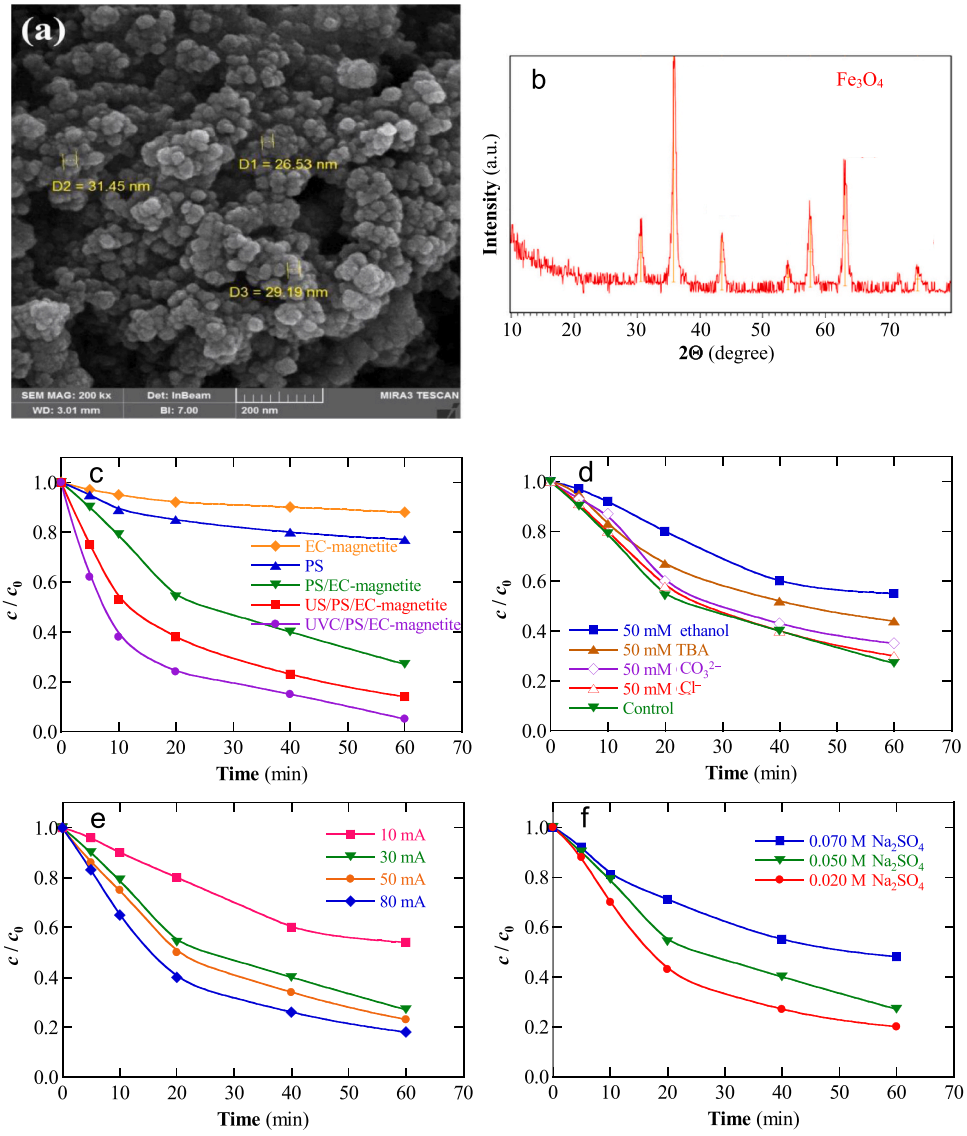

Fig. 21. (a) Scanning electron microscopy (SEM) image and (b) X-Ray diffraction pattern of the magnetite obtained from the electrocoagulation (EC) of 100 mL of 0.050 M Na_2SO_4 at pH = 4.0 filling a stirred undivided cell with a Fe anode and a graphite cathode at current (I) of 30 mA. (c) Normalized amoxicillin concentration with time for different treatments of the above solution with 50 mg L^{-1} antibiotic and 80 mM PS, as well as by illuminating with a 6 W UVC light or introducing the cell in a US bath of 37 kHz. Effect on the antibiotic degradation in the above PS/EC-magnetite process of: (d) ethanol, TBA, CO_3^{2-}, and Cl^-, (e) applied current, and (f) electrolyte concentration.
Adapted from ref. [145]. Fig. 21a and b with permission 5644860133880 from Elsevier.

agents in the order: $Cl^- < NO_3^- < H_2PO_4^- < SO_4^{2-} < HCO_3^-$. Specific.

scavengers also decelerated ciprofloxacin degradation, more rapidly for: methanol < ethanol < TBA < L-histidine. Despite this unexpected trend because the inhibition with TBA should be smaller than with methanol or ethanol, the authors concluded that $^1O_2$ acted as major oxidant than $SO_4^{\bullet-}$ and $^\bullet OH$ (see Table 3). 9 primary by-products were identified by LC-MS analysis.

The characteristics of the hybrid UVC/PS/Fe^{3+} process has been investigated by Zeng et al. [159] considering de degradation of 5.0 mg L^{-1} of tetracycline in pure water with 0.4 mM PS and 0.4 mM Fe^{3+} at pH = 3.0–7.0 using a stirred dish exposed to a 75 W UVC light. Fig. 23a schematizes the mechanism proposed for the generation of radicals like $SO_4^{\bullet-}$, $^\bullet OH$, $O_2^{\bullet-}$ and non-radical Fe(IV) for the degradation of the antibiotic. $SO_4^{\bullet-}$ was generated from PS reduction with Fe^{2+} via its two-electron oxidation to Fe(IV), $^\bullet OH$ was produced either from the UVC activation of PS from reaction (22) followed by reactions (5) or (6) or from the photo-Fenton reaction (40) involving the photolysis of $Fe(OH)_2^+$ species, and $O_2^{\bullet-}$ was formed from O_2 reduction with Fe^{2+} by reaction (41). Fig. 23b depicts the increasing normalized tetracycline abatement for the processes as UVC < PS < UVC/Fe^{3+} < UVC/PS < PS/Fe^{3+} < UVC/PS/Fe^{3+}. For the latter process, total disappearance of the antibiotic was reached after the consumption of a UVC fluence of 220 mJ cm^{-2} with a $k_1 = 0.0222$ cm^2 mJ^{-1} (see Table 3). Fig. 23c shows the percentage of oxidizing agent generated that were determined from several specific scavengers as function of pH. $^\bullet OH$ usually followed by $SO_4^{\bullet-}$ were always the pre-eminent oxidant. Less significant was the contribution of $O_2^{\bullet-}$ and the action of Fe(IV) + others was enhanced at neutral pH = 7.0. This can explain the loss of degradation rate found with increasing pH.

$$Fe(OH)_2^+ + h\nu \rightarrow Fe^{2+} + {}^\bullet OH \quad (40)$$

$$O_2 + Fe^{2+} \rightarrow O_2^{\bullet-} + Fe^{3+} \quad (41)$$

It is also noticeable the sequential treatment of 250 mL of 20 mg L^{-1} of tetracycline in pure water introduced in a conical flask in a shaker at 200 rpm with 0.1 mM of PS, 10 g L^{-1} of nano-

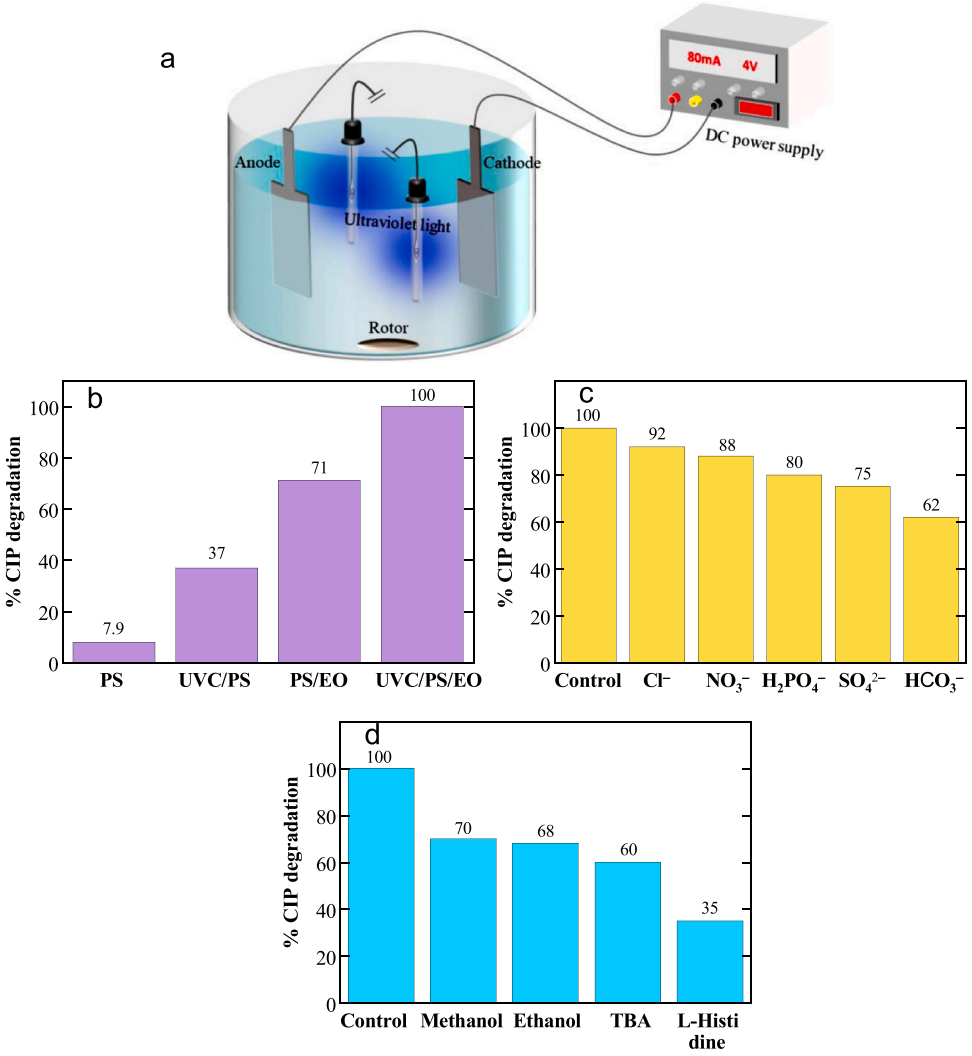

Fig. 22. (a) Set-up of the stirred undivided cell with a $Ti/RuO_2/IrO_2$ anode, an activated carbon felt (ACF) cathode, and two inner UVC lamps providing a 6 W light used for the UVC/PS/EO remediation of ciprofloxacin solutions. (b) Percentage of ciprofloxacin degradation after120 min of different processes for 500 mL of 100 mg L^{-1} of antibiotic in pure water with 20 mM PS at pH = 7.0 by applying a cell voltage of 4.0 V. Effect on the percentage of ciprofloxacin degradation at 120 min of the solution treated by UVC/PS/EO of: (c) inorganic anions at 100 mM concentration and (d) scavengers like 8.8 M methanol, 6.1 M ethanol, 3.6 M TBA, and 4 g L^{-1} L-histidine.
Adapted from ref. [153]. Fig. 22a with permission 5644860867090 Elsevier.

Fe_3O_4 catalyst at pH = 3.0 or 6, followed by biodegradation with microbes of the resulting wastewater after magnetic separation of the catalyst [160]. After 360 min, a 30% and 47% of degradation was achieved for the individual PS and biodegradation processes, respectively. The addition of nano-Fe_3O_4 activated the PS of the suspension, as stated above, and the tetracycline concentration was reduced by 77% at pH = 3.0. In contrast, a 95% abatement was achieved by the sequential PS/nano-Fe_3O_4-biodegradation at pH = 6.0 (see Table 3), indicating its preferred application for tetracycline remediation. The use of biodegradation post-treatment should be more investigated because it ensures the cheap treatment of large wastewater volumes.

4. Change of toxicity of antibiotic waters during the PS based AOPs

The reuse of antibiotic waters is linked to the loss of their toxicity after PS treatment. The lower toxicity of a treated water can be assessed by: (i) direct methods usually involving its antibacterial inhibition, e.g., for the marine bacteria *Vibrio fischeri* or the algae *Microcystis aeruginosa*, or its bioactivity reduction with TTC dehydrogenase, or (ii) indirect methods such as the decay of its oxygen consumption.

Several works have reported the almost overall detoxification of antibiotic waters because of the fast degradation of the non-toxic intermediates formed. This is the case of tetracycline in groundwater with PS/MnO_x catalyst [75] and in mariculture wastewater with UVC/PS [103], chloramphenicol in pure water with Vis/PS/4:1 graphene foam @FeS_2/α-Fe_2O_3 photocatalyst [113], ampicillin in pure water with PS/heat [124], cephalexin in pure water with electrochemically activated PS [136], and ciprofloxacin in pure water with US/PS/Fe^{2+} catalyst [152]. Fig. 24a shows the progressive decay of inhibition of *Vibrio fischeri* for 0.1 mM cephalexin in several media at pH = 7.0 by 1.0 mM PS at 60 °C [125]. At 240 min, an almost total detoxification was achieved, even slightly more rapidly in the presence of HCO_3^- and Cl^-, indicating the scarce influence of such scavengers on the mineralization process involving non- toxic by-products. Similarly, Fig. 24b highlights the practical loss of toxicity vs. *Vibrio fischeri* after 15–20 min of treatment of a suspension with 5 mg L^{-1} norfloxacin, 0.25 mM PS, and 1.5 g L^{-1} C-$ZnFe_2O_4$ catalyst in pure water at pH = 6.7 and 60 °C under 400 W microwaves [78].

However, the toxicity attained a maximal at 10 min due to the rapid

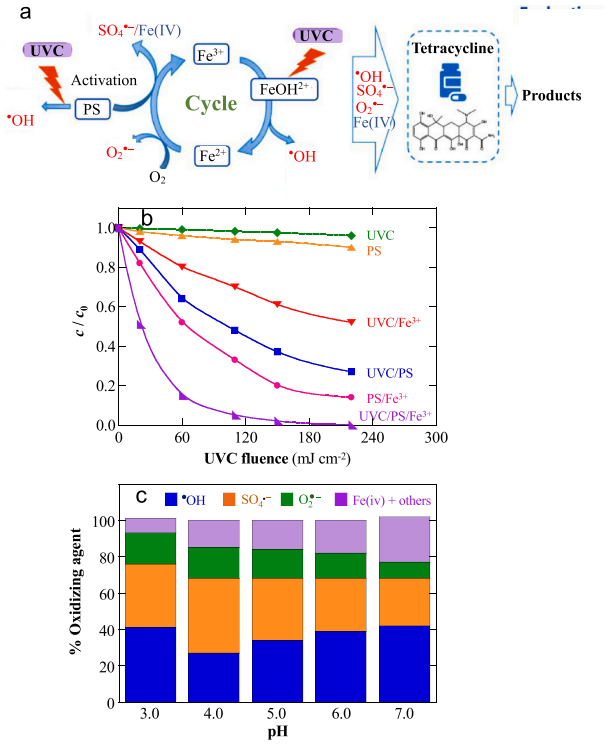

Fig. 23. (a) Mechanism proposed for the generation of radicals and non-radicals for the oxidation of tetracycline by a combined UVC/PS/Fe^{3+} process using a stirred dish illuminated with a 75 W UVC light. (b) Normalized antibiotic concentration as a function of the UVC fluence for the degradation of 5.0 mg L^{-1} of antibiotic in pure water with 0.4 mM PS and/or 0.4 mM Fe^{3+} at pH = 3.0 and 22 ºC by several processes, (c) Percentage of oxidizing agents at different pH values for the UVC/PS/Fe^{3+} process.
Adapted from . [159]. Mechanism (a) with permission 5644861507945 Elsevier.

formation of primary toxic derivatives that are quickly degradeed at longer time. Note that TOC was only reduced by 70% in 40 min, pointing to the non-toxic nature of the remaining final by-products.

In contrast, other antibiotics generate toxic derivatives that only caused as much a partial detoxification of their solutions, as has been described for florfenicol [96] and sulfaquinoxaline [102] with UVC/PS. Other examples are given in Fig. 24c-f. So, Fig. 24c highlights the small change in acute toxicity determined from TCT dehydrogenase for 50 mL of 5.0 mg L^{-1} of levofloxacin or ofloxacin in pure water by UVC/PS with 150 μM PS at pH= 3.0, as result of the toxic primary by-products formed [98]. A total inhibition of *Vibrio fischeri* for the PS generation in a BDD/stainless steel cell filled with 250 mL of 30 mg L^{-1} florfenicol in 0.050 M Na_2SO_4 at pH 3.0 was found for Periyasamy et al. [139] due to the large production of toxic primary derivatives, as can be seen in Fig. 24d. Similarly, Fig. 24e depicts a very little inhibition of *Microcystis aeruginosa* after treating 1.0 mg L^{-1} carbamazepine in pure water with 0.4 mg L^{-1} PS and Fe catalyst at pH = 5.0 under a 240 W and 40 kHz US for 60 min [146]. This behavior was confirmed by the slight difference of the algae concentration produced for the untreated and treated suspensions after several culture days. Fig. 24f shows the small detoxification obtained from the percent of oxygen consumption for the combined activation processes of 50 mg L^{-1} of amoxicillin presented in Fig. 21c. An enhancement in toxicity can be observed at the beginning of the US/PS/EO-magnetite and UVC/PS/EO-magnetite processes as expected by the initial generation of more toxic primary derivatives.

Recently, the relative toxicity of the by-products formed from several antibiotics, previously identified by LC-MS, has been theoretically calculated. So, the evolution of the solution toxicity during the PS treatment can be predicted. This study has been performed for sulfamethoxazole with PS/Fe^{3+}-sulfite catalyst [23] and PS/DBD plasma [133], tetracycline with PS/Fe,Co,O-g-C_3N_4 catalyst [67], ampicillin with near-IR/PS [140], and UVC/PS/Fe^{3+} [159].

5. Conclusions and prospects

It has been shown that activated PS is very effective to remove antibiotics from synthetic and real waters and wastewaters. Radical and non-radical mechanisms for antibiotic degradation with the oxidants detected have been proposed and the inhibition effect of specific scavengers, common inorganic ions, and NOM has been widely assessed. In some cases, the partial or total loss of toxicity of the treated solutions was determined. Comparison with other weaker oxidants, mainly H_2O_2, has also been reported, but with a lack of techno-economic studies to confirm the possible beneficial of PS-based AOPs respect to other conventional treatments for their applicability to antibiotic remediation. Such studies need to be developed in future works.

Most present works over PS-based AOPs have been carried out at bench scale without offering a significant information for their application at large scale. This experimental drawback needs to be solved in the next future by studying the oxidation power and characteristics of such processes using pilot flow plants for treating large volumes of natural and real wastewaters. The mixture of the effluent with the PS solution at different flow rates should be examined and the effect of the activator should be clarified to find the best operating conditions. When using heterogeneous catalysts, its optimal dosage should be determined along with the establishment of an appropriated procedure for its recovery and reuse with cleaning. In such a case, the catalyst should not release toxic ions for ensuring water reuse for their possible scaled-up at industrial level. On the other hand, it is very interesting to explore the use of novel photocatalysts activated with free direct sunlight to significantly improve the oxidation power of the PS systems giving rise to the most favorable conditions for industrial application.

A little number of works have reported the homogeneous catalytic activation of PS mainly with Fe^{2+}. The electron-transfer reaction between PS and Fe^{2+} originated $SO_4^{\bullet-}$ that partially evolved to $^{\bullet}OH$. Good antibiotic degradations have been obtained operating in acidic media to avoid the precipitation of iron hydroxides. The use of specific scavengers such as ethanol and TBA allowed detecting the generation of the above oxidizing radicals. The presence of scavengers like inorganic ions and NOM caused a decay of the loss of antibiotics in real waters and wastewaters. The PS/Fe^{2+} process was superior to Fenton reagent to mineralize a WWTP effluent contaminated with trimethoprim. Fe^{3+} was also checked as homogeneous catalysts but SO_3^{2-} was added to be reduced to the active Fe^{2+} in solution.

Many solid materials have been used as PS activators including biochar, modified biochar, carbonaceous materials, iron and iron compounds, non-ferrous metal oxides, and other catalysts. Biochar was synthesized from waste biomass in the absence of O_2 and its positive action as activator has been explained by the oxidation of surface -OH groups or -C-O-Fe(II) bridges by PS to originate the oxidant $SO_4^{\bullet-}$, also being formed $^{\bullet}OH$, $O_2^{\bullet-}$, and the non-radical $^1O_2$. The composites of modified biochar with metal and metal oxides enhanced the oxidation power of PS activated with biochar alone, promoting the non-radical mechanism. With Fe_3O_4/biochar, non-radical mechanisms involving Fe(IV) and the oxidation of the adsorbed antibiotic onto the catalyst by direct electron-transfer with surface PS were envisaged as well. The preponderance of the radical or non-radical mechanism depended on the kind of modified biochar, but most of them presented a low reusability, except FeCu/biochar, mainly due to the progressive loss of the metal coating. The existence of non-radical mechanisms have also been detected with carbonaceous materials like S,N-carbon. For iron and iron compounds like nZVI and S-nZVI, the surface Fe(II) and Fe^0 reduced PS, and the corrosion of Fe^0 yielded Fe^{2+} to react with PS in the medium. These processes enhanced the antibiotic degradation. Good performance using non-ferrous metal oxides in pure water have been described with

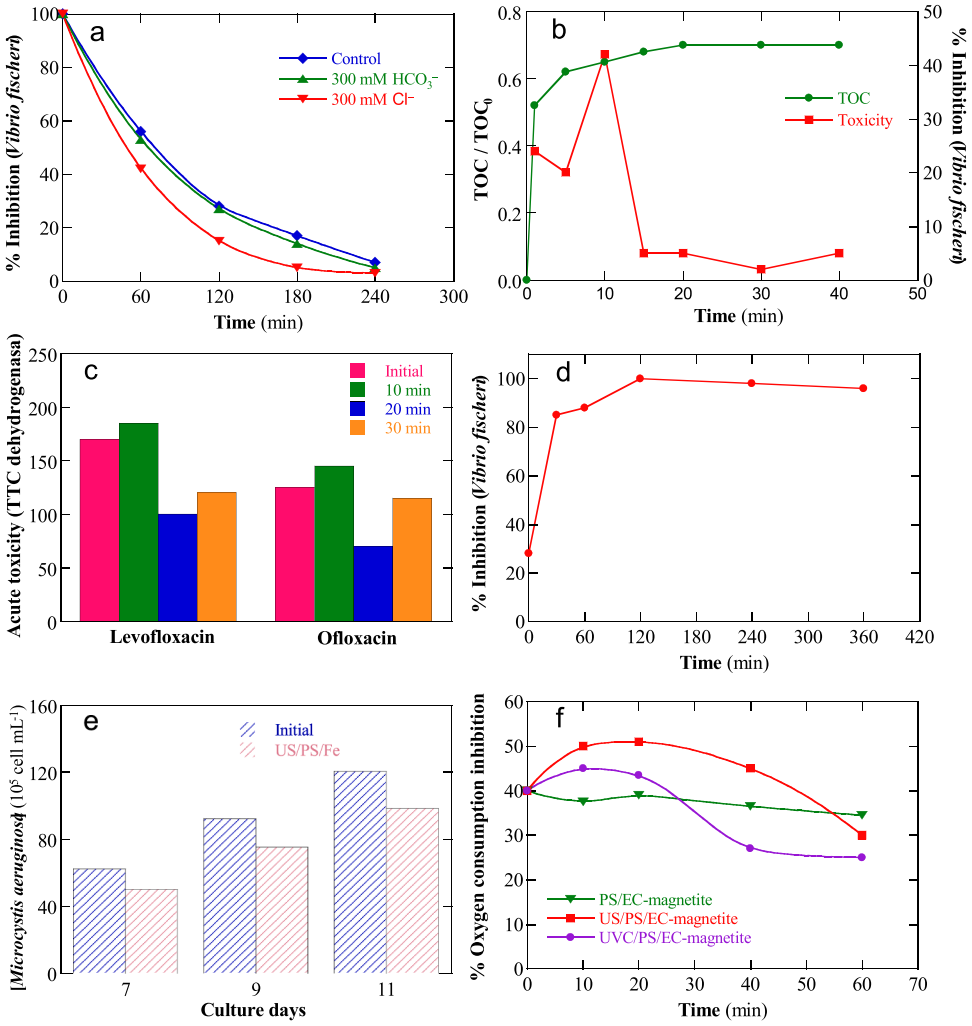

Fig. 24. (a) Percentage of inhibition of Vibrio fischeri with time for 100 mL of 0.1 mM cephalexin in several media of 10 mM phosphate buffer with 1.0 mM PS at pH 7.0 and 60 °C (b) Change of normalized TOC concentration and percent of inhibition of Vibrio fischeri with time for 5 mg L^{-1} norfloxacin with 0.25 mM PS and 1.5 g L^{-1} C-ZnFe2O4 at pH = 6.7 and 60 °C upon 400 W microwaves (c) Time course of acute toxicity determined as TTC dehydrogenase activity for 50 mL of 5.0 mg L^{-1} of levofloxacin or ofloxacin in pure water with 150 μM PS at pH= 3.0 under a 25 W UVC light. (d) Percentage of inhibition of Vibrio fischeri vs. time for 250 mL of 30 mg L^{-1} florfenicol in 0.050 M Na_2SO_4 at pH 3.0 with a BDD/stainless steel cell to generate PS at 60 mA cm^{-2} (e) Content of Microcystis aeruginosa produced during several culture days from 105 cell mL^{-1} introduced into 1.0 mg L^{-1} carbamazepine at pH = 5.0 (initial) and after treating with 0.4 mg L^{-1} PS and Fe upon 240 W and 40 kHz US for 60 min. (f) Percent of oxygen consumption with time determined for the amoxicillin assays of Fig. 21c
(a) (adapted from ref. [125]). (b) (adapted from ref. [78]). (c) (adapted from ref. [98]).(d) (adapted from ref. [139]) (e) (adapted from ref. [146]).(f) (adapted from ref. [145]).

the generation of $SO_4^{\bullet-}$, $^{\bullet}OH$, and in some cases $O_2^{\bullet-}$ as well as an excellent reusability for $LaNiO_3$ and MnO_x. However, the fast removal achieved with $LaNiO_3$ catalyst in pure water was strongly inhibited in bottled water and a WWTP effluent, reason for which this catalyst does not seem useful for the treatment of real waters and wastewaters. Other catalysts like tourmaline also yielded excellent degradation of sulfamethazine in pure water. For the heterogeneous catalysts, the rise of PS and catalyst dosage and the lowering of antibiotic content and pH enhanced the degradation rate in pure water, but the oxidation power strongly decreased in real effluents by the scavenging effect of their components. The scavenging of humic and/or fulvic acid and of common inorganic ions, with larger inhibition for HCO_3^- and CO_3^{2-}, was confirmed in most studies.

UVC irradiation caused the energetic decomposition of PS to $SO_4^{\bullet-}$ to degrade antibiotics. The degradation rate was increased with the UVC fluence. $SO_4^{\bullet-}$ and $^{\bullet}OH$ were usually reported as oxidants. Fast decay of antibiotics and good TOC abatement of their solutions in pure water were determined by UVC/PS, much greater than those of UVC/ClO^- and UVC/H_2O_2. However, the applicability of the UVC/PS treatment can be limited by the expensive cost of the UVC lamp, being more reasonable the use of suitable photocatalysts illuminated with free sunlight for PS activation. Pd/$BiVO_4$, MIL-101(Fe)− 1-(4-(methyl)phenyl)urea, carbonyl modified g-C_3N_4, 4:1 graphene foam @FeS_2/α-Fe_2O_3, α-Fe_2O_3/ZnO/rGO, and CuO_x/$BiVO_4$ photocatalysts under simulated sunlight or visible LED light showed a rapid total degradation of antibiotics and in some cases, a large mineralization. In these photocatalytic processes, $SO_4^{\bullet-}$, $^{\bullet}OH$, $O_2^{\bullet-}$, $^1O_2$, and holes were usually detected as oxidants, indicating the existence of radical and non-radical mechanisms for antibiotic removal. A 39 L pilot flow plant with a solar CPC photoreactor and a conventional TiO_2 photocatalyst rapidly degraded 1.0 mg L^{-1} trimethoprim in natural water by TiO_2/solar/PS, much faster than using solar/H_2O_2/PS, demonstrating the interest of these systems to characterize the solar photocatalytic activation of PS. The development of solar pilot flow plants in the next future should be combined with the application of novel solar photocatalysts to enhance the degradation rate and mineralization of antibiotic waters.

The PS/heat process yielded a relatively fast total removal of antibiotics, which raised with increasing temperature due to the increase in

rate of the energetically decomposition of PS to $SO_4^{\bullet-}$ with generation of more $^{\bullet}OH$. It was also enhanced at lower antibiotic concentration and pH and at higher PS dosage. The treatment was potent enough to mineralize up to a 97% of 100 mg L^{-1} metronidazole in pure water at 60 ºC. The DBD activation of PS has shown an excellent effectiveness to remove antibiotics like metronidazole and sulfamethoxazole with generation of O_3, H_2O_2. $SO_4^{\bullet-}$, $^{\bullet}OH$, $O_2^{\bullet-}$, and $^1O_2$ as oxidants, However, the high energetic requirements of the DBD system limits its actual application to large water volumes in practice. Several approaches have been proposed for the electrochemical activation of PS. Apart from the cathodic reduction of this compound to $SO_4^{\bullet-}$, a recent work has proposed that a SnO_2/Ni@N-CNTs anode was able to remove cephalexin by direct oxidation of mediated oxidation with physisorbed $^{\bullet}OH$ or $SO_4^{\bullet-}$ formed from PS reduction with the hydroxyl group of its surface. This is an exciting field that requires more attention in further research. Treatments with other activators of PS like gamma irradiation, O_3, and microwaves have also shown an excellent effectiveness to remediate antibiotic solutions.

The use of combined processes for activating PS facilitates the degradation of antibiotics, but with greater energetic requirements than the individual ones. Among the hybrid processes with independent activators, good results have been reported for electrochemical processes with or without Fe_3O_4 generation coupled to UVC light and for UVC/PS/Fe^{3+} with production of oxidants like $SO_4^{\bullet-}$, $^{\bullet}OH$, $O_2^{\bullet-}$ and the non-radical Fe(IV). Up to 95% abatement of 20 mg L^{-1} of tetracycline was achieved by a sequential process of PS/nano-Fe_3O_4 followed by biodegradation at pH = 6.0, indicating that biodegradation post-treatment should be more investigated because it ensures the cheap treatment of large wastewater volumes.

The toxicity of treated antibiotic solutions has been assessed by direct methods based on the antibacterial inhibition of the bacteria *Vibrio fischeri* or the algae *Microcystis aeruginosa*, or its bioactivity reduction with TTC dehydrogenase, as well as indirect methods as the decay of its oxygen consumption. Solutions with ampicillin, cephalexin, ciprofloxacin, norfloxacin, and tetracycline can be completely detoxified by PS-based AOPs, whereas a scarce detoxification has been found for solutions of other antibiotics like amoxicillin, carbamazepine, florfenicol, levofloxacin, and sulfaquinoxaline due to the formation of toxic by-products. Recently, the theoretical relative toxicity of the by-products formed from several antibiotics has been theoretically calculated to predict the evolution of the solution toxicity during the PS treatment. All this knowledge is needed to know the possible reusability of treated wastewaters.

Declaration of Competing Interest

The authors declare that they have no known competing financial interests or personal relationships that could have appeared to influence the work reported in this paper.

Data Availability

Data will be made available on request.

References

[1] A.J. dos Santos, M.S. Kronka, G.V. Fortunato, M.R.V. Lanza, Recent advances in electrochemical water technologies for the treatment of antibiotics: a short review, Curr. Opin. Electrochem. 26 (2021), 100674, https://doi.org/10.1016/j.coelec.2020.100674.

[2] S. Li, Y. Liu, R. Ge, S. Yang, Y. Zhai, T. Hua, B.S. Ondon, Q. Zhou, F. Li, Microbial electro-Fenton: a promising system for antibiotics resistance genes degradation and energy generation, Sci. Total Environ. 699 (2020), 134160, https://doi.org/10.1016/j.scitotenv.2019.134160.

[3] E. Brillas, Progress of homogeneous and heterogeneous electro-Fenton treatments of antibiotics in synthetic and real wastewaters. A critical review on the period 2017–2021, Sci. Total Environ. 819 (2022), 153102, https://doi.org/10.1016/j.scitotenv.2022.153102.

[4] J. Meijide, P.S.M. Dunlop, M. Pazos, M.A. Sanromán, Heterogeneous electro-Fenton as "Green" technology for pharmaceutical removal: a review, Catalysts 11 (1) (2021) 22, https://doi.org/10.3390/catal11010085.

[5] X. Liu, Y. Zhou, J. Zhang, L. Luo, Y. Yang, H. Huang, H. Peng, L. Tang, Y. Mu, Insight into electro-Fenton and photo-Fenton for the degradation of antibiotics: mechanism study and research gaps, Chem. Eng. J. 347 (2018) 379–397, https://doi.org/10.1016/j.cej.2018.04.142.

[6] H. Monteil, Y. Péchaud, N. Oturan, M.A. Oturan, A review on efficiency and cost effectiveness of electro- and bio-electro-Fenton processes: application to the treatment of pharmaceutical pollutants in water, Chem. Eng. J. 376 (2019), 119577, https://doi.org/10.1016/j.cej.2018.07.179.

[7] E. Brillas, S. Garcia-Segura, Benchmarking recent advances and innovative technology approaches of Fenton, photo-Fenton, electro-Fenton, and related processes: a review on the relevance of phenol as model molecule, Sep. Purif. Technol. 237 (2020) 11633, https://doi.org/10.1016/j.seppur.2019.116337.

[8] E. Brillas, A critical review on ibuprofen removal from synthetic waters, natural waters, and real wastewaters by advanced oxidation processes, Chemosphere 286 (2022), 131849, https://doi.org/10.1016/j.chemosphere.2021.131849.

[9] A. Hassani, J. Scaria, F. Ghanbari, P.V. Nidheesh, Sulfate radicals-based advanced oxidation processes for the degradation of pharmaceuticals and personal care products: a review on relevant activation mechanisms, performance, and perspectives, Environ. Res. 217 (2023), 114789, https://doi.org/10.1016/j.envres.2022.114789.

[10] A.J. dos Santos, I. Sirés, E. Brillas, Removal of bisphenol A from acidic sulfate medium and urban wastewater using persulfate activated with electroregenerated Fe^{2+}, Chemosphere 263 (2021), 128271 https://doi.org/10.1016/j.chemosphere.2020.128271.

[11] Z. Honarmandrad, X. Sun, Z. Wang, M. Naushad, G. Boczkaj, Activated persulfate and peroxymonosulfate based advanced oxidation processes (AOPs) for antibiotics degradation - a review, Water Res. Ind. 29 (2023), 100194, https://doi.org/10.1016/j.wri.2022.100194.

[12] M. Pirsaheb, H. Hossaini, H. Janjani, An overview on ultraviolet persulfate based advances oxidation process for removal of antibiotics from aqueous solutions: a systematic review, Desal. Water Treat. 165 (2019) 382–395, https://doi.org/10.5004/dwt.2019.24559.

[13] Y. Zhang, Y.-G. Zhao, F. Maqbool, Y. Hu, Removal of antibiotics pollutants in wastewater by UV-based advanced oxidation processes: influence of water matrix components, processes optimization and application: a review, J. Water Process Eng. 45 (2022), 102496, https://doi.org/10.1016/j.jwpe.2021.102496.

[14] S. Anandan, V. Kumar Ponnusamy, M. Ashokkumar, A review on hybrid techniques for the degradation of organic pollutants in aqueous environament, Ultrason. Sonochem. 67 (2020), 105130, https://doi.org/10.1016/j.ultsonch.2020.105130.

[15] E. Calcio Gaudino, E. Canova, P. Liu, Z. Wu, G. Cravotto, Degradation of antibiotics in wastewater: new advances in cavitational treatments, Molecules 26 (2021), https://doi.org/10.3390/molecules26030617.

[16] G. Chen, Y. Yu, L. Liang, X. Duan, R. Li, X. Lu, B. Yan, N. Li, S. Wang, Remediation of antibiotic wastewater by coupled photocatalytic and persulfate oxidation system: a critical review, J. Hazard. Mater. 408 (2021), 124461, https://doi.org/10.1016/j.jhazmat.2020.124461.

[17] Z. Li, J. Wang, J. Chang, B. Fu, H. Wang, Insight into advanced oxidation processes for the degradation of fluoroquinolone antibiotics: removal, mechanism, and influencing factors, Sci. Total Environ. 857 (2023), 159172, https://doi.org/10.1016/j.scitotenv.2022.159172.

[18] Y. Ji, C. Ferronato, A. Salvador, X. Yang, J.-M. Chovelon, Degradation of ciprofloxacin and sulfamethoxazole by ferrous-activated persulfate: Implications for remediation of groundwater contaminated by antibiotics, Sci. Total Environ. 472 (2014) 800–808, https://doi.org/10.1016/j.scitotenv.2013.11.008.

[19] I. Epold, M. Trapido, N. Dulova, Degradation of levofloxacin in aqueous solutions by Fenton, ferrous ion-activated persulfate and combined Fenton/persulfate systems, Chem. Eng. J. 279 (2015) 452–462, https://doi.org/10.1016/j.cej.2015.05.054.

[20] G. Ayoub, A. Ghauch, Assessment of bimetallic and trimetallic iron-based systems for persulfate activation: application to sulfamethoxazole degradation, Chem. Eng. J. 256 (2014) 280–292, https://doi.org/10.1016/j.cej.2014.07.002.

[21] S. Wang, J. Wang, Comparative study on sulfamethoxazole degradation by Fenton and Fe(II)-activated persulfate process, RSC Adv. 7 (2017) 48670–48677, https://doi.org/10.1039/c7ra09325j.

[22] S. Wang, J. Wang, Trimethoprim degradation by Fenton and Fe(II)-activated persulfate processes, Chemosphere 191 (2018) 97–105, https://doi.org/10.1016/j.chemosphere.2017.10.040.

[23] D. Yuan, C. Zhang, S. Tang, M. Sun, Y. Zhang, Y. Rao, Z. Wang, J. Ke, Fe^{3+}-sulfite complexation enhanced persulfate Fenton-like process for antibiotic degradation based on response surface optimization, Sci. Total Environ. 727 (2020), 138773, https://doi.org/10.1016/j.scitotenv.2020.138773.

[24] T. Wang, Y. Zhou, S. Cao, J. Lu, Y. Zhou, Degradation of sulfanilamide by Fenton-like reaction and optimization using response surface methodology, Ecotoxicol. Environ. Saf. 172 (2019) 334–340, https://doi.org/10.1016/j.ecoenv.2019.01.106.

[25] A.C. Velosa, C.A.O. Nascimento, Evaluation of sulfathiazole degradation by persulfate in Milli-Q water and in effluent of a sewage treatment plant, Environ. Sci. Pollut. Res. 24 (2017) 6270–6277, https://doi.org/10.1007/s11356-016-7036-z.

[26] Y.-P. Chen, C.-H. Zheng, Y.-Y. Huang, Y.-R. Chen, Removal of chlortetracycline from water using spent tea leaves-based biochar as adsorption-enhanced

persulfate activator, Chemosphere 286 (2022), 131770, https://doi.org/10.1016/j.chemosphere.2021.131770.
[27] Y. Zhang, M. Xu, S. Liang, Z. Feng, J. Zhao, Mechanism of persulfate activation by biochar for the catalytic degradation of antibiotics: synergistic effects of environmentally persistent free radicals and the defective structure of biochar, Sci. Total Environ. 794 (2021), 148707, https://doi.org/10.1016/j.scitotenv.2021.148707.
[28] L. Kemmou, Z. Frontistis, J. Vakros, I.D. Manariotis, D. Mantzavinos, Degradation of antibiotic sulfamethoxazole by biochar-activated persulfate: factors affecting the activation and degradation processes, Catal. Today 313 (2018) 128–133, https://doi.org/10.1016/j.cattod.2017.12.028.
[29] Y. Zhang, M. Xu, X. Liu, M. Wang, J. Zhao, S. Li, M. Yin, Regulation of biochar mediated catalytic degradation of quinolone antibiotics: important role of environmentally persistent free radicals, Biores. Technol. 326 (2021), 124780, https://doi.org/10.1016/j.biortech.2021.124780.
[30] S. Zhang, K. Zheng, G. Xu, B. Liang, Q. Yin, Enhanced removal of tetracycline via advanced oxidation of sodium persulfate and biochar adsorption, Environ. Sci. Pollut. Res. 29 (2022) 72556–72567, https://doi.org/10.1007/s11356-022-20817-7.
[31] X. Fan, W. Zhang, Y. Liu, S. Shi, Y. Cui, Z. Zhao, J. Hou, Hydrothermal synthesis of sewage sludge biochar for activation of persulfate for antibiotic removal: efficiency, stability and mechanism, Environ. Res. 218 (2023), 114937, https://doi.org/10.1016/j.envres.2022.114937.
[32] B. Lv, W. Zhang, Y. Liu, D. Xu, X. Fan, Excess sludge biochar facilitates persulfate activation for highly efficient tetracycline removal, Water Sci. Technol. 86 (2022) 2059–2070, https://doi.org/10.2166/wst.2022.338.
[33] X. Kang, Q. Zhang, X. Liu, J. Song, H. Guo, L. Wang, The interface mechanism of sludge biochar activating persulfate to remove tetracycline: the role of the C-O-Fe bridge at the carbon surface, J. Clean. Prod. 384 (2023), 135514, https://doi.org/10.1016/j.jclepro.2022.135514.
[34] E. Grilla, J. Vakros, I. Konstantinou, I.D. Manariotis, D. Mantzavinos, Activation of persulfate by biochar from spent malt rootlets for the degradation of trimethoprim in the presence of inorganic ions, J. Chem. Technol. Biotechnol. 95 (2020) 2348–2358, https://doi.org/10.1002/jctb.6513.
[35] H. Song, Q. Li, Y. Ye, F. Pan, D. Zhang, D. Xia, Degradation of cephalexin by persulfate activated with magnetic loofah biochar: performance and mechanism, Sep. Purif. Technol. 273 (2021), 118971, https://doi.org/10.1016/j.seppur.2021.118971.
[36] Z. Jiang, J. Wei, Y. Zhang, X. Niu, J. Li, Y. Li, G. Pan, M. Xu, X. Cui, N. Cui, J. Li, Electron transfer mechanism mediated nitrogen-enriched biochar encapsulated cobalt nanoparticles catalyst as an effective persulfate activator for doxycycline removal, J. Clean. Prod. 384 (2023), 135641, https://doi.org/10.1016/j.jclepro.2022.135641.
[37] S. Cai, T. Wang, C. Wu, W. Tang, J. Chen, Efficient degradation of norfloxacin using a novel biochar-supported CuO/Fe_3O_4 combined with peroxydisulfate: insights into enhanced contribution of nonradical pathway, Chemosphere 329 (2023), 138589, https://doi.org/10.1016/j.chemosphere.2023.138589.
[38] F.-X. Dong, L. Yan, S.-T. Huang, J.-Y. Liang, W.-X. Zhang, X.-W. Yao, X. Chen, W. Qian, P.-R. Guo, L.-J. Kong, W. Chu, Z.-H. Diao, Removal of antibiotics sulfadiazine by a biochar based material activated persulfate oxidation system: performance, products and mechanism, Process Saf. Environ. Prot. 157 (2022) 411–419, https://doi.org/10.1016/j.psep.2021.11.045.
[39] J. Liang, X. Duan, X. Xu, K. Chen, Y. Zhang, L. Zhao, H. Qiu, S. Wang, X. Cao, Persulfate oxidation of sulfamethoxazole by magnetic iron-char composites via nonradical pathays: Fe(IV) versus surface-mediated electron transfer, Environ. Sci. Technol. 55 (2021) 10077–10086, https://doi.org/10.1021/acs.est.1c01618.
[40] M. Zhang, K. Huang, Y. Ding, X. Wang, Y. Gao, P. Li, Y. Zhou, Z. Guo, Y. Zhang, D. Wu, N, S, Co-doped carbons derived from Enteromorpha prolifera by a molten salt approach: antibiotics removal performance and techno-economic analysis, Nanomaterials 12 (2022), https://doi.org/10.3390/nano12234289.
[41] G. Papatheodorou, P. Ntzoufra, E. Hapeshi, J. Vakros, D. Mantzavinos, Hybrid biochar/ceria nanomaterials: synthesis, characterization and activity assessment for the persulfate-induced degradation of antibiotic sulfamethoxazole, Nanomaterials 12 (2022), https://doi.org/10.3390/nano12020194.
[42] S. Cai, Y. Liu, J. Chen, FeCu/biochar enhances the removal of antibacterial sulfapyridine from groundwater by activation of persulfate, Environ. Chem. Lett. 18 (2020) 1693–1700, https://doi.org/10.1007/s10311-020-01026-5.
[43] Z. Pi, X. Li, D. Wang, Q. Xu, Z. Tao, X. Huang, F. Yao, Y. Wu, L. He, Q. Yang, Persulfate activation by oxidation biochar supported magnetite particles for tetracycline removal: performance and degradation pathway, J. Clean. Prod. 235 (2019) 1103–1115, https://doi.org/10.1016/j.jclepro.2019.07.037.
[44] J. Xu, X. Zhang, C. Sun, J. Wan, H. He, F. Wang, Y. Dai, S. Yang, Y. Lin, X. Zhan, Insights into removal of tetracycline by persulfate activation with peanut shell biochar coupled with amorphous Cu-doped FeOOH composite in aqueous solution, Environ. Sci. Pollut. Res. 26 (2019) 2820–2834, https://doi.org/10.1007/s11356-018-3777-1.
[45] F. Shao, Y. Wang, Y. Mao, T. Shao, J. Shang, Degradation of tetracycline in water by biochar supported nanosized iron activated persulfate, Chemosphere 261 (2020), 127844, https://doi.org/10.1016/j.chemosphere.2020.127844.
[46] Z. Guo, G. Bai, B. Huang, N. Cai, P. Guo, L. Chen, Preparation and application of a novel biochar-supported red mud catalyst - active sites and catalytic mechanism, J. Hazard. Mater. 408 (2021), 124802, https://doi.org/10.1016/j.jhazmat.2020.124802.
[47] H. Zeng, J. Li, J. Xu, W. Qi, R. Hao, G. Gao, D. Lin, D. Li, J. Zhang, Preparation of magnetic N-doped iron sludge based biochar and its potential for persulfate activation and tetracycline degradation, J. Clean. Prod. 378 (2022), 134519, https://doi.org/10.1016/j.jclepro.2022.134519.
[48] J. Wang, M. Dou, X. Wang, B. Gao, Y. Zhuang, Z. Ma, Synergetic mechanism of defective g-C_3N_4 activated persulfate on removal of antibiotics and resistant bacteria: ROSs transformation, electron transfer and noncovalent interaction, Chemosphere 294 (2022), 133741, https://doi.org/10.1016/j.chemosphere.2022.133741.
[49] M. Forouzesh, A. Ebadi, A. Aghaeinejad-Meybodi, Degradation of metronidazole antibiotic in aqueous medium using activated carbon as a persulfate activator, Sep. Purif. Technol. 240 (2019) 145–151, https://doi.org/10.1016/j.seppur.2018.07.066.
[50] J. Kang, X. Duan, L. Zhou, H. Sun, M.O. Tadé, S. Wang, Carbocatalytic activation of persulfate for removal of antibiotics in water solutions, Chem. Eng. J. 288 (2016) 399–405, https://doi.org/10.1016/j.cej.2015.12.040.
[51] F. Qian, H. Yin, F. Liu, J. Sheng, S. Gao, Y. Shen, The in situ catalytic oxidation of sulfamethoxazole via peroxydisufate activation operated in a NG/rGO/CNTs composite membrane filtration, Environ. Sci. Pollut. Res. 28 (2021) 26828–26839, https://doi.org/10.1007/s11356-021-12545-1.
[52] W. Tian, J. Lin, H. Zhang, X. Duan, H. Wang, H. Sun, S. Wang, Kinetics and mechanism of synergistic adsorption and persulfate activation by N-doped porous carbon for antibiotics removals in single and binary solutions, J. Hazard. Mater. 423 (2022), 127083, https://doi.org/10.1016/j.jhazmat.2021.127083.
[53] O. Vieira, R.S. Ribeiro, M. Pedrosa, A.R. Lado Ribeiro, A.M.T. Silva, Nitrogen-doped reduced graphene oxide-PVDF nanocomposite membrane for persulfate activation and degradation of water organic micropollutants, Chem. Eng. J. 402 (2020), 126117, https://doi.org/10.1016/j.cej.2020.126117.
[54] X. Huo, P. Zhou, J. Zhang, Y. Liu, X. Cheng, Y. Liu, W. Li, Y. Zhang, N, S-Doped porous carbons for persulfate activation to remove tetracycline: nonradical mechanism, J. Hazard. Mater. 291 (2020), 122055, https://doi.org/10.1016/j.jhazmat.2020.122055.
[55] C. Yang, Y. Zhu, J. Chen, T. Wu, J. Wang, X. Zhao, W. Sun, H. Lin, S. Lv, Graphene/Fe@N-doped carbon hybrid derived from spent MOF adsorbent as efficient persulfate activator for degradation of tetracycline hydrochloride, Chem. Eng. J. 431 (2022), 133443, https://doi.org/10.1016/j.cej.2021.133443.
[56] N. Osouleddini, L. Tajik, M. Moradi, Degradation of amoxicillin by persulfate activated with Fe_3O_4/GO nanocomposite in aqueous solution, Des. Water Treat. 153 (2019) 392–401, https://doi.org/10.5004/dwt.2019.23970.
[57] F. He, W. Ma, D. Zhong, Y. Yuan, Degradation of chloramphenicol by α-FeOOH-activated two different double-oxidant systems with hydroxylamine assistance, Chemosphere 250 (2020), 126150, https://doi.org/10.1016/j.chemosphere.2020.126150.
[58] G. Wu, W. Kong, Y. Gao, Y. Kong, Z. Dai, H. Dan, Y. Shang, S. Wang, F. Yin, Q. Yue, B. Gao, Removal of chloramphenicol by sulfide-modified nanoscale zero-valent iron activated persulfate: performance, salt resistance, and reaction mechanisms, Chemosphere 286 (2022), 131876, https://doi.org/10.1016/j.chemosphere.2021.131876.
[59] M. Li, X. Yang, D. Wang, J. Yuan, Enhanced oxidation of erythromycin by persulfate activated iron powder-H_2O_2 system: role of the surface Fe species and synergistic effect of hydroxyl and sulfate radicals, Chem. Eng. J. 317 (2017) 103–111, https://doi.org/10.1016/j.cej.2016.12.126.
[60] J. Wu, J. Li, G. Owens, Z. Chen, Toward green nano adsorbents and catalysts: highly active Fe/Mn nanoparticles for enhanced oxidation of oxytetracycline and levofloxacin, J. Colloid Interface Sci. 632 (2023) 299–310, https://doi.org/10.1016/j.jcis.2022.11.074.
[61] C. Chokejaroenrat, C. Sakulthaew, A. Angkaew, T. Satapanajaru, A. Poapolathep, T. Chirasatienpon, Remediating sulfadimethoxine-contaminated aquaculture wastewater using ZVI-activated persulfate in a flow-through system, Aquac. Eng. 84 (2019) 99–105, https://doi.org/10.1016/j.aquaeng.2018.12.004l.
[62] L. Du, W. Xu, Y. Liu, X. Li, D. Huang, S. Wu, Removal of sulfamethoxazole in aqueous solutions by iron-based advanced oxidation processes: performances and mechanisms, Water, Air, Soil Pollut. 231 (2020), https://doi.org/10.1007/s11270-020-04534-w.
[63] X. Yu, X. Jin, N. Wang, Y. Yu, X. Zhu, M. Chen, Y. Zhong, J. Sun, L. Zhu, Transformation of sulfamethoxazole by sulfidated nanoscale zerovalent iron activated persulfate: mechanism and risk assessment using environmental metabolomics, J. Hazard. Mater. 428 (2022), 128244, https://doi.org/10.1016/j.jhazmat.2022.128244.
[64] R.S. Ribeiro, Z. Frontistis, D. Mantzavinos, A.M. T Silva, J.L. Faria, H.T. Gomes, Screening of heterogeneous catalysts for the activated persulfate oxidation of sulfamethoxazole in aqueous matrices. Does the matrix affect the selection of catalyst? J. Chem. Technol. Biotechnol. 94 (2019) 2425–2432, https://doi.org/10.1002/jctb.6080.
[65] L. Niu, G. Zhang, G. Xian, Z. Ren, T. Wei, Q. Li, Y. Zhang, Z. Zou, Tetracycline degradation by persulfate activated with magnetic γ-Fe_2O_3/CeO_2 catalyst: performance, activation mechanism and degradation pathway, Sep. Purif. Technol. 259 (2021), 118156, https://doi.org/10.1016/j.seppur.2020.118156.
[66] L. Xie, F.-Y. Chen, Y.-B. Tang, C.-C. Hao, Tetracycline degradation by persulfate activated with novel magnetic composite ferrocene/chitosan@Fe_3O_4, J. Chem. Technol. Biotechnol. 97 (2022) 2766–2774, https://doi.org/10.1002/jctb.7145.
[67] Z. Wu, Z. Tong, Y. Xie, H. Sun, X. Gong, P. Qin, Y. Liang, X. Yuan, D. Zou, L. Jiang, Efficient degradation of tetracycline by persulfate activation with Fe, Co and O co-doped g-C_3N_4: performance, mechanism and toxicity, Chem. Eng. J. 434 (2022), 134732, https://doi.org/10.1016/j.cej.2022.134732.
[68] J. Fan, Y. Cai, S. Shen, L. Gu, New insights into FeS/persulfate system for tetracycline elimination: iron valence, homogeneous-heterogeneous reactions

and degradation pathways, J. Environ. Sci. (China) 112 (2022) 48–58, https://doi.org/10.1016/j.jes.2021.04.031.
[69] J. Ma, X. Wang, X. Zhang, Z. Ye, S. Sun, L. Zhou, Preparation of $FeSe_2$-based Fenton catalysts loaded on chloro-methyl styrene-based resins and study of activated persulfate degradation of tetracycline, Sustain. (Switz.) 25 (2023), https://doi.org/10.3390/su15043657.
[70] C. Li, N. de Melo Costa Serge, R.F.P. Nogueira, S. Chiron, V. Goetz, Peroxydisulfate activation by CuO pellets in a fixed-bed column, operating mode and assessments for antibiotics degradation and urban wastewater disinfection, Environ. Sci. Pollut. Res. 29 (2022) 71709–71720, https://doi.org/10.1007/s11356-022-20847-1.
[71] Y. Zhang, C. Zhang, S. Xing, Fabrication of NiO/Mg-Al layered double hydroxide with superior performance for peroxydisulfate activation, J. Solid State Chem. 304 (2021), 122565, https://doi.org/10.1016/j.jssc.2021.122565.
[72] A. Petala, O.S. Arvaniti, M. Christofili, A. Safakas, Z. Frontistis, D. Mantzavinos, Lanthanum nickel oxide: an effective heterogeneous activator of sodium persulfate for antibiotics elimination, Catalysts 10 (2020) 1–17, https://doi.org/10.3390/catal10121373.
[73] C. Gkika, A. Petala, Z. Frontistis, G. Bampos, D. Hela, L. Konstantinou, D. Mantzavinos, Heterogeneous activation of persulfate by lanthanum strontium cobaltite for sulfamethoxazole degradation, Catal. Today 361 (2021) 130–138, https://doi.org/10.1016/j.cattod.2020.01.046.
[74] Z. Liu, Z. Gao, Q. Wu, Activation of persulfate by magnetic zirconium-doped manganese ferrite for efficient degradation of tetracycline, Chem. Eng. J. 423 (2021), 130283, https://doi.org/10.1016/j.cej.2021.130283.
[75] T. Wang, K.-M. Xu, K.-X. Yan, L.-G. Wu, K.-P. Chen, J.-C. Wu, H.-L. Chen, Comparative study of the performance of controlled release materials containing mesoporous MnOx in catalytic persulfate activation for the remediation of tetracycline contaminated groundwater, Sci. Total Environ. 846 (2022), 157217, https://doi.org/10.1016/j.scitotenv.2022.157217.
[76] C. Geçgel, O. Görmez, B. Gözmen, M. Turabik, D. Kalderis, A dual purpose aluminum-based metal organic framework for the removal of chloramphenicol from wastewater, Chemosphere 308 (2022), 136411, https://doi.org/10.1016/j.chemosphere.2022.136411.
[77] T. Olmez-Hanci, I. Arslan-Alaton, M. Dogan, S. Khoei, H. Fakhri, G. Korkmaz, Enhanced degradation of micropollutants by zero-valent aluminum activated persulfate: assessment of toxicity and genotoxic activity, Water Sci. Technol. 76 (2017) 3195–3204, https://doi.org/10.2166/wst.2017.489.
[78] Y. Gao, W. Wang, M. Xu, Y. Hao, D. Zou, The magnetically recoverable C-$ZnFe_2O_4$ as a microwave absorption catalyst for the degradation of norfloxacin by persulfate: mechanism, degradation pathway, toxicity, and stability, J. Environ. Chem. Eng. 10 (2022), 107434, https://doi.org/10.1016/j.jece.2022.107434.
[79] H. Mohan, J.-M. Lim, S.-W. Lee, M. Cho, Y.-J. Park, K.-K. Seralathan, B.-T. Oh, V_2O_5/RGO/Pt nanocomposite on oxytetracycline degradation and pharmaceutical effluent detoxification, J. Chem. Technol. Biotechnol. 95 (2020) 297–307, https://doi.org/10.1002/jctb.6238.
[80] J. Kang, H. Zhang, X. Duan, H. Sun, X. Tan, S. Wang, Nickel in hierarchically structured nitrogen-doped graphene for robust and promoted degradation of antibiotics, J. Clean. Prod. 218 (2019) 202–211, https://doi.org/10.1016/j.jclepro.2019.01.323.
[81] Y. Jiao, Y. Zhang, W. Wang, Comparison of four tourmalines for ps activation to degrade sulfamethazine: efficiency, kinetics and mechanisms, Int. J. Environ. Res. Public Health 19 (2022), https://doi.org/10.3390/ijerph19063244.
[82] C. Alexopoulou, A. Petala, Z. Frontistis, C. Drivas, S. Kennou, D.I. Kondarides, D. Mantzavinos, Copper phosphide and persulfate salt: a novel catalytic system for the degradation of aqueous phase micro-contaminants, Appl. Catal. B: Environ. 244 (2019) 178–187, https://doi.org/10.1016/j.apcatb.2018.11.058.
[83] A. Ioannidi, P. Oulego, S. Collado, A. Petala, V. Arniella, Z. Frontistis, G. N. Angelopoulos, M. Diaz, D. Mantzavinos, Persulfate activation by modified red mud for the oxidation of antibiotic sulfamethoxazole in water, J. Environ. Manag. 270 (2020), 110820, https://doi.org/10.1016/j.jenvman.2020.110820.
[84] H. Shan, X. Dong, X. Cheng, Y. Si, J. Yu, B. Ding, Highly flexible, mesoporous structured, and metallic Cu-doped C/SiO_2 nanofibrous membranes for efficient catalytic oxidative elimination of antibiotic pollutants, Nanoscale 11 (2019) 14844–14856, https://doi.org/10.1039/c9nr04118d.
[85] E. Kattel, B. Kaur, M. Trapido, N. Dulova, Persulfate-based photodegradation of a beta-lactam antibiotic amoxicillin in various water matrices, Environ. Technol. (U. Kingd.) 41 (2020) 202–210, https://doi.org/10.1080/09593330.2018.1493149.
[86] S. Patel, J. Sharma, V.L. Gole, Removal of antibiotic cefixime from wastewater using UVC/sodium persulphate system, Mater. Today.: Proc. 78 (2023) 69–73, https://doi.org/10.1016/j.matpr.2022.11.198.
[87] M. Sizykh, A. Batoeva, G. Matafonova, Enhanced catalyst-free degradation and mineralization of ceftriaxone by UV/H_2O_2 and UV/$S_2O_8^{2-}$ processes using KrCl excilamp (222 nm), J. Photochem. Photobiol. A: Chem. 436 (2023), 114357, https://doi.org/10.1016/j.jphotochem.2022.114357.
[88] Y. Sun, D.-W. Cho, N.J.D. Graham, D. Hou, A.C.K. Yip, E. Khan, H. Song, Y. Li, D. C.W. Tsang, Degradation of antibiotics by modified vacuum-UV based processes: mechanistic consequences of H_2O_2 and $K_2S_2O_8$ in the presence of halide ions, Sci. Total Environ. 664 (2019) 312–321, https://doi.org/10.1016/j.scitotenv.2019.02.006.
[89] C. Wenhai, C. Tengfei, D. Erdeng, Y. Deng, G. Yingqing, G. Naiyun, Increased formation of halomethanes during chlorination of chloramphenicol in drinking water by UV irradiation, persulfate oxidation, and combined UV/persulfate pre-treatments, Ecotoxicol. Environ. Saf. 124 (2016) 147–154, https://doi.org/10.1016/j.ecoenv.2015.10.016.
[90] A. Ghauch, A. Baalbaki, M. Amasha, R. El Asmar, O. Tantawi, Contribution of persulfate in UV-254 nm activated systems for complete degradation of chloramphenicol antibiotic in water, Chem. Eng. J. 317 (2017) 1012–1025, https://doi.org/10.1016/j.cej.2017.02.133.
[91] J.-S. Ye, J. Liu, H.-S. Ou, L.-L. Wang, Degradation of ciprofloxacin by 280 nm ultraviolet-activated persulfate: degradation pathway and intermediate impact on proteome of *Escherichia coli*, Chemosphere 165 (2016) 311–319, https://doi.org/10.1016/j.chemosphere.2016.09.031.
[92] H. Yang, Y. Li, Y. Chen, G. Ye, X. Sun, Comparison of ciprofloxacin degradation in reclaimed water by UV/chlorine and UV/persulfate advanced oxidation processes, Water Environ. Res. 91 (2019) 1576–1588, https://doi.org/10.1002/wer.1144.
[93] H. Milh, X. Yu, D. Cabooter, R. Dewil, Degradation of ciprofloxacin using UV-based advanced removal processes: comparison of persulfate-based advanced oxidation and sulfite-based advanced reduction processes, Sci. Total Environ. 764 (2021), 144510, https://doi.org/10.1016/j.scitotenv.2020.144510.
[94] J.-A. Macías-Vargas, M.-L. Díaz-Ramírez, T.-A. García-Mejía, R.-M. Ramírez-Zamora, Enhanced ciprofloxacin degradation via photo-activated persulfate using the effluent of a large wastewater treatment plant, Top. Catal. 65 (2022) 1128–1138, https://doi.org/10.1007/s11244-022-01666-7.
[95] I. Michael-Kordatou, M. Iacovou, Z. Frontistis, E. Hapeshi, D.D. Dionysiou, D. Fatta-Kassinos, Erythromycin oxidation and ERY-resistant Escherichia coli inactivation in urban wastewater by sulfate radical-based oxidation process under UV-C irradiation, Water Res 85 (2015) 346–358, https://doi.org/10.1016/j.watres.2015.08.050.
[96] Y.-Q. Gao, N.-Y. Gao, Y. Deng, D.-Q. Yin, Y.-S. Zhang, Degradation of florfenicol in water by UV/$Na_2S_2O_8$ process, Environ. Sci. Pollut. Res. 22 (2015) 8693–8701, https://doi.org/10.1007/s11356-014-4054-6.
[97] X. He, S.P. Mezyk, I. Michael, D. Fatta-Kassinos, D.D. Dionysiou, Degradation kinetics and mechanism of β-lactam antibiotics by the activation of H_2O_2 and $Na_2S_2O_8$ under UV-254nm irradiation, J. Hazard. Mater. 279 (2014) 375–383, https://doi.org/10.1016/j.jhazmat.2014.07.008.
[98] X. Liu, Y. Liu, S. Lu, Z. Wang, Y. Wang, G. Zhang, X. Guo, W. Guo, T. Zhang, B. Xi, Degradation difference of ofloxacin and levofloxacin by UV/H_2O_2 and UV/PS (persulfate): efficiency, factors and mechanism, Chem. Eng. J. 385 (2020), 123987, https://doi.org/10.1016/j.cej.2019.123987.
[99] Y. Liu, X. He, Y. Fu, D.D. Dionysiou, Kinetics and mechanism investigation on the degradation of oxytetracycline by UV-254 nm activation of persulfate, J. Hazard. Mater. 305 (2016) 229–239, https://doi.org/10.1016/j.jhazmat.2015.11.043.
[100] L. Gao, Q. Mao, S. Luo, L. Cao, X. Xie, Y. Yang, Y. Deng, Z. Wei, Experimental and theoretical insights into kinetics and mechanisms of hydroxyl and sulfate radicals-mediated degradation of sulfamethoxazole: similarities and differences, Environ. Pollut. 259 (2020), 113795, https://doi.org/10.1016/j.envpol.2019.113795.
[101] Z. Liu, W. Hu, H. Zhang, H. Wang, P. Sun, Enhanced degradation of sulfonamide antibiotics by UV irradiation combined with persulfate, Processes 9 (2021) 1–9, https://doi.org/10.3390/pr9020226.
[102] L. Boudriche, Z. Safaei, D. Ramasamy, M. Sillanpaa, A. Boudjemaa, Sulfaquinoxaline oxidation by UV-C activated sodium persulfate: degradation kinetics and toxicological evaluation, Water Environ. Res. 91 (2019) 1412–1419, https://doi.org/10.1002/wer.1136.
[103] Y. Zhang, Y.-G. Zhao, Y. Hu, M. Gao, L. Guo, J. Ji, Insight in degradation of tetracycline in mariculture wastewater by ultraviolet/persulfate advanced oxidation process, Environ. Res. 212 (2022), 113324, https://doi.org/10.1016/j.envres.2022.113324.
[104] M.H. Rasoulifard, H. Majidzadeh, F.T. Demneh, E. Babaei, M.H. Rasoulifard, Photocatalytic degradation of tylosin via ultraviolet-activated persulfate in aqueous solution, Int. J. Ind. Chem. 3 (1) (2012) 5, https://doi.org/10.1186/2228-5547-3-16.
[105] E.A. Serna-Galvis, F. Ferraro, J. Silva-Agredo, R.A. Torres-Palma, Degradation of highly consumed fluoroquinolones, penicillins and cephalosporins in distilled water and simulated hospital wastewater by UV254 and UV254/persulfate processes, Water Res 122 (2017) 128–138, https://doi.org/10.1016/j.watres.2017.05.065.
[106] B. A. Ospino-Atehortúa, H. Zúñiga-Benítez, G. A. Peñuela, Potential application of persulfate and simulated sunlight radiation on azithromycin removal, Environ. Eng. Res. 26 (2021), https://doi.org/10.4491/eer.2020.189.
[107] Y.-C. Lin, S.C. Panchangam, L.-C. Liu, A.Y.-C. Lin, The design of a sunlight-focusing and solar tracking system: a potential application for the degradation of pharmaceuticals in water, Chemosphere 214 (2019) 452–461, https://doi.org/10.1016/j.chemosphere.2018.09.114.
[108] F. Chen, Q. Yang, D. Wang, F. Yao, Y. Ma, X. Li, J. Wang, L. Jiang, L. Wang, H. Yu, Highly-efficient degradation of amiloride by sulfate radicals-based photocatalytic processes: reactive kinetics, degradation products and mechanism, Chem. Eng. J. 354 (2018) 983–994, https://doi.org/10.1016/j.cej.2018.08.095.
[109] M. Liu, L. Zhang, B.-D. Xi, S. Yu, X. Hu, L.-A. Hou, Degradation of ciprofloxacin by TiO_2/Fe_2O_3/zeolite catalyst-activated persulfate under visible LED light irradiation, RSC Adv. 7 (2017) 51512–51520, https://doi.org/10.1039/c7ra08475g.
[110] G.N. Coulibaly, S. Bae, J. Kim, A.A. Assadi, K. Hanna, Enhanced removal of antibiotics in hospital wastewater by Fe-ZnO activated persulfate oxidation, Environ. Sci.: Water Res. Technol. 5 (2019) 2193–2201, https://doi.org/10.1039/c9ew00611g.
[111] L. Wang, J. Fu, Y. Chen, H. Ou, Persulfate-based visible photocatalysis with a novel stability enhanced Fe-based metal-organic framewor, J. Solid State Chem. 313 (2022), 123297, https://doi.org/10.1016/j.jssc.2022.123297.

[112] K. Xu, K. Cui, M. Cui, X. Liu, X. Chen, Carbonyl heterocycle modified mesoporous carbon nitride in photocatalytic peroxydisulfate activation for enhanced ciprofloxacin removal: performance and mechanism, J. Hazard. Mater. 444 (2023), 130412, https://doi.org/10.1016/j.jhazmat.2022.130412.
[113] M.M. Mohamed, E.E. Abdelmonem, G.O. El-Sayed, Graphene foam mediated FeS_2/α-Fe_2O_3 composites for chloramphenicol photodegradation using persulfate activation under visible light irradiation, J. Water Process Eng. 53 (2023), 103633, https://doi.org/10.1016/j.jwpe.2023.103633.
[114] A. Sanei, K. Dashtian, J. Yousefi Seyf, F. Seidi, E. Kolvari, Biomass derived reduced-graphene-oxide supported α-Fe_2O_3/ZnO S-scheme heterostructure: robust photocatalytic wastewater remediation, J. Environ. Manag. 332 (2023), 117377, https://doi.org/10.1016/j.jenvman.2023.117377.
[115] M. Berkani, A. Smaali, Y. Kadmi, F. Almomani, Y. Vasseghian, N. Lakhdari, M. Alyane, Photocatalytic degradation of Penicillin G in aqueous solutions: kinetic, degradation pathway, and microbioassays assessment, J. Hazard. Mater. 421 (2022), 126719, https://doi.org/10.1016/j.jhazmat.2021.126719.
[116] K. Kouvelis, A.A. Kampioti, A. Petala, Z. Frontistis, Degradation of sulfamethoxazole using a hybrid CuO_x-$BiVO_4$/SPS/solar system, Catalysts 12 (2022), https://doi.org/10.3390/catal12080882.
[117] X. Zhang, W. Liu, T. Gao, D. Cao, X. Che, S. Zhou, J. Shang, X. Cheng, A novel iron molybdate photocatalyst with heterojunction-like band gap structure for organic pollutant degradation by activation of persulfate under simulated sunlight irradiation, Environ. Sci. Pollut. Res. 30 (2023) 53157–53176, https://doi.org/10.1007/s11356-023-26056-8.
[118] O. Tuna, E. Bilgin Simsek, D. Berek, Assembling of orthorhombic $CaTiO_3$ particles with carbon fiber with rich surface oxygen vacancies and interfacial charge transfer for enhanced decomposition of recalcitrant antibiotic under visible light, Opt. Mater. 134 (2022), 113193, https://doi.org/10.1016/j.optmat.2022.113193.
[119] L. Zhu, Y. Zhou, L. Fei, X. Cheng, X. Zhu, L. Deng, X. Ma, Z-scheme CuO/Fe_3O_4/GO heterojunction photocatalyst: enhanced photocatalytic performance for elimination of tetracycline, Chemosphere 309 (2022), 136721, https://doi.org/10.1016/j.chemosphere.2022.136721.
[120] T. Song, X. Meng, H. Wang, C. Zhang, M. Ge, Visible-LED-light-driven photocatalytic activation of peroxydisulfate by magnetic $ZnFe_2O_4$/Ag nanocomposite for efficient tetracycline degradation, Sep. Purif. Technol. 297 (2022), 121474, https://doi.org/10.1016/j.seppur.2022.121474.
[121] E. Grilla, V. Matthaiou, Z. Frontistis, I. Oller, I. Polo, S. Malato, D. Mantzavinos, Degradation of antibiotic trimethoprim by the combined action of sunlight, TiO_2 and persulfate: a pilot plant study, Catal. Today 328 (2019) 216–222, https://doi.org/10.1016/j.cattod.2018.11.029.
[122] Y. Vasseghian, D. Sezgin, D.C. Nguyen, H.Y. Hoang, M. Sari Yilmaz, A hybrid nanocomposite based on CuFe layered double hydroxide coated graphene oxide for photocatalytic degradation of trimethoprim, Chemosphere 322 (2023), 128243, https://doi.org/10.1016/j.chemosphere.2023.138243.
[123] E. Brillas, S. Garcia-Segura, Recent progress of applied TiO_2 photoelectrocatalysis for the degradation of organic pollutants in wastewaters, J. Environ. Chem. Eng. 11 (2023), 109635, https://doi.org/10.1016/j.jece.2023.109635.
[124] K. Lalas, O.S. Arvaniti, E. Zkeri, M.-C. Nika, N.S. Thomaidis, D. Mantzavinos, A. S. Stasinakis, Z. Frontistis, Thermally activated persulfate oxidation of ampicillin: linetics, transformation products and ecotoxicity, Sci. Total. Environ. 846 (2022), 157378, https://doi.org/10.1016/j.scitotenv.2022.157378.
[125] Y. Qian, G. Xue, J. Chen, J. Luo, X. Zhou, P. Gao, Q. Wang, Oxidation of cefalexin by thermally activated persulfate: kinetics, products, and antibacterial activity change, J. Hazard. Mater. 354 (2018) 153–160, https://doi.org/10.1016/j.jhazmat.2018.05.004.
[126] Y. Qian, X. Liu, K. Li, P. Gao, J. Chen, Z. Liu, X. Zhou, Y. Zhang, H. Chen, X. Li, G. Xue, Enhanced degradation of cephalosporin antibiotics by matrix components during thermally activated persulfate oxidation process, Chem. Eng. J. 384 (2020), 123332, https://doi.org/10.1016/j.cej.2019.123332.
[127] C. Jiang, Y. Ji, Y. Shi, J. Chen, T. Cai, Sulfate radical-based oxidation of fluoroquinolone antibiotics: kinetics, mechanisms and effects of natural water matrices, Water Res 106 (2016) 507–517, https://doi.org/10.1016/j.watres.2016.10.025.
[128] R. Zhou, T. Li, Y. Su, T. Ma, L. Zhang, H. Ren, Oxidative removal of metronidazole from aqueous solution by thermally activated persulfate process: kinetics and mechanisms, Environ. Sci. Pollut. Res. 25 (2018) 2466–2475, https://doi.org/10.1007/s11356-017-0518-9.
[129] L. Liu, S. Lin, W. Zhang, U. Farooq, G. Shen, S. Hu, Kinetic and mechanistic investigations of the degradation of sulfachloropyridazine in heat-activated persulfate oxidation process, Chem. Eng. J. 346 (2018) 515–524, https://doi.org/10.1016/j.cej.2018.04.068.
[130] Y. Ji, W. Xie, Y. Fan, Y. Shi, D. Kong, J. Lu, Degradation of trimethoprim by thermo-activated persulfate oxidation: reaction kinetics and transformation mechanisms, Chem. Eng. J. 286 (2016) 16–24, https://doi.org/10.1016/j.cej.2015.10.050.
[131] S. Song, Y. Huang, Y. Du, S. Xiao, S. Han, K. Hu, H. Zhang, H. Wang, C. Wu, A. Qiong, Oxidation of ciprofloxacin by the synergistic effect of DBD plasma and persulfate: reactive species and influencing factors analysis, Plasma Sci. Technol. 25 (2022), https://doi.org/10.1088/2058-6272/ac8dd4.
[132] B. Wang, X. Li, Y. Wang, Degradation of metronidazole in water using dielectric barrier discharge synergistic with sodium persulfate, Sep. Purif. Technol. 303 (2022), 122173, https://doi.org/10.1016/j.seppur.2022.122173.
[133] K. Shang, R. Morent, N. Wang, Y. Wang, B. Peng, N. Jiang, N. Lu, J. Li, Degradation of sulfamethoxazole (SMX) by water falling film DBD Plasma/Persulfate: reactive species identification and their role in SMX degradation, Chem. Eng. J. 431 (2022), 133916, https://doi.org/10.1016/j.cej.2021.133916.
[134] S. Tang, D. Yuan, Y. Rao, N. Li, J. Qi, T. Cheng, Z. Sun, J. Gu, H. Huang, Persulfate activation in gas phase surface discharge plasma for synergetic removal of antibiotic in water, Chem. Eng. J. 337 (2018) 446–454, https://doi.org/10.1016/j.cej.2017.12.117.
[135] J. Lei, P. Duan, W. Liu, Z. Sun, X. Hu, Degradation of aqueous cefotaxime in electro-oxidation-electro-Fenton-persulfate system with Ti/CNT/SnO_2-Sb-Er anode and Ni@NCNT cathode, Chemosphere 250 (2020), 126163, https://doi.org/10.1016/j.chemosphere.2020.126163.
[136] P. Duan, D. Chen, X. Hu, Tin dioxide decorated on Ni-encapsulated nitrogen-doped carbon nanotubes for anodic electrolysis and persulfate activation to degrade cephalexin: mineralization and degradation pathway, Chemosphere 269 (2021), 128740, https://doi.org/10.1016/j.chemosphere.2020.128740.
[137] M. Malakootian, M. Ahmadian, Removal of ciprofloxacin from aqueous solution by electro-activated persulfate oxidation using aluminum elèctrodes, Water Sci. Technol. 80 (2019) 587–596, https://doi.org/10.2166/wst.2019.306.
[138] M. Malakootian, M. Ahmadian, Ciprofloxacin removal by electro-activated persulfate in aqueous solution using iron elèctrodes, Appl. Water Sci. 9 (2019), https://doi.org/10.1007/s13201-019-1024-7.
[139] S. Periyasamy, X. Lin, S.O. Ganiyu, S.-K. Kamaraj, A. Thiam, D. Liu, Insight into BDD electrochemical oxidation of florfenicol in water: kinetics, reaction mechanism, and toxicity, Chemosphere 288 (2022), 132433, https://doi.org/10.1016/j.chemosphere.2021.132433.
[140] N. Xu, C. Hu, Z. Zhu, W. Wang, H. Peng, B. Liu, Establishment of a novel system for photothermal removal of ampicillin under near-infrared irradiation: persulfate activation, mechanism, pathways and bio-toxicology, J. Colloid Interface Sci. 640 (2023) 472–486, https://doi.org/10.1016/j.jcis.2023.02.131.
[141] L. Chu, R. Zhuan, D. Chen, J. Wang, Y. Shen, Degradation of macrolide antibiotic erythromycin and reduction of antimicrobial activity using persulfate activated by gamma radiation in different water matrices, Chem. Eng. J. 361 (2019) 156–166, https://doi.org/10.1016/j.cej.2018.12.072.
[142] S. Adil, B. Maryam, E.-J. Kim, N. Dulova, Individual and simultaneous degradation of sulfamethoxazole and trimethoprim by ozone, ozone/hydrogen peroxide and ozone/persulfate processes: a comparative study, Environ. Res. 189 (2020), 109889, https://doi.org/10.1016/j.envres.2020.109889.
[143] Amina, Q. Abbas, A. Shakoor, M. Naushad, B. Yousaf, In-situ oxidative degradation of sulfamethoxazole by calcium peroxide/persulfate dual oxidant system in water and soil, Process Saf. Environ. Prot. 164 (2022) 696–705, https://doi.org/10.1016/j.psep.2022.06.052.
[144] Y. Gao, S. Cong, Y. He, D. Zou, Y. Liu, B. Yao, W. Sun, Study on the mechanism of degradation of tetracycline hydrochloride by microwave-activated sodium persulfate, Water Sci. Technol. 82 (2020) 1961–1970, https://doi.org/10.2166/wst.2020.479.
[145] F. Sepyani, R. Darvishi Cheshmeh Soltani, S. Jorfi, H. Godini, M. Safari, Implementation of continuously electro-generated Fe_3O_4 nanoparticles for activation of persulfate to decompose amoxicillin antibiotic in aquatic media: UV254 and ultrasound intensification, J. Environ. Manag. 224 (2018) 315–326, https://doi.org/10.1016/j.jenvman.2018.07.072.
[146] W. Wei, D. Zhou, L. Feng, X. Li, L. Hu, H. Zheng, Y. Wang, The graceful art, significant function and wide application behavior of ultrasound research and understanding in carbamazepine (CBZ) enhanced removal and degradation by Fe^0/PDS/US, Chemosphere 278 (2021), 130368, https://doi.org/10.1016/j.chemosphere.2021.130368.
[147] B. Kaur, L. Kuntus, P. Tikker, E. Kattel, M. Trapido, N. Dulova, Photo-induced oxidation of ceftriaxone by persulfate in the presence of iron oxides, Sci. Total. Environ. 676 (2019) 165–175, https://doi.org/10.1016/j.scitotenv.2019.04.277.
[148] C.M. Garcìa Perdomo, P.A. Ramírez Minota, H. Zúñiga-Benítez, G.A. Peñuela, Cephalexin removal by persulfate activation using simulated sunlight and ferrous ions, Water Sci. Technol. 85 (2022) 52–62, https://doi.org/10.2166/wst.2021.509.
[149] V.M.M.C. Starling, E.P. Costa, F.A. Souza, E.C. Machado, J.C. de Araujo, C. C. Amorim, Persulfate mediated solar photo-Fenton aiming at wastewater treatment plant effluent improvement at neutral pH: emerging contaminant removal, disinfection, and elimination of antibiotic-resistant bacteria, Environ. Sci. Pollut. Res. 28 (2021) 17355–17368, https://doi.org/10.1007/s11356-020-11802-z.
[150] A.R. Rahmani, H. Rezaei-Vahidian, H. Almasi, F. Donyagard, Modeling and optimization of ciprofloxacin degradation by hybridized potassium persulfate / zero valent-zinc/ultrasonic process, Environ. Process. 4 (2017) 563–572, https://doi.org/10.1007/s40710-017-0251-x.
[151] S. Ahmadi, C. Osagie, S. Rahdar, N.A. Khan, S. Ahmed, H. Hajini, Efficacy of persulfate-based advanced oxidation process (US/PS/Fe_3O_4) for ciprofloxacin removal from aqueous solutions, Appl. Water Sci. 10 (2020), https://doi.org/10.1007/s13201-020-01271-7.
[152] G.Z. Kyzas, N. Mengelizadeh, M.K. Saloot, S. Mohebi, D. Balarak, Sonochemical degradation of ciprofloxacin by hydrogen peroxide and persulfate activated by ultrasound and ferrous ions, Colloids Surf. A: Physicochem, Eng. Asp. 642 (2022), 128627, https://doi.org/10.1016/j.colsurfa.2022.128627.
[153] Y. Ma, Z. Wang, J. Li, B. Song, S. Liu, Electrochemical-assisted ultraviolet light coupled peroxodisulfate system to degrade ciprofloxacin in water: kinetics, mechanism and pathways, Chemosphere 295 (2022), 133838, https://doi.org/10.1016/j.chemosphere.2022.133838.
[154] J. Gu, G. Wei, Y. Zhu, C. Lu, L. Zhang, Z. Huang, Q. Su, S. Pan, Photoelectric activation of persulfate with a new type of red mud-based $CuFe_2O_4$ particle electrode for the efficient degradation of ciprofloxacin: preparation, influencing

factors and mechanism, J. Environ. Chem. Eng. 11 (2023), 109137, https://doi.org/10.1016/j.jece.2022.109137.
[155] M. Li, X. Yang, D. Wang, J. Yuan, Enhanced oxidation of erythromycin by persulfate activated iron powder-H_2O_2 system: role of the surface Fe species and synergistic effect of hydroxyl and sulfate radicals, Chem. Eng. J. 317 (2017) 103–111, https://doi.org/10.1016/j.cej.2016.12.126.
[156] T. Zhang, Y. Yang, X. Li, H. Yu, N. Wang, H. Li, P. Du, Y. Jiang, X. Fan, Z. Zhou, Degradation of sulfamethazine by persulfate activated with nanosized zero-valent copper in combination with ultrasonic irradiation, Sep. Purif. Technol. 239 (2020), 116537, https://doi.org/10.1016/j.seppur.2020.116537.
[157] H.-C. Zhang, P.-C. Guo, X. Zhang, G.-P. Sheng, Developing a solar photothermal method for peroxydisulfate activation for water purification: taking degradation of sulfamethoxazole as an exemple, Chem. Eng. J. 403 (2021), 126324, https://doi.org/10.1016/j.cej.2020.126324.
[158] R.D.C. Soltani, M. Mashayekhi, M. Naderi, G. Boczkaj, S. Jorfi, M. Safari, Sonocatalytic degradation of tetracycline antibiotic using zinc oxide nanostructures loaded on nano-cellulose from waste straw as nanosonocatalyst, Ultrason. Sonochem. 55 (2019) 117–124, https://doi.org/10.1016/j.ultsonch.2019.03.009.
[159] H. Zeng, S. Shen, A. Cai, Q. Sun, L. Wang, S. Zhu, X. Li, J. Deng, Degradation of tetracycline by UV/Fe^{3+}/persulfate process: kinetics, mechanism, DBPs yield, toxicity evaluation and bacterial community analysis, Chemosphere 307 (2022), 136072, https://doi.org/10.1016/j.chemosphere.2022.136072.
[160] L. Wang, Y. Ye, Z. Zeng, Y. Wang, M. Han, X. Pei, D. Wang, F. Pan, Efficient removal of tetracycline in water by a Fe_3O_4-mediated persulfate activation and biodegradation coupled system: performance, validation, and mechanism, J. Water Process Eng. 53 (2023), 103718, https://doi.org/10.1016/j.jwpe.2023.103718.
[161] L. Vazquez, L.M.M.T. Gomes, P.H. Presumido, D.G.D. Rocca, R.F.P.M. Moreira, T. Dagnac, M. Llompart, A.I. Gomes, V.J.P. Vilar, Tubular membrane photoreactor for the tertiary treatment of urban wastewater towards antibiotics removal: application of different photocatalyst/oxidant combinations and ozonation, J. Environ. Chem. Eng. 11 (2023), 109766, https://doi.org/10.1016/j.jece.2023.109766.